NPS-PH-11-005

NAVAL POSTGRADUATE SCHOOL

MONTEREY, CALIFORNIA

THE LEGACY OF MANFRED HELD WITH CRITIQUE

by

EV2 Florian Bouvenot

Thesis Advisor:	Prof. Brown,	NPS
First Thesis Supervisor:	Prof. Rothe,	HSU
Second Thesis Supervisor:	Prof. Dickmann,	HSU

August 2011

Approved for public release; distribution is unlimited.

THIS PAGE INTENTIONALLY LEFT BLANK

REPORT DOCUMENTATION PAGE

Form Approved
OMB No. 0704-0188

1. REPORT DATE *(DD-MM-YYYY)* 01-08-2011	**2. REPORT TYPE** Technical Report	**3. DATES COVERED** *(From - To)*
4. TITLE AND SUBTITLE THE LEGACY OF MANFRED HELD WITH CRITIQUE		**5a. CONTRACT NUMBER**
		5b. GRANT NUMBER
		5c. PROGRAM ELEMENT NUMBER
6. AUTHOR(S) EV2 Florian Bouvenot		**5d. PROJECT NUMBER**
		5e. TASK NUMBER
		5f. WORK UNIT NUMBER
7. PERFORMING ORGANIZATION NAME(S) AND ADDRESS(ES) Naval Postgraduate School Monterey, CA 93943-5000		**8. PERFORMING ORGANIZATION REPORT NUMBER** NPS-PH-11-005
9. SPONSORING / MONITORING AGENCY NAME(S) AND ADDRESS(ES) Helmut Schmidt University University of the Federal Armed Forces Holsenhofweg 85, 22043 Hamburg Germany		**10. SPONSOR/MONITOR'S ACRONYM(S)**
		11. SPONSOR/MONITOR'S REPORT NUMBER(S)

12. DISTRIBUTION / AVAILABILITY STATEMENT
Approved for public release; distribution is unlimited

13. SUPPLEMENTARY NOTES
The views expressed in this thesis are those of the authors and do not reflect the official policy or position of the Department of Defense or the United States Government.

14. ABSTRACT
Impact initiation of explosives is one of the more frequent referred to topics of Prof (Dr) Manfred Held, an internationally renown ballistician, who passed away in 2011. This thesis includes a cross-referenced bibliography of most of his published papers and patents and focuses on one of his more frequently referred topics, the impact of initiation of explosives. Experimental data from impacts against bare explosives, covered and confined with and without air gaps, and explosive and projectile dimensions are first used to validate finite difference computations required to extend and properly evaluate the database. The analyses include explosives (PBX 9404, Comp. B (65/35), Octol (70/30), H6, TNT) and projectiles (aluminum, steel, copper, tantalum) of much varied properties and sensitivities. Assuming that close examination of the experimental data proposed by Held and others to rate the relative threshold sensitivity of explosives to impact (incl., (v^2d), (u^2d), ($\rho v^2 d$) and ($\rho^{1/2} v^2 d$)) deviate significantly from constancy, in some cases greater than 50 percent. It is found that the product of interfacial impact pressure and well-defined projectile diameter is a much more reliable predictor of the impact sensitivity of a bare explosive based on the smaller deviation from mean values relative to the aforementioned terms. Importantly, this energy term takes into account the density and Hugoniot properties of both impactor and explosive.

15. SUBJECT TERMS
Manfred Held, Impact initiation, Explosive sensitivity, AUTODYN®, Initiation criterions, Explosives, PBX 9404, Comp. B, H6, Octol, TNT

16. SECURITY CLASSIFICATION OF:			**17. LIMITATION OF ABSTRACT**	**18. NUMBER OF PAGES**	**19a. NAME OF RESPONSIBLE PERSON** Ronald Brown
a. REPORT UNCLASSIFIED	**b. ABSTRACT** UNCLASSIFIED	**c. THIS PAGE** UNCLASSIFIED	UU	217	**19b. TELEPHONE NUMBER** *(include area code)* 831-656-2635

Standard Form 298 (Rev. 8-98)
Prescribed by ANSI Std. Z39.18

THIS PAGE INTENTIONALLY LEFT BLANK

NAVAL POSTGRADUATE SCHOOL
Monterey, California 93943-5000

Daniel T. Oliver
President

Leonard A. Ferrari
Executive Vice President and
Provost

The report entitled "The Legacy of Manfred Held with Critique" contains the results of research conducted at the Naval Postgraduate School, under an exchange agreement with the Helmut Schmidt University (German Armed Forces), in partial fulfillment of the requirements for the Degree Master of Science in Electrical Engineering.

Further distribution of all or part of this report is authorized.

This report was prepared by:

Florian Buvenot
B.Sc.

Approved by:

Ronald E. Brown
Professor and Lead Advisor
Physics Department

Reviewed by:

Andres Larraza, Chairman
Physics Department

Released by:

Karl A. van Bibber
Vice President and
Dean of Research

THIS PAGE INTENTIONALLY LEFT BLANK

ABSTRACT

Impact initiation of explosives is one of the more frequent referred to topics of Prof (Dr) Manfred Held, an internationally renown ballistician, who passed away in 2011. This thesis includes a cross-referenced bibliography of most of his published papers and patents and focuses on one of his more frequently referred topics, the impact of initiation of explosives. Experimental data from impacts against bare explosives, covered and confined with and without air gaps, and explosive and projectile dimensions are first used to validate finite difference computations required to extend and properly evaluate the database. The analyses include explosives (PBX 9404, Comp. B (65/35), Octol (70/30), H6, TNT) and projectiles (aluminum, steel, copper, tantalum) of much varied properties and sensitivities. Assuming that close examination of the experimental data proposed by Held and others to rate the relative threshold sensitivity of explosives to impact (incl., (v^2d), (u^2d), (ρv^2d) and ($\rho^{1/2}v^2d$)) deviate significantly from constancy, in some cases greater than 50 percent. It is found that the product of interfacial impact pressure and well-defined projectile diameter is a much more reliable predictor of the impact sensitivity of a bare explosive based on the smaller deviation from mean values relative to the aforementioned terms. Importantly, this energy term takes into account the density and Hugoniot properties of both impactor and explosive.

THIS PAGE INTENTIONALLY LEFT BLANK

TABLE OF CONTENTS

LIST OF FIGURES

LIST OF TABLES

THIS PAGE INTENTIONALLY LEFT BLANK

PREFACE

Mr. Held's contributions cover a wide range within the ballistics sciences, as illustrated in the exhibit below:

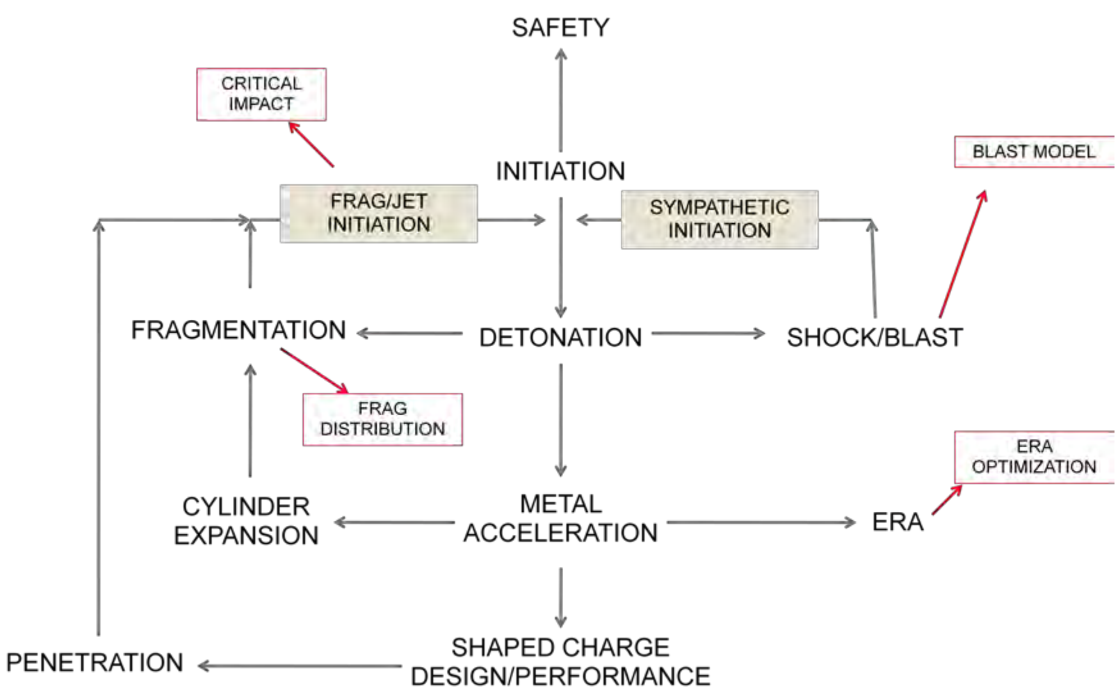

THIS PAGE INTENTIONALLY LEFT BLANK

EXECUTIVE SUMMARY

Prof (Dr) Manfred Held, an internationally renowned ballistician, passed away in February 2011 leaving behind an extraordinary number of technical accomplishments. A bibliography of published and unpublished reports and patents along with the full contents and cross-index of some these reports are recorded on a CD accompanying this thesis.

Along with the survey of his accomplishments another objective of the thesis research reported herein is to critique one of the more frequently referred to aspects of centerpieces of his work: that is the topic of impact initiation of explosives. Dr Held not only recognized the value of defining means for rating explosive sensitivity, but his interest extended to closely rated areas of detonation breakup and divergency (i.e., "retonation"), shock initiation, safety and the development of extremely useful diagnostic techniques for examining the associated phenomenologies.

Close examination of the experimental data proposed by Held and others to rate the relative threshold sensitivity of explosives to impact (incl., (v^2d), (u^2d), (ρv^2d) and ($\rho^{1/2}v^2d$)) are found, however, to deviate significantly from constancy. These deviations might result in part to shaped charge jet impact data, since accurate measure of impactor characteristics at impact are difficult. There is concluded, on the other hand, that the product of interfacial impact pressure and well-defined projectile diameter is a much more reliable predictor of the impact sensitivity of a bare explosive based on the smaller deviation from mean values relative to the aforementioned terms. As important is that this energy term takes into account the density and Hugoniot properties of the impactor and explosive.

Experimental data from impacts against bare explosives, covered and confined with and without air gaps, and explosive and projectile dimensions are used to validate finite

difference computations required to extend and properly evaluate the database. The analyses include explosives and projectiles of much varied properties and sensitivities.

Explosives: PBX9404, Composition B (65/35), Octol(70/30), H6 and TNT.
Projectiles: Tungsten, Copper, Steel, and Aluminum

The average Pd-values for the explosives are reported below:

Explosive	**Pd (cal/cm^2)**	**% Deviation**
PBX9404	793±32	4.0
Comp. B	691±150	21.7
Octol	1460±208	14.3
H6	1572±337	21.4
TNT	3049±849	27.9

Table 1: Pd values and % deviation established in this thesis.

Deviations from mean values of v^2d, u^2d, ρv^2d and $\rho^{1/2}v^2$ are from former treatments in most cases greater than 50 percent.

The differences in deviation between PBX9404 and the other explosives most likely results at least in part to preparation. That is, final content distribution and grain size are dependent on the rate of sedimentation of the denser components and the column length and rate of cool-down. Each of these factors can affect impact and shock sensitivity.

DECLARATION

Hereby I declare that the following Master's Thesis has been created by myself, without assistance of others, using only named sources and supplementary materials. Furthermore, I certify that the digital version is exactly the same as the printed one.

Monterey, the . . . .

(Date) (Signature)

THIS PAGE INTENTIONALLY LEFT BLANK

EHRENWÖRTLICHE ERKLÄRUNG

Hiermit versichere ich, dass ich diese Arbeit selbständig verfasst, keine anderen als die im Quellen- und Literaturverzeichnis genannten Quellen und Hilfsmittel, insbesondere keine dort nicht genannten Internet-Quellen benutzt, alle aus Quellen und Literatur wörtlich oder sinngemäß entnommenen Stellen als solche kenntlich gemacht habe und dass die auf einem elektronischen Speichermedium abgegebene Fassung der Arbeit der gedruckten entspricht.

Monterey, den . . . .

(Datum) (Unterschrift)

THIS PAGE INTENTIONALLY LEFT BLANK

ACKNOWLEDGMENT

The last five months I have spent at the Physics Department of the Naval Postgraduate School have been for me a very interesting experience from every point of view. All the expectations I had, like the diversification of my scientific knowledge, the autonomy at work and the acquisition of engineering skills, have been successfully performed by the resolution of an engineering challenge in a field in which I was not absolutely active and familiar.

At this point, I would like much to give thanks to my Thesis advisor at the Naval Postgraduate School, Professor Brown. Each time I had important questions to ask, he took his time to meet me and to answer in detail my questions. His wide scientific knowledge, his permanent helpfulness as well as his natural kindness, have been helping and motivating me for five months to solve this engineering challenge as good as I can. The compliance and the writing of this Master's Thesis would have been undeniably much more complicated without his help and support. The routinely meetings, presentations and reports we had these last five months have been very meaningful to control the state of the Thesis and to allow potential adjustments.

I would like to give thanks to my both advisors at the Helmut Schmidt University, Professor Rothe and Professor Dickmann for the enablement and the organization of this exchange too.

Mentioned in this acknowledgment should be evenly Richard Cook, English instructor at the Naval Postgraduate School, as well as my German fellow and good friend second Lieutenant Andreas Lück, for the Help by the error checking and correction concerning the English and German Orthography and Grammatik.

THIS PAGE INTENTIONALLY LEFT BLANK

DANKSAGUNG

Die letzten fünf Monaten, die ich an der Naval Postgraduate School im „Physics Department“ verbracht habe, waren für mich in allen Bereichen eine sehr interessante Erfahrung. Jede meiner Erwartungen, sei es die Erweiterung meines wissenschaftlichen Wissens, die Selbstständigkeit bei der Arbeit, sowie das Erlernen der Ingenieurtätigkeiten, wurde bei der Lösung einer Ingenieuraufgabe, in einem Bereich indem ich ursprunglich nicht unbedingt tätig und vertraut war, erfolgreich erfüllt.

An dieser Stelle möchte ich mich bei meinem Betreuer an der Naval Postgraduate School, Professor Brown, ganz herzlich bedanken. Jedes Mal, wenn ich wichtige Fragen hatte, nahm er sich die Zeit, um mich zu empfangen und diese im Detail zu beantworten. Sein sehr umfangreiches wissenschaftliches Wissen, seine ständige Hilfsbereitschaft, sowie seine natürliche Freundlichkeit haben mir immer geholfen und mich immer motiviert, weiterhin fleißig zu arbeiten, um diese Ingenieuraufgabe so gut wie möglich lösen zu können. Die Erfüllung und das Schreiben dieser Master-Arbeit wären zweifellos ohne seine Hilfe und Unterstützung viel komplizierter gewesen. Die regelmäßigen Treffen, die Präsentationen und Berichte, die wir im Laufe dieser fünf Monaten hatten, waren auch hilfreich, um den Stand der Arbeit kontrollieren zu können und eventuelle Änderungen vorzunehmen.

Ich möchte mich ebenso bei meinen beiden Betreuern an der Helmut Schmidt Universität, Professor Rothe und Professor Dickmann, für das Ermöglichen und für die Organisation dieses Austausches bedanken.

Erwähnen bei dieser Danksagung möchte ich auch Richard Cook, Sprachlehrer an der Naval Postgraduate School, sowie meinen deutschen Kamerad und guten Freund Leutnant Andreas Lück, für die Hilfe bei der Korrektur der Orthographie und Grammatik, sei es auf englisch oder auf deutsch.

THIS PAGE INTENTIONALLY LEFT BLANK

HONNEUR PATRIE VALEUR DISCIPLINE

"La véritable école du Commandement est la culture générale"

Charles de Gaulle

THIS PAGE INTENTIONALLY LEFT BLANK

I. INTRODUCTION

A. INTRODUCTION OF THE THESIS

The field of ballistics, which deals with all aspects of flight, behavior and effects of projectiles used in combination with explosives, has been researched by a lot of scientists in the last decades, furnishing plenty of results which have been mainly used for the development and the performing of weapons in the defense industry.

Dr. Manfred Held was one of these scientists who spent his entire life doing research in this immense field. Unfortunately, he passed away on the 08th of February 2011 at the age of seventy seven, leaving behind him more than fifty years of work documented in more than one hundred and fifty patents as well as more than five hundred publications. His research dealt with all topics of this field. His research dealt with many of the topics of this field: for example, detonation processes, metal acceleration and cylinder expansion, the invention of Explosive Reactive Armor (ERA), and high-speed diagnostics. One of these topics was also the process of initiation, especially impact initiation.

It is the aim of this thesis to review this last topic, to present and to check the results obtained by Dr. Held and to make critiques by using the family of ANSYS AUTODYN® codes and state-of-the-art material response models.

After having reviewed some of the statements concerning impact initiation formulated by Dr. Held and after having clearly defined the objectives of this thesis, some definitions, process descriptions and analysis tools will be presented as a technical background. Then, the technical issues will be listed and technical approaches will be submitted. After that, the results obtained by the simulations set up in AUTODYN® have been presented and discussed. Assumptions and potential implications will also be formulated. Furthermore, a conclusion regrouping all the important results obtained in this thesis will be presented and some recommendations for future works will be made. Last but not least, some additional information concerning the properties of the materials needed to set up the simulations as well as a description of the tools and functions of the AUTODYN® software are available in the Appendix. Important simulation results have been tabulated in the Appendix.

In this thesis, it has first be shown that the simulation software AUTODYN® is best adapted to set up the experiments concerning impact initiation. With the help of this software, it has been shown that the computational techniques developed agree well with experiments reported by several investigators, including Moulard whose results were used to define the technique. As a result of this comprehensive examination of projectile impacts against explosives under a wide range of conditions (incl. explosive type, dimensions, protection, confinement and projectile material), a new parameter for rating impact sensitivity against bare explosives is derived. This alternative term is found to be closer to constancy for each explosive compared with other terms such as the v^2d and u^2d criterions proposed by Held, and the $\sqrt{\rho v^2 d}$ and $\rho v^2 d$ criterions proposed by Chick and Mader respectively.

B. BIOGRAPHY OF MANFRED HELD

Born in Regensburg, the 4th biggest city of the state of Bavaria (south-east Germany) on the 28th of September 1933, Manfred Held studied physics and completed his doctorate on ultra violet spectroscopy in Physical Chemistry at the Technical University of Munich (*TU-Muenchen*) in 1959 [001]. After he graduated, he joined the *EADS-Thomson-DASA-Wirksysteme* (MBDA Germany), previously known as the *Messerschmidt-Boelkow-Blohm-Apparatebau/Schrobenhausen* (MBB), in 1960 and specialized in the physics of explosions. This former German weapon company, now owned by the European armaments giant EADS, was cofounded by Franz Rudolf Thomanek (1913-1990), an Austrian physics engineer who became famous in the 1930's and during the Second World War for the development of portable anti-tank weapons using the shaped-charge principle. Franz Rudolf Thomanek promptly saw in Doctor Held a potential successor at the directorship of this establishment, so took Held under his wing and consequently worked closely with him over the years. Professor Doctor Manfred Held worked for this company for more than fifty years, beginning as a simple research scientist, coming then the head of "research and development of conventional warheads and armour" [001].

Although very attached to his home Bavaria, where he worked and used to teach terminal ballistics at the military university of the German armed forces[1] (*UniBw Muenchen*) in Bibenberg, next to Munich, Dr. Held travelled a lot to present his newest papers at conferences all around the world [002]. The most popular conferences for him were the *Symposium of Detonation* and, above, all the *International Symposium on Ballistics,* which first took place in 1974 and at which he was always present over the years. He was also a member of the editorial board of the *Propellants, Explosives, Pyrotechnics* journal, of the Chinese journal of *Energetic Materials*, and an independent expert to the *Scientific Monitoring and Advisoring Publication* of the *Australian Institute of High Energetic Materials*. As a direct consequence of his engagement with the scientific community, he obtained a lot of titles and gratifications from different research organizations [003]: he was a respected member of the *Scientific Committees of the International Seminars* at the *University of Pardubice* (Czech Republic), member of the *Board of Trustees of the Fraunhofer Institute for Chemical Technology* (ICT) in Germany, professor honoris causa[2] of the *Chinese Nanching University*, and the first person in the *International Ballistics Society* (IBS) to be named a Ballistics Science Fellow with an honorary Lifetime Membership and membership number 001. He also attained the Diesel-Medal in Silver for his more than significant number of patents [001].

---

[1] There are actually two military universities of the German armed forces in Germany: the *UniBw Muenchen* in Bibenberg (Munich), and the *UniBw Hamburg* in Hamburg, also known as *Helmut Schmidt University*.

[2] A degree honoris causa is an academic degree which is conferred as a way of honoring a distinguished visitor's contribution to a specific field.

Figure 1: Dr. Held (right) receiving a reward from Jack Riegel, Chairman of the International Ballistics Society, at the 25th *International Symposium on* Ballistics.

Professor Doctor Manfred Held passed away from a sudden heart attack on the 08th of February 2011, at his 50th wedding anniversary in Schrobenhausen, a small town in Bavaria where he took up residence some years ago [004]. He left behind his wife, four children, a lot of friends in the scientific community as proven by all the condolence letters left publicly for him in different journals and on the internet, and his achievements in more than fifty years of research documented in more than five hundred publications and one hundred fifty patents [003].

Figure 2 [001]: Dr. Held working on one of his paper during a conference

His legacy covers a lot of main and secondary topics in the science of ballistics : investigations into the structure of initiation, detonation, fragmentation, cylinder expansion, penetration, metal acceleration and so on. He developed techniques which are still used today, such as techniques for measuring detonic events, including symmetry of detonation, wave shaping, corner turning effects, v^2d initiation criterion, synchro-streak techniques and more [002]. He also performed investigations concerning shaped charges, especially shaped-charge warhead systems such as the Milan, Hot, Kormoran, Roland and dispenser munitions, EFPs (explosive-formed projectiles), up to fragmenting warheads with directional effects [001]. But he was above all known for the invention and the development of Explosive Reactive Armour (ERA) in the late 60's which was successfully used for the first time in 1982 by the Israelis during the Arab-Israeli conflict and later by the Russians [004]. One of his last fields of research was the development of the "momentum method" for determining and characterizing blast effects.

THIS PAGE INTENTIONALLY LEFT BLANK

II. MOTIVATION

A. HELD'S RESULTS CONCERNING IMPACT INITIATION

In the immense field of ballistics, Held did a lot of studies concerning impact initiation, an important process with regards to explosive detonation. The *Held's Publications Chronology*, attached on the Compact Disc joined to this thesis, contains 225 of his published articles. This is approximately one-half of the total of his works.

In one of his papers [005], Held reported that the initiation threshold value of high explosives could be defined with regards to fragment impact velocities, the fragment impact masses and the barrier thickness in front of the acceptor charge. Changing one of this variable by keeping the two other ones fixed gives the possibility to describe exhaustively the initiation threshold value within a defined study area. Figure 3 illustrates this statement. Furthermore, he noticed that the length of the projectile didn't affect the probability of detonation [006], which means that the pressure duration is irrelevant. In other words, the mass of the projectile can actually be reduced to the impact area, in this case the projectile surface. For cylindrical projectiles, this surface is a circle which can be defined through its diameter. Under these particular circumstances, the term "mass" of Figure 3 can also be replaced by the term "diameter". More generally, it can be replaced by the term "impact surface". In this way, it is meaningful to plot the projectile velocity as a function of the projectile diameter to describe the initiation threshold value of high explosives.

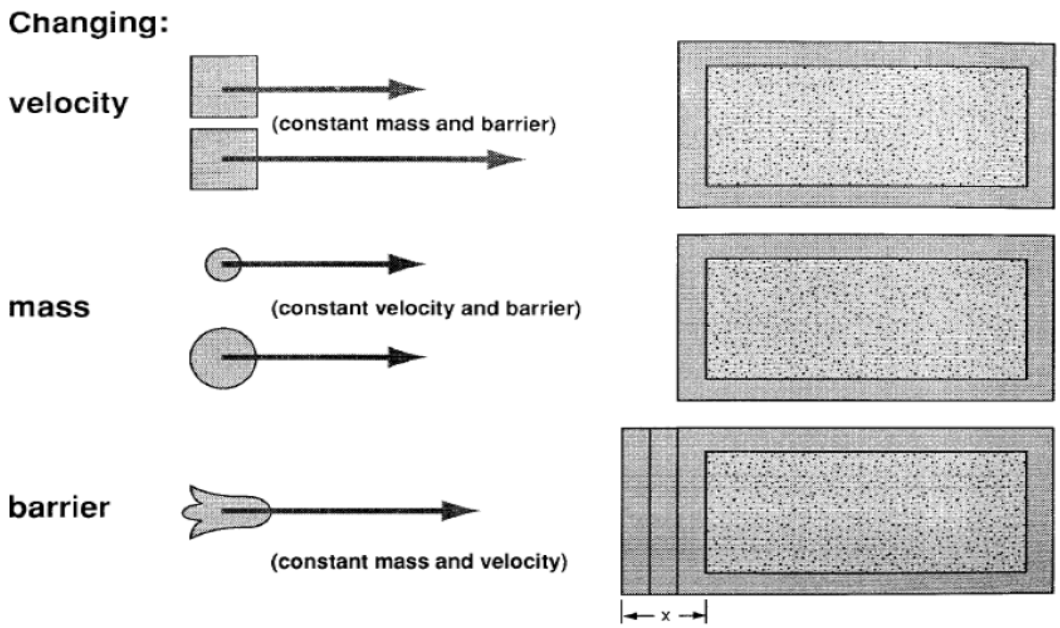

Figure 3 [005]: Definition of the initiation threshold value of high explosives with regards to the fragment impact velocities, the fragment masses and the barrier thickness in front of the acceptor charge.

Doing some research about the ability of Patriot systems to destroy TBM missiles and using the quoted initiation threshold value description method, he impacted, among others, a 40 g heavy steel fragment with a velocity of 2400 m/s against a 3 kg heavy block of Comp B at 1.71 g/cm^3. He did the same by adding a steel barrier in front of the acceptor charge and then by increasing this steel barrier while conducting a double fragment shot. All his results have been reported in his paper [005]. The velocities needed to obtain a detonation were higher in case of barriers.

Held has also observed that an unconfined high explosive charge directly in contact with a barrier, surprisingly, was less easily initiated by a jet impact than a one with an air gap between [006]. He has listed three effects which appear to be responsible for this effect. The first one is that the high explosive should be pre-compressed by the bulging of the barrier plate while being perforated. The second one is that the loading of the test charge generated by the bulging target plate and by the pressure of the cratering jet is relatively slow and there is no such high, one dimensional pressure as in the case of a free jet. The third one is that the high explosive charge in contact with the barrier is exposed in a smaller area than the charge with an air gap between because of the large-area spray of fragments emerging from the barrier. He has also described the differences between the detonation in confined and unconfined high explosive charges. He found that the threshold value between detonation and reaction, and between reaction and no reaction, was in the case of confined charges at considerably lower jet penetration velocities, because the confinement held the test charge together for a considerably longer time, so that a reaction that started more slowly could still run up to a full detonation [006].

In 1983 [007], Held noticed that the energy density criterion by Walker and Wasley [008] was certainly a well suitable criterion for many of high explosive charges (HE), but it does not provide any information about the minimum required impact area which is necessary for an initiation. Using his own empirical results [009] and evaluations from literature [010, 011, 012], and taking the stagnation pressure for the initiation of HE as a rough rule, he derived an empirical rule for the minimum required initiation area. With v_{cr} as the critical velocity and A_{cr} the critical area required for detonation, this assumption is:

He transformed the critical area A_{cr} for cylindrical projectiles:

As a consequence,

If the product is constant, the quotient is constant too.

As a result, the Held's criterion is obtained [006]:

This criterion, known as Held v^2d criterion, has been generally accepted and used for rating the sensitivity of explosives over a wide range of conditions[3] by many scientists including Held himself [006, 013, 014, 015]. Some of the results are presented in table 2 and figure 4.

Type of HE	v^2d in $mm^3/\mu s^2$	Reference
HNAB	3	Hasman
PBX 9404	4	Bahl
RDX/Wax 88/12	5	Griffiths
TNT/RDX 35/65	6	Held
PETN 1.77	13	Vigil
Comp B	16	Chick, Moulard
H6	16.5	Chick
Detasheet	36-53	Weickert
C3 9407	40	Vigil
Tetryl	44	Vigil
C4	64	Weickert
TATB	108	Weingart
9502	128	Campell

Table 2 [003]: Initiation criterion v^2d

[3] To be discussed in later sections of this thesis.

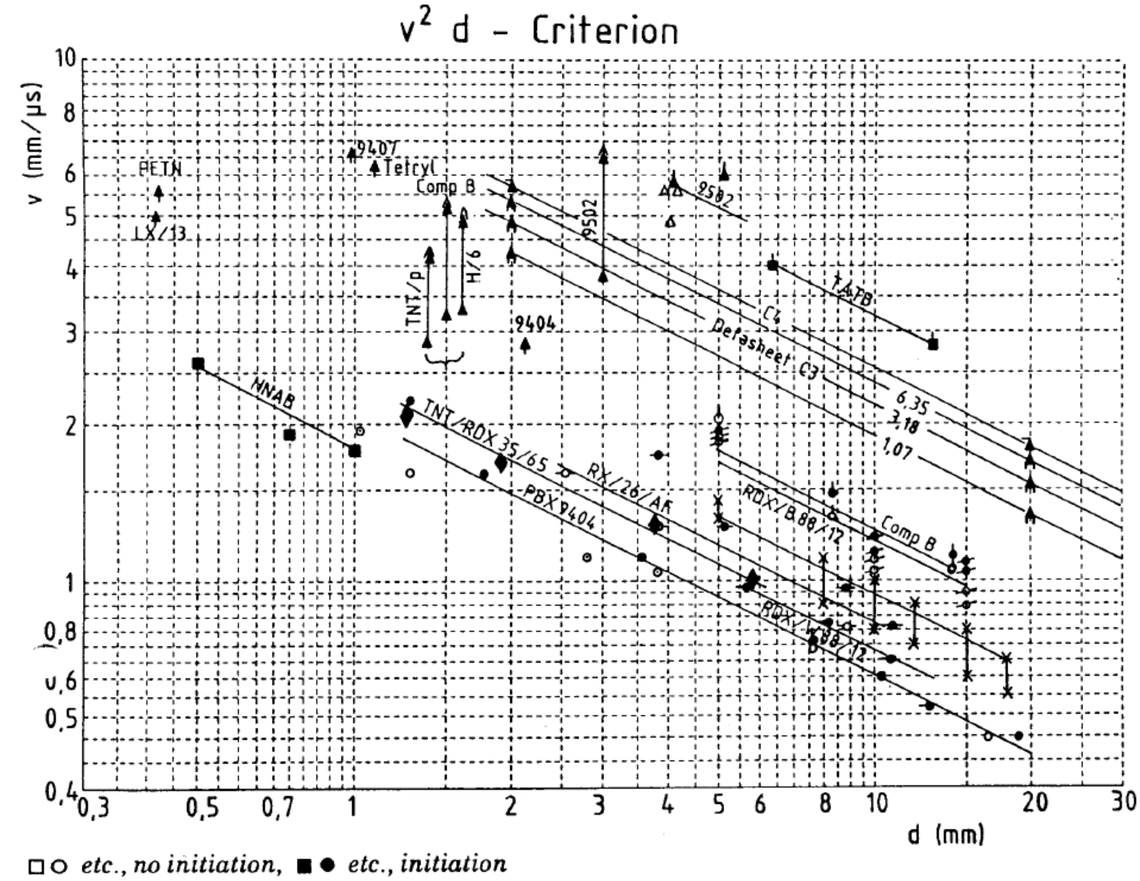

Figure 4 [006]: Threshold impact velocity as a function of the diameter of shaped charge jets, projectiles or flyer foil for different high explosive charges in a logarithmic scale.

Aware of the fact that almost all the experiences to determine the v^2d criterion of high explosive charges had been done with copper and steel projectiles, therefore with similar densities[4]. Later, Held modified his v^2d statement to take into account the projectile density [016]. He defined the cratering velocity v_{cr}:

[4] Copper has a density of 8.94 g/cm^3 and Steel has a variable density due to the different alloying constituents but generally comprised between 7.75g/cm^3 and 8.05 g/cm^3.

with ρ_t as the density of the target, also the density of the acceptor charge, and ρ_p as the density of the projectile.

Using the cratering velocity, he made following statement:

Chick and Mader defined two similar criterions, respectively the $\sqrt{\rho_p}v^2d$ and $\rho_p v^2 d$ criterions, which are compared with the Held u^2d criterion in one study [016].

B. RESEARCH GOALS AND OBJECTIVES

The main objective of this thesis is to review the statements concerning impact initiation, that Held was able to formulate and which have been mentioned just above, in order to confirm or contradict in the context of data found in the literature survey, concluded as part of this research. Comparisons between experimental results obtained by some scientists in the past and simulation results obtained with AUTODYN® should confirm the ability of this software to be used for impact initiation problems, and the analysis of different effects potentially affecting impact initiation should help to set up the computational technique. Topics covered are listed below:

- Moulard experiment for PBX 9404
- Effect of the length on impact initiation
- Effect of the acceptor charge diameter on impact initiation
- Effect of a barrier on impact initiation
- Effect of a confinement on impact initiation
- Effect of an air gap between barrier and acceptor charge on impact initiation
- Effect of the projectile material on impact initiation
- Study of other explosives

- v^2d, u^2d, ρv^2d, $\sqrt{\rho} v^2d$ and Pd energy criterion
- Impact pressure at interfaces, run distances and rarefaction effect

THIS PAGE INTENTIONALLY LEFT BLANK

III. TECHNICAL BACKGROUND

A. HISTORY

Accidentally fabricated in China in 220 BC by separating gold from silver during a low-temperature reaction, black powder was the first explosive developed on the Earth. Its diffusion has however not been instantly: the Arabs first used it for military operations at the end of the 7th century, while the Chinese only started producing it in large quantities for civil and military uses, especially for fireworks and blast purposes, during the 11th century. The Europeans had to wait till the middle of the 13th decade to discover it and one more decade before propagating it everywhere on the old continent. It has been first used for military purposes before finding its utility in mining after 1650.

Black powder has always been extremely dangerous to use, mainly because it is so easily ignited by any spark. Furthermore, its action is unpredictable, mainly because its burning rate and the pressure developed depend on the strength of the rock confining it. All these facts made it inappropriate for uses in large quantities during the industrial revolution, when mining in hard rock and destroying difficult landscapes (mountains, rivers,...) to build thousands kilometers of railroads became a national priority for many countries [020]. A need of new explosives was born...

This new need of explosives, which should be in the first place safer to handle, cheaper to produce and more powerful to use, made plenty of scientists from the middle of the 19th century take up doing research and finding or developing new types of explosives like Nitroglycerine (Sobrero, 1846), TNT (Wilbrand, 1863) and Dynamite (Nobel, 1867). Many of the advances, which have especially been done in the decades after that, have come from military researches, which have been done in all aspects of the explosives and their common uses, for example security and safety, blast/shock and penetration capacities as well as blast/shock and penetration protections. A name has been given to this enhanced field of research: the ballistics field. Research in this immense field has then been done by numbers of scientists, like Dr. Held, in the last decades.

B. THE BALLISTICS FIELD

1. Organization of the ballistics field

The ballistics field is defined as the science of mechanics which deals with all aspects of flight, behavior and effects of projectiles used in combination with explosives. This field covers a lot of different topics which can be classified in different main categories:

- Initiation: Start of a chemical reaction due to an input of energy and leading to a chain reaction whose produced energy becomes more and more important.
- Detonation: Explosion observed in both conventional solid and liquid explosives, as well as in reactive gases, and involving a supersonic exothermic front accelerating through a medium that eventually drives a shock front propagating directly in front of it.
- Shock/Blast: Sudden acceleration or deceleration caused by an impact or an explosion.
- Metal acceleration: Metal acceleration as a result of a detonation leading to a cylinder expansion. It is a function of the detonation velocity, the energy released and the produced gases. Description is given by the Gurney equations.
- Cylinder expansion: Deformation of the confinement of an explosive due to metal acceleration
- Fragmentation: Process by which the casing of an explosive (artillery shell, bomb, grenade, ...) is shattered by its detonation.
- Shaped charge design/performance: Design and performance of an explosive charge which has been shaped to focus the effect of the explosive's energy. Shaped charges can be used to initiate nuclear weapons or to penetrate armors.

- Penetration: Entry of a projectile into a target and evolution of this projectile in the target.
- Explosive Reactive Armour (ERA): Armour that reacts by exploding to the impact of a weapon to reduce the damages done to the object being protected. It is generally used against shaped charges.
- Safety: Protection against unwanted initiations, detonations or all other effects which could affect high explosives (HE) or ammunitions.

The figure below shows areas of Held's interests, which reflect a broad range of ballistics:

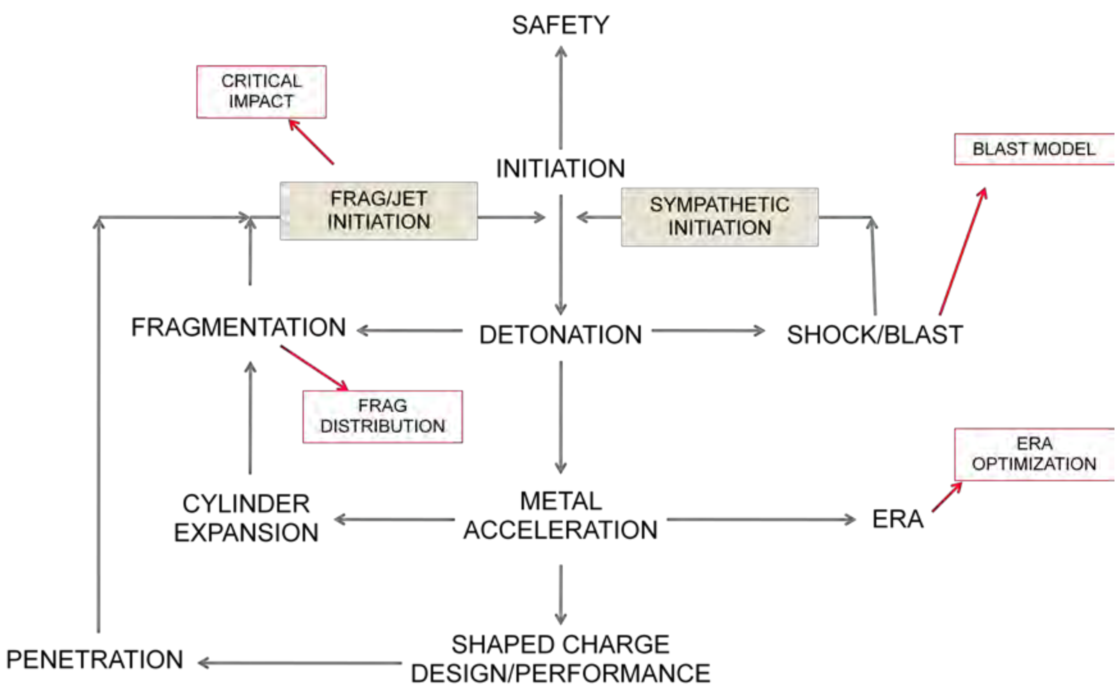

Figure 5 [021]: Organization of the ballistics field. The papers are organized according to the outline in the figure.

2. Explosion and explosives

a) Definition of explosion

There are two types of explosions [021]:

- Physical explosions, which are characterizing by a sudden release of internal from a contained volume and fragmentation of the containment
- Chemical explosions, which are characterizing by a rapid exothermic reaction leading to ignition and autocatalytic reaction (or burning) and the production of large volumes of gas products

The second ones are responsible for the deflagration and detonation processes[5].

b) Definition and properties of explosives

Explosives are substances which are capable of undergoing exothermic chemical reaction at extremely fast rates to produce gaseous and/or condensed reaction products at high temperature and pressure, leading to an explosion with deflagration and detonation processes. They contain atomic bonds of a specific nature which generate the explosive character (called "explosophore" groups) as well as a high density of nitrogen dioxide (NO_2), which allows the reaction to take place. They react with different sensibility with the environment (temperature, shock, pressure, ...) making them more or less difficult to initiate[6].

Pure explosives are generally not used as they are, but are mixed with other explosives and energetic and/or inert additives which change their properties, making them for example less sensitive or easier to manufacture. It is for example the case of polymer-

[5] See subchapter C of this chapter.

[6] See subchapter C of this chapter.

bonded explosives, also called plastic-bonded explosives (PBX), whose explosive powder is bound together in a matrix using small quantities of a synthetic polymer, making it less sensitive.

Explosives are generally divided into two main categories:

- primary explosives, used as initiators, which are easy to initiate (low activation energies) but have a low energy gain
- secondary explosives, used as boosters or main charges, which are more difficult to initiate (high activation energies) but have a high energy gain

Furthermore, pure explosives or explosive mixtures are usually worked in various ways to form specific products, whose the most widely used are plastic-bonded explosives (PBX)[7], pressed explosives and cast explosives. Pressed explosives can be of two types: canned or cartridged (pure explosives with no additives), and free standing (explosives with binder). Generally, additives blended with the explosives are needed to desensitize them and to held the pressed pellets together during pressing. Cast explosives, generally machineable, are based on mixtures of relatively higher-melting crystalline explosives and molten TNT, sometimes completed with oxidizers like nitrates [022].

c) Applications and attributes

Explosives are principally used for commercial and military purposes, or as aid to research. In these fields, explosives are used for applications as different as the mining and rock blasting, metal forming, fire fighting, high speed photography, artillery shells, guided missiles or propellants.

For optimum use, explosives have to possess some specific attributes. They have to be economical to produce, to have a high energy gain, to be safe to prepare and to handle, to

[7] See above.

detonate when they are required to, to be sensitive enough to be initiated in the manner desired and to have a small initiation stimuli compared with the detonation output [021]. That's why initiation studies and explosive properties are very important.

d) Presentation of the explosives used for the purposes of this thesis

Since it is one of the main objectives of this investigation to examine the usefulness of the Held's impact initiation criterion (i.e. the v^2d and u^2d criterions), the five explosives listed below, which cover a wide range of sensitivities, were selected for this investigation:

- PBX 9404, a Plastic-Bonded explosive made of 94% HMX (a nitroamine high explosive), 3% Nitrocellulose and 3% CEF widely used as initiator in nuclear weapons
- Cast TNT, also called Trinitrotoluene, a pure and insensitive explosive which is very useful in a large range of different applications and possesses convenient handling properties (can be easily cast poured for warhead loading because of its relatively low melting temperature). The explosive yield of TNT is also considered to be the standart mesure of strength of explosives.
- H6, a military composition composed of 45% RDX, 30% TNT, 20% powdered aluminum and 5% paraffin wax as a phlegmatizing agent to stabilize and desensitize it notably used in underwater munitions
- Comp. B, a military composition consisting of castable mixtures of RDX and TNT, used as the main explosive filling in artillery projectiles, rockets, land mines and hand grenades. The main common compositions are comp. B (60/40) and comp. B (65/35). Generally, 1% wax is added to it.

- Octol 7030, a melt-castable high explosive mixture consisting of 70% HMX and 30% TNT used in the military for shaped charges and warhead in guide missiles and submunitions.

C. FROM INITIATION TO DETONATION

As already mentioned, it is very important to get very precise information concerning the initiation of explosives, mainly to make them detonating only when required and to obtain the effects desired.

1. Initiation

Initiation is the start of a chemical reaction due to an input of energy and leading to a chain reaction whose produced energy becomes more and more important and ideally leading to detonation.

a) Form of initiations

The input of energy needed to initiate an explosive can take different forms [020]:

- <u>Heat</u>: it consists of a thermal initiation of hot-spots, which are randomly distributed in the explosives. The uncertainties concerning their location and the temperatures at which they are formed make thermal initiation however relatively unreliable for the directly initiation of secondary explosives or propellants but adapted for initiation trains[8], where especially friction-sensitive initiatory materials may be highly receptive to hot-spot initiation and reliable output can be obtained from relatively low-power inputs.

[8] See part d) of this subchapter.

- Friction or Stabbing: it consists, by using friction forms, to produce immense quantities of hot-spots in explosives or compositions where they can grow reliably to detonation. It is generally used in initiation trains, and the preferred form of friction input is the action of stabbing a composition through a metal foil septum into a friction sensitive composition which responds igniferously.
- Flash or Flame: it consists of using a flame or a flash for a very short time to initiate most of energetic materials.
- Percussion: it consists of initiating reliably an explosive by a sharp blow, like in a small-arms cartridge. Initiation occurs via crushing of crystalline particles and the generation of hot spots from which the process grows reliably.
- Electrical: it consists of using electricity to initiate weapon systems. Especially with the introduction of new types of separated electrolyte batteries, electrical detonators and igniters are designed with sensitivities from the order of microjoules to ten of joules of input electrical energy. The most common form of electrical device is the bridgewire, or foil, where the conductor is part of an electrical circuit and is stimulated either by a continuous electrical current or the discharge from a capacitor. It is very reliable technique.
- Coherent light (laser): it consists in providing highly intense radiation levels in very precise time periods at predicted wavelengths to initiate explosives. Laser-initiated devices have safety advantages over electrically and mechanically initiated systems because they eliminate the possibility of initiation through electrostatic discharge, which is a big problem on board ship and in all air-carried ordnance.

b) Impact initiation

The special case of initiation which has been studied in this thesis concerns impact initiation, also called shock initiation, and consisting in impacting projectiles into an explosive to supply the amount of energy needed to make it detonating. With regards to impact initiation, initiation criterions have been developed by Held and some of his colleagues like Mader and Chick. Examples are the v^2d and the ρv^2d criterions, which have been presented in chapter II and which will be checked in this thesis.

c) Initiation energy

This amount of energy needed to initiate explosives has been studied in the past, delivering a critical time dependent energy initiation criterion called "critical energy fluence". This time dependant energy criterion is given by:

with	P ... Pressure applied to the explosive in Pa
	t ... Time period during which P is applied in s
	ρ_0 ... Density of unshocked material in kg/m^3
	U ... Hugoniot relationship
with	s ... Velocity Hugoniot coefficient
	c_0 ... Bulk sound speed in $m.s^{-1}$
	u ... Particle velocity in $m.s^{-1}$

Some explosives have been tested and average values concerning this criterion have been found. They have been noted down in table 3[022]:

Explosive	**Density** (g.cm^3)	**Critical Energy** (cal/cm^2)
Comp. B	1.73	44
Comp. B-3	1.727	33
PBX 9404	1.84	15
RDX	1.55	16
TNT (cast)	1.60	100
TNT (pressed)	1.62	32

Table 3 [022]: Critical time dependent energy fluence values for some explosives

It is however important to notify that these critical energy fluence values have been calculated by using square-wave shock pulses with a certain duration. Some differences with other different energy values, obtained with different methods, like the Pd time independent criterion which will be developed later in this thesis, can also be different.

The initial impact pressure is also important to estimate the amount of energy coming into the explosive. This pressure can be estimated, giving an important tool for impact initiation studies[9].

d) Initiation trains

The aim of initiation trains is to translate a low-power input to an explosive in order to obtain a high-power output: a very insensitive high explosive (secondary explosive) is lead to detonation by initiating first a sensitive explosive (primary explosive) and by going through different charges increasing slowly the amount of energy, giving the necessary energy to initiate the main charge. It generally involves a series of four or five different explosives, and the chain reaction initiating them should be safe and reliable. Initiation trains are widely used in nuclear bombs.

9 See subchapter D, part 1 of this chapter.

e) The mechanism of initiation

The input of energy into the explosive initiates a chemical reaction, whose rate depends on the amplitude of the input and on the chemical reactivity of the explosive. This chemical reaction goes on and starts to release substantial amounts of energy.. As a consequence, the pressure rises and compression waves are generated: deflagration occurs. The reaction rate becomes more and more important while the speed of the pressure wave into the explosives raises. After a certain time, the pressure wave overtakes the shock and merge with it. The detonation takes over. Figure 6 shows this "closed loop" leading, at term, to detonation.

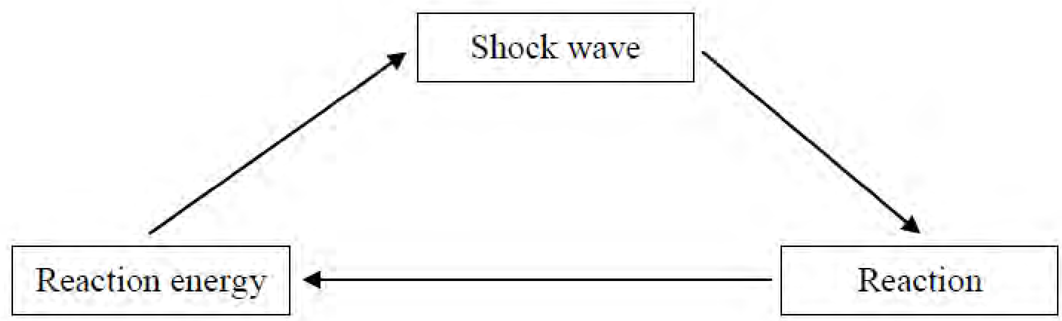

Figure 6: The closed loop of the initiation process

2. Detonation

The v-d parameterization proposed by Held and others for rating projectile impact sensitivity of explosives has been of value to many workers in the field of ballistics. These parameters have been used for example in establishing criteria for neutralizing unexploded ordnance using various projectile devices and shaped charges, and for designing shielding for protecting explosive components. Careful study of published data on this subject has, however, revealed a degree of uncertainty with these relationships. Thus, in addition to the collection and organization of Held's publication, research was directed towards assessing the general usefulness of these relationships, particularly the effect of the material response that lead to explosive detonation.

Steps leading to detonation after impact include the following:

1. Compressional densification and heating
2. Exothermic decomposition (i.e., deflagration)
3. Pressure wave development
4. Transition to shock formation
5. High-order detonation

a) P-v relationship and Rayleigh line

At high rates of impact (i.e., kilometers/second) the explosive and projectile exhibit plastic behavior. Stresses exerted are far above the elastic limit where permanent material deformation results. Under conditions where the projectile and target are chemically inert, pressure waves can reach shock conditions accompanied by severe densification and thermal excitation. Relationships, based on mass, momentum, and energy conservation, and experimental Hugoniot data allow to predict pressure-volume behavior much better than the "ideal" gas law does, see the equation below and figure 7.

with P ... Pressure in Pa

c_0 ... Bulk sound velocity in m/s

ν_0... Specific volume of the unreacted explosive, — with ρ_0 density of the unreacted explosive in kg/m^3

ν ... Specific volume of the explosive at the pressure P

s ... Hugoniot constant dimensionless

The parameters c_0 and s are obtained from experiments. They are available in the Appendix C, subchapter C, for the explosives and inert materials used in this thesis.

The slope of the Rayleigh line, connecting a coordinate on the P-v curve and the ambient condition, provides an estimate of the resulting shock velocity (see equation below). The P-v integral represents the changes in specific energy. It is this extremely compacted high energy zone that leads to exothermic pyrolitic decomposition of explosive molecules and recombination reactions that continual drive the early stages of shock development and eventually led to steady state high order detonation. The equation of the Rayleigh line is:

with $U = c_0 + su$, where u is the particle velocity in m/s

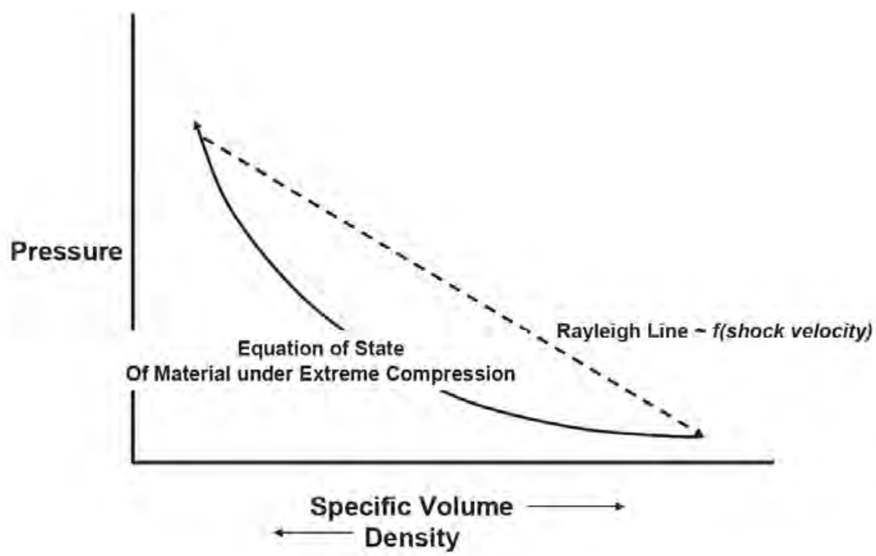

Figure 7 [021]: P-v relationship and Rayleigh line.

b) Steady state detonation and CJ-pressure

Steady state detonation involves an extremely fast cycling back and forth between the so-called Von Neumann spike and the Chapman Jouguet state (see figures 8 and 9). The VN-spike is at the intersection between the Rayleigh line and the P-v EOS. The VN-spike, just behind the shock front (see figures 8 and 9) dictates the density and energy state of the material. Product cases from the detonation are released at and expand away from the CJ state which is at the identical sonic condition as is the shock.

The pressure at the CJ state is:

with ρ_0 ... Initial unreacted explosive density in $kg.m^{-3}$

D ... Detonation velocity in $m.s^{-1}$

γ ... Specific heats ratio of the detonation product gases

γ is normally different for each explosive. However, similitudes in the product composition make that γ is approximately equal to 3 for a large range of explosives whose densities are comprised between 1 g/cm^3 and 1.8 g/cm^3. This leads to:

The CJ pressure is furnished for every explosive by AUTODYN® and can be seen under the properties of the considered explosive[10]. It is also not necessary to calculate it for the explosives available in the AUTODYN® library.

---

[10] See Appendix A, part 1.

The specific volumes at the VN-spike and CJ-state are easily found from the plots shown in figure 9:

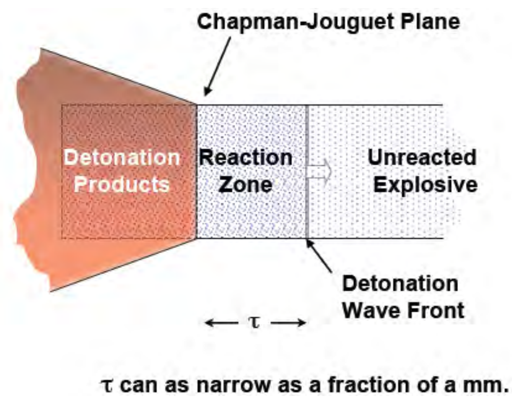

Figure 8 [021]: Evolution of the detonation wave front in the explosive.

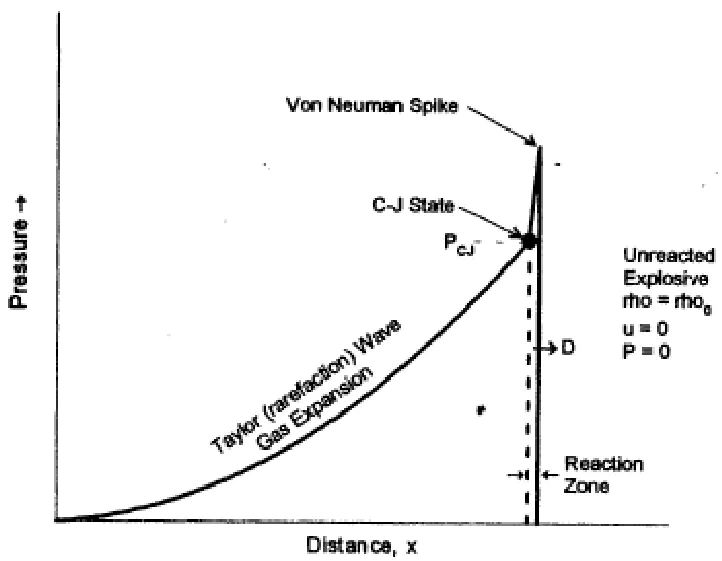

Figure 9 [021]: Evolution of the pressure in the explosive as a function of the distance.

c) Interfacial pressures

Hugoniot equations in the P-u are employed for making first approximations of the interfacial pressures resulting from projectile-explosive. The set of equations include expressions for the projectile and the explosive. The impact velocity is expressed as u_o, the reflected particle motion as u_o-u. As already mentioned, the bulk sound velocity c_o and the Hugoniot dimensionless constant s are determined from experiment.

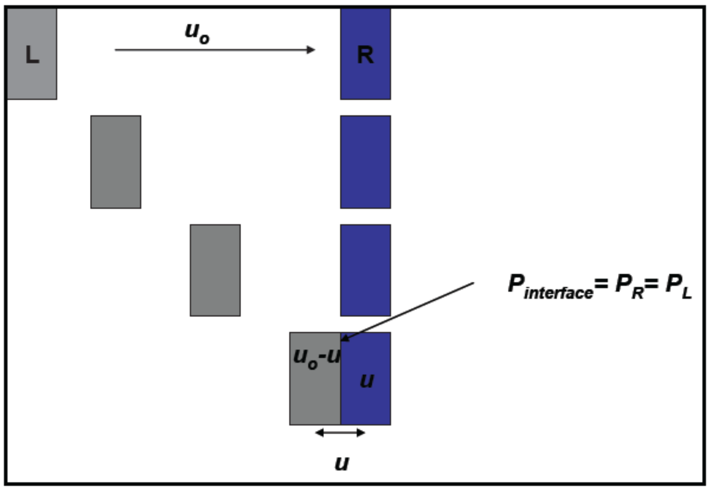

Figure 10 [021]: Interfacial pressures setup.

It is:

At the interface:

The solution of this interface problem has the form $au^2 + bu + c = 0$. Examples will be given later[11]

[11] See chapter V, subchapter J, part1.

d) Equations Of State (EOS)

The analytical analyses using the Hugoniot relationship provide first-cut approximation of initial interfacial pressure. Finite difference computations using the ANSYS AUTODYN code are then used for purposes of simulating actual experimental data and for extrapolation. Models in the code include the Hugoniot equations of state of the projectile and explosive, and thereby provide interfacial response and more importantly bulk effects of impact.

The Lee-Tarver model is used to predict whether explosive ignition follows impact and whether ignition will grow to full detonation based on the pressure exerted on and energy buildup that is expected to occur. Equation of the Lee-Tarver model is given below:

with I, b, a, x, G_1, c, d, y, G_2, e, g, z ... Constants

F ... Reaction ratio (ratio of the mass of the gaseous explosive to the total mass of the explosive)

P ... Pressure in the explosive

μ ... compression,

with ρ ... Density of the explosive at the pressure P

ρ_0 ... Density of the unreacted explosive

The value of F is hereby used to predict whether detonation occurs[12].

An equation of state for the product gases is linked to Lee-Tarver. This equation, most applicable and based on vast experience, was derived by Jones, Wilkins and Lee (referred

[12] See ALPHA, chapter V, subchapter A.

to as JWL). It includes P-v of the gases that expand from the CJ state and the energy released by the detonation of the explosive. The JWL equation is:

with A, B, C, R_1, R_2 and ω ... constants to be calibrated (A, B, C in Pa, R1, R2, ω dimensionless)

It is important to note that modeling product gas behavior is quite challenging since they do not behavior anyway close to that under ambient conditions. The density of detonation products at the CJ state are near 33% greater than the ambient density of the explosive from which they form from. For example densities of the order of aluminum metal result from the detonation of an explosive like HMX, which has a density of 1.9 grams/cc.

Predicted pressure growth in the explosive is used to estimate whether an impact will lead to 1st order detonation. That is, a peak pressure rising to the von-Neumann condition indicates 1st order detonation. On the contrary, an initial pressure first increasing and then falling off indicates a non-detonation. Examples of both cases are presented in chapter V, subchapter A.

e) Distance to detonation

As already mentioned, an explosive does not instantly reach full steady-state detonation. Before steady-state detonation is reached and achieved, the impact has to travel some distance into the acceptor charge (this is the deflagration process). This distance, named run distance, is not constant but depends on the impact pressure and consequently on the materials (projectile and acceptor charge) and on the initial impact velocity. The higher the pressure, the shorter the run distance. This relation is given in the following equation from Alfonse Popalato [022]:

$$\log P = a - b*\log x$$

with P ... Initial impact pressure in GPa

x ... Run distance to detonation in mm

a,b ... constants in Pa

The run distance as a function of pressure is therefore:

The parameters a and b are determined experimentally and listed by Cooper [022].

As the impact pressure is a function of the initial velocity and of parameters taken from the nature of the projectile and from the nature of the acceptor charge[13], the run distance can also be calculated as a simple function of the initial impact velocities and material constants. This formulation is however restricted to a certain range of pressures, determined by the nature of the explosive [022].

f) Rarefaction effect

When a projectile impacts an explosive, a rarefaction wave is also formed. This rarefaction wave first go back into the projectile before being reflected and coming back into the explosive. After a certain time, the rarefaction wave catches up with the shock front and starts attenuating the shock front peak pressure.

It is possible to estimate the distance x' in the explosive over which the shock maintains constant peak pressure. If the run distance x is smaller than the distance x', the rarefaction effects doesn't affect the detonation process. On the contrary, if x is larger than x', which

[13] See above in this subchapter.

is called a "thin-pulse" condition, the rarefaction wave may affect the detonation process and eventually avoid a detonation. This critical distance x' is given by [022]:

with U_{HE} ... Shock velocity in $m.s^{-1}$ in the explosive, $U_{HE} = c_0 + su$

c_0 ... Bulk sound speed in $m.s^{-1}$, specific to the material/explosive

s ... Velocity Hugoniot coefficient, specific to the material/explosive

u ... Particle velocity in $m.s^{-1}$ obtained from the "interface problem"[14]

R_{HE} ... Rarefaction wave velocity in m.s-1 in the explosive, $R_{HE} = c_0 + 2su$

t' ... Pulse width in s,

with x_p ... Projectile length in m

U_p ... Shock velocity in $m.s^{-1}$ in the projectile

R_p ... Rarefaction wave velocity in $m.s_{-1}$ in the projectile

[14] See part 1 of this subchapter.

IV. NATURE OF THE PROBLEM (TECHNICAL ISSUES)

A. LITERATURE RESEARCH AND ACQUISITION

The ballistics and detonics fields are typical armament topics, which is why the military keeps a very close eye on them. As a consequence, most of the studies done in these very specific fields are kept more or less secret and are not available for the general public. Furthermore, all his papers over the last fifty years, either in the civilian word or declassified from the military or the armament industry, have been published in a lot of different journals, books or anthologies held in only a few different public or private libraries around the word. It was also not an easy job to find and get them. In memory of Dr. Held, to whom this thesis is dedicated, all the publications (about two hundred twenty of a total of five hundred obtained during research at the *Naval Postgraduate School* (NPS) of Monterey (California, USA) are listed with abstract and literature sources in a digital document on a separated Compact Disc joined to this thesis.

Writing a thesis about the legacy of Dr. Held implies to have general knowledge about his work. After the literature research comes also the literature acquisition. By more than two hundred twenty papers covering very different topics, it is impossible to read everything before starting working on the thesis. Identifying the different topics treated in his papers and classifying them by topics-interests seems to be a good solution to save time. Then, the papers covering the initiation process and especially the impact initiation process, can be analyzed in more details. This classification by topics-interests is joined in another data on the same disc. Both data should help future researchers interested in Dr. Held's work save time in literature searches and acquisition.

B. SIMULATIONS VS. EXPERIMENTS

1. General observations

Most of the results that have been exposed from Held have been obtained and partially confirmed through different experiments performed by different scientists all around the world, using streak end framing camera, high speed photography, flash radiography and other diagnostics. The obtained pressures have generally been measured with the help of diagnostics tubes with carbon resistors which have been used as pressure gauges [005]. Most of these results, nearly all of them actually, have also been more or less purely obtained through experimentations. No simulations, using thermodynamic codes, have been performed. One of the reason for this is probably the fact that many findings about impact initiation took place some years ago at a period during which simulations software were inexistent or at least not efficient enough, making such tools inappropriate to obtain significant results.

Experimentation results are of course more representative of the reality than simulations, and nothing will replace them before bringing a new product on the military or civil market, but they are also more dependent on outside parameters like temperature, humidity, pressure and so on. Special cameras and other techniques as well as diverse gauges may not be able in initiation and detonation processes (because of very important velocities, pressures,...) to give the accuracy which is necessary to provide good analysis results.

Furthermore, experiments take generally a long time to be prepared, and much time is also needed to do calculations and to analyze the results. Between work, explosive and instrument costs, performing experiments in ballistics is a very costly operation. Simulations are on the contrary generally quite fast to be designed and to be solved, and the results easy to analyze. Concerning the costs, only a relatively small one-time investment for computer equipments and software is needed, making them a very economic tool for research purposes.

2. Is AUTODYN® adapted?

The software which has been used in this thesis is ANSYS AUTODYN®, an engineering simulation software for modeling nonlinear dynamics of solids, fluids, gas and their interaction. This product, which has been developed by the company ANSYS, Inc. based in Canonsburg, Pennsylvania (United States of America), provides advanced capabilities within a robust, easy-to-use software tool to solve many nonlinear dynamics problems of the type required in this thesis.

However, only comparisons between simulation results obtained with AUTODYN® and very similar experimental results obtained from scientists can confirm the ability of AUTODYN® to simulate with a sufficient accuracy some special problems, especially problems concerning impact initiation, which is the main topic of this thesis. This check should be the starting point of this thesis before using this very useful simulation tool to make some general statements.

3. Problems and solutions

Using a simulation tool like AUTODYN® instead of performing some experiments, if it saves time, money and complicated calculations and analysis, brings also with it new problems which have to be taken into consideration and to be solved. The most important ones, with which we had to be confronted in this thesis, are presented below.

For most of the simulations, one important point was to identify the detonation pressure, also called "Chapman-Jouguet" pressure, and indicated in the material properties under "C-J pressure"[15], in the results plots furnished by AUTODYN®. After having spent some

[15] See chapter III, subchapter C, part 2, section b).

time thinking that the abnormally high steady state value obtained in the plots was the detonation pressure and trying to find explanations in, for example, reflections effects to justify it, it was found that this value was not the "Chapman-Jouguet" pressure but the "Von Neumann spike". Finding the "Chapman Jouguet" pressure became also the next aim[16].

During the first problems set up in this thesis, the simulations used to stop after only a few seconds, delivering an error message as following: "Error, degenerate cells in...". This could be solved by selecting the option "Prevent erosion of degenerate elements" in the "Interaction" panel, which allows the interaction calculation to be used to stop elements from becoming degenerate. However, it is to notice that this option only works for Lagrange volume elements and can lead to unphysical results, especially if a large air gap exists between two elements. On the same way, the "Retain inertia of eroded notes", just above, is selected to prevent the eroded nodes from being removed from the model[17].

4. Limits of AUTODYN®

On the same way, some simulations stopped because the energy error was too high. Increasing this value is manually possible[18], but can also lead to unphysical results. Because of that, some problems, generally featuring very small projectile diameters (less than 3 mm) and important projectile velocities (more than 3500 m/s), could not be set up.

Using the finest zoning in AUTODYN® would have been of course the best way to obtain the most accurate simulation results. But it would have required a unaffordable runtime to perform each simulation. By the very important number of simulations which had to be performed in this thesis, choosing the finest zoning was impossible to finish it

[16] See chapter V, subchapter A.

[17] See Appendix B, subchapter C, part 6.

[18] See Appendix B, subchapter C, part 8.

within four months, the time allowed for this research project. Some inaccuracies are also possible and are identified in later sections.

Directly connected to the zoning is the air gap size limit. This size must be in the range 1/10 to 1/2 the dimension of the smallest element face of parts involved in interactions[19]. In a case of a zoning of 2 cells/mm, which has been nearly used for all simulations in this thesis, the air gap is also limited to 0.05 mm, making eventually some problems impossible to set up.

C. CONSISTENCE OF THE STATEMENTS

1. General observations

Most of the experiments which have been realized by Dr. Held have been done for copper-lined shaped charges, that means with important velocities in the range from 4 km/s to 10 km/s, long broken lengths and small jet diameters. Despite the fact that only a few results concerning the behavior of acceptor charges by impact initiation of projectiles are available, the general implementations or rules, established by Held or his confreres for shaped charges, are assumed as valid.

Also, the rare experiments concerning impact initiation with steel projectiles which have been performed used quite large projectile diameters, generally larger than 12 mm. Impact initiation with projectiles in a range from 2 mm to 12 mm are also practically inexistent. It is in the later range which this research is concentrated.

2. Variability of jet diameters

As already mentioned, most of the experiment results concerning impact initiation have been obtained with copper-lined jets. One of the major problems of a jet is its "broken"

[19] See Appendix B, subchapter C, part 6.

diameter. Indeed, a jet has not a fixed diameter, as it is the case for projectiles, but a variable diameter from the tip of the jet to the tail. It remains complicated to estimate the exact jet diameter, mainly because of all the small fragments present in the neighbor area. What jet diameter has been taken during the experiments? Has this diameter been really well estimated? That are two important question which have not been answered very well in most of the reports consulted for the purposes of this thesis.

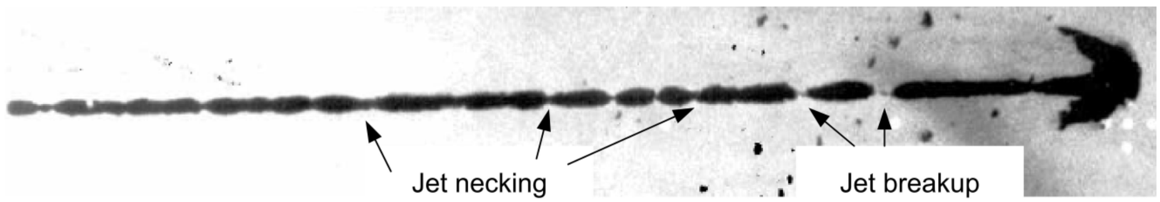

Figure 11 [024]: Jet picture with jet necking and jet breakup

3. Nature of the projectile

Furthermore, and as already mentioned, most of the experimental tests which have been realized used copper jets. On the contrary, most of the experimental tests realized with projectiles used steel material. Copper and steel, because of their similar density (8.93 g/cm^3 vs. 7.90 g/cm^3 respectively), have, according to Held, the same effect on impact initiation [016]. They should also be equivalent to use. However, some tests should be provided to confirm it and we should handle this with attention.

4. Nature of the explosive

There are a lot of explosives, especially explosive compositions, which are having the same name but have quite different compositions proportions. The explosives used by Held or some of his coworkers or colleagues to perform some experiments about impact initiation are sometimes not well described giving a doubt about the exact composition used. And sometimes, even if the composition proportions are given, having a look at the density[20] of this composition shows that it could be a different one from another one whom the given proportions are the same. Different explosives have generally different properties and different behaviors. It is also sometimes quite difficult to compare the results with each other.

5. Variation of v^2d and u^2d for steel projectile impacts

The Held v^2d criterion is given by himself as a constant. Having a look at his results and at the results contained in the references mentioned in his papers supplies however more a certain range of values than fixed ones [006, 009]. The results are also often given for shaped charges, whom jet diameter, as already mentioned, is difficult to estimate, and not for projectiles. Other results are given for very particular conditions like for example only one type of flyer with a unique thickness. Some of the results are tabulated in table 5. Sometimes, the results are given with no regards to the barrier in front of the acceptor charge or with no regards if the explosive is "pressed" or "cast". The results concerning some bare explosives which have been obtained by different scientists are given in table 4. A report concerning technical demining and addressed to the "*Office of Special Technology*" at Fort Washington, Maryland, contains other values of v^2d concerning a large range of explosives and obtained, mainly, through initiation with copper jets [025].

Furthermore, the u^2d criterion is also given by Held as a constant, which describes better the initiation threshold value than the Mader ρv^2d criterion or the Chick $\sqrt{\rho}v^2d$ criterion [016]. However, this statement is only based on the results of two different projectiles, which have been tested with only one diameter. A more range of projectiles and diameters should also be tested.

Thus, it is important to reiterate the fact that the v^2d values, for a large range of steel projectile impacts on different explosives, are not constant. Some examples are given in table 4 as evidence for it.

[20] This is due to the conservation of mass.

Explosive	Scientists	Experimental conditions (steel projectile)	Projectile diameters tested (mm)	Held values of v^2d ($mm^3/\mu s^2$)	Estimated ranges[21] of v^2d ($mm^3/\mu s^2$)
PBX9404 (1.84 g/cm^3)	Weingart, [026]	Flat nosed projectiles	2 - 12	4	3.9 - 4.5
	Moulard [027]	Small cylindrical projectiles	2 - 8		4 - 5.5
	LeRoy Green [028]	Long cylindrical tool projectile	2 - 12		4.5 - 8.5
	James [029]	Flat nosed projectiles	2 - 12		3 - 4.5
Comp. B (35/65) (1.73 g/cm^3)	Moulard [027]	Small cylindrical projectiles	6 - 12	16	13 - 19.5
Comp. B-3 (60/40) (1.70 g/cm^3)	LeRoy Green [028]	Flat nosed projectiles	4 - 12		14.5 - 16
TNT (cast) (1.59 g/cm^3)	Zoellner [030]	0.25 mm thick flyer	13 - 17		325 - 425
Octol7030 (1.81 g/cm^3)	Zoellner [030]	0.25 mm thick flyer	3 - 8		44 - 83
TATB (1.80 g/cm^3)	Weingart [026]	0.25 mm thick flyer	6 - 12	108	87 - 96

Table 4: v^2d values of some explosives found in the literature

[21] Reinterpretation of Held data.

V. TECHNICAL APPROACHES (SOLUTION ISSUES)

First of all, the ability of the software ANSYS AUTODYN®, which should provide impact initiation simulations by using the Lagrange solver and the Lee-Tarver model, to simulate impact initiation problems had to be checked and confirmed. Therefore, the Moulard experiment had first to be set up, and the results had to be compared with experimental results obtained by different scientists. These data used to compare with code computations are compiled in Appendix C, subchapter A.

Furthermore, the check of some parameters which could potentially affect the results of impact initiations problems had to be done. After that, and assuming the points mentioned above, the review of some results of Held concerning impact initiation had to be presented using AUTODYN®.

A cylindrical geometry was used. A complete description of this solver as well as this model together with further information about the ANSYS AUTODYN® software and its options are contained in Appendix B. These simulations are described below.

A. MOULARD EXPERIMENT FOR PBX 9404

This experiment has first to be performed because it provides means for assessing the predictive accuracy of the computational technique, by comparing the simulation results with some experimental results obtained in the past, under the same conditions, by Moulard.

Moulard, a French scientist, conducted some impact initiation experiments at the French-German research institute of Saint-Louis in France in 1981 [012, 027]. These experiments consisted in launching cylindrical steel projectiles against PBX 9404 cylinders. These launchings were performed at close distance to prevent the results from drag and flight stability problems. His aim was to find the "Go/No Go" threshold velocity, which is the minimum impact velocity required to initiate the explosive to high-order detonation as a function of the projectile diameter. His results have been well documented. As a consequence, they allow a good comparison with some simulation results, under naturally the same conditions, which could be obtained by using AUTODYN®.

In these simulations, a block of explosive (acceptor charge) PBX 9404, known as PBX9404JJ3 in the AUTODYN® library, has been impacted by a projectile made from Steel and known as STEEL1006 in the AUTODYN® library. The characteristics of these two materials are contained in Appendix A. In accordance with Moulard's setup, the block of PBX 9404 has a length of 50 mm and a width of 15 mm. The projectile has a length of 10 mm and variable diameters going from 2 mm to 10 mm. The velocity of the projectile is variable and was continually adjusted with a 100 m/s step in order to find the "Go/No Go" marginal velocity. Acceptor charge and projectile are separated by a 1.0 mm air gap in order to facilitate computations. This air gap has no physical consequence on the results obtained. The computational setup is illustrated in the figure below:

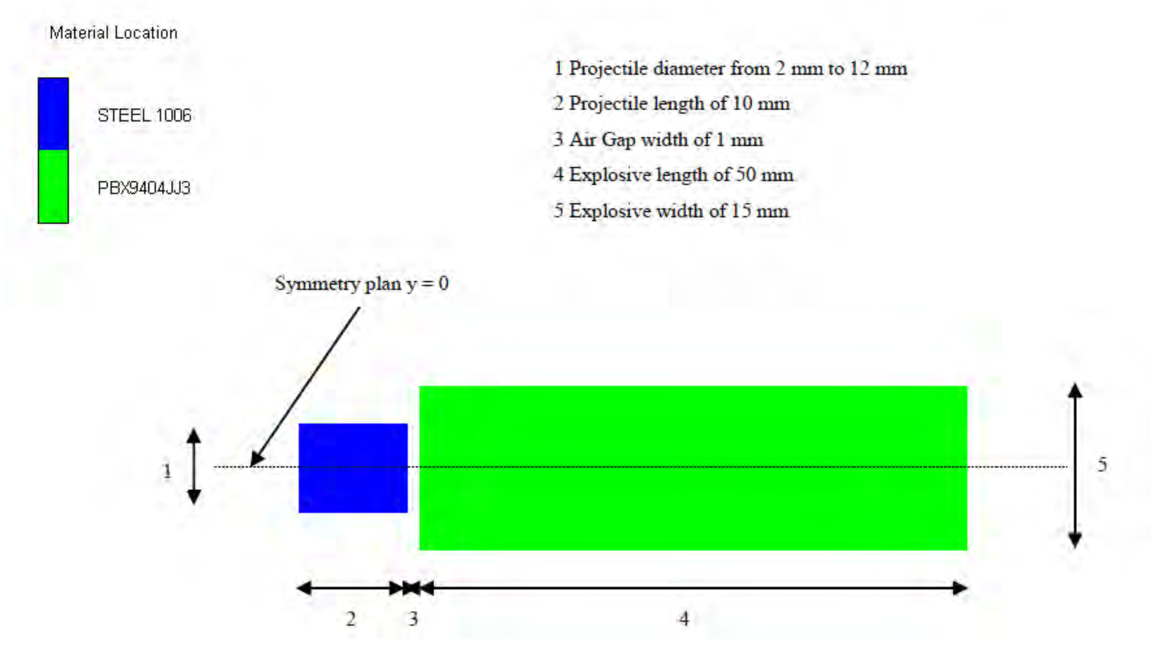

Figure 12: Disposal designed in AUTODYN® to simulate the Moulard experiment.

Three different series have been simulated. They differentiate themselves by the chosen zone size[22]. A coarse zoning has the advantage of giving short simulation times but sometimes inaccurate results while a fine zoning improves the results accuracy by longer simulation times. That's why three different zone sizes ("coarse", "fine" and "super fine") are chosen here. The first serial has a zoning of 1cell/mm, the second serial a zoning of 2 cells/mm and the third serial a zoning of 4 cells/mm.

Some fixed gauges[23] were placed on the acceptor charge in the axial- (x-direction) along the centerline, as well as in the radial-direction (y-direction). As mentioned in the Appendix B[24], it is not very meaningful to put more than one gauge per cell. This remark has been taken into consideration by placing them. For these simulations, assuming that the gauges are used for purposes of observing trends - for example, the growth to steady state detonation is used to confirm complete detonation state - , 1 gauge/mm has been put along the centerline from the impact surface to the bottom of the acceptor charge (total of 50 gauges) and 1 gauge/mm by the planes y = 1 mm, y = 2 mm, y = 3 mm, y = 4 mm, y = 5 mm and y = 7.5 mm from the impact surface to half of the acceptor charge. This disposal is exactly the same for the three series and is to see in figure 13:

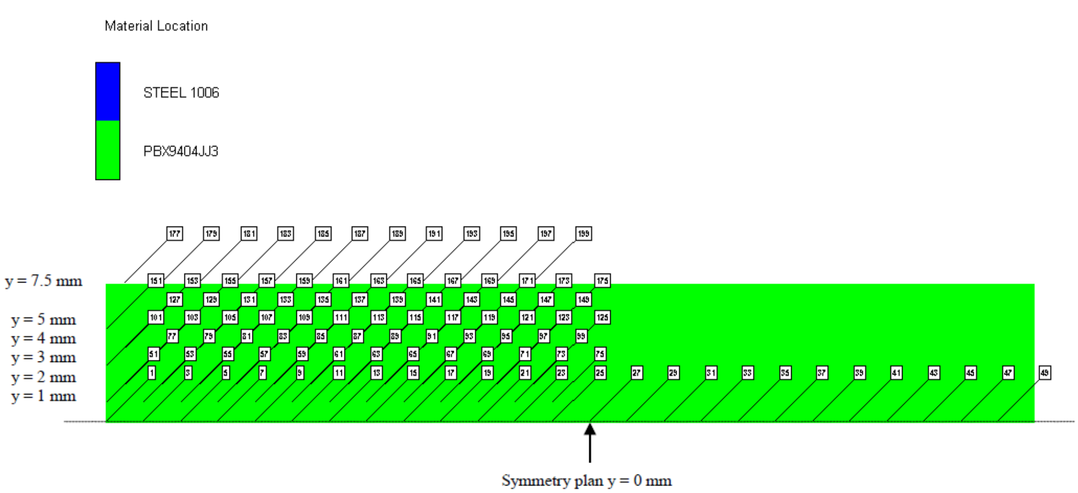

Figure 13: Gauges disposal (only odd numbers shown) on the acceptor charge PBX 9404 for the Moulard experiment.

22 See Appendix B, subchapter C, part 3.

23 See Appendix B, subchapter C, part 7.

24 See Appendix B, subchapter C, part 7.

The Lee-Tarver parameter F, which is denoted by ALPHA in AUTODYN®[25], is also used to estimate conditions resulting in first-order detonation. A Value of 1 means that the explosive detonated, values around 0 mean, on the contrary, that the explosive didn't detonate. This affirmation can be performed by observing the pressures in the axial- and radial-directions, which are stored by the gauges. An augmentation of the pressure along both directions, especially along the centerline, until a steady state value is reached means a "Go". A diminution of the pressures is au contraire a "No Go". By searching and finding this steady state value, the differences between the "Chapman Jouguet" pressure and the "Von Neumann" spike should be known: the detonation pressure is given by the "Chapman-Jouguet" pressure, which is quite smaller than the "Von Neumann" spike[26]. Examples of the interpretation of these two criterions are given in figures 14, 15, 17 and 18 and the differences the Chapman Jouguet pressure and the von Neumann spike are presented in figure 16:

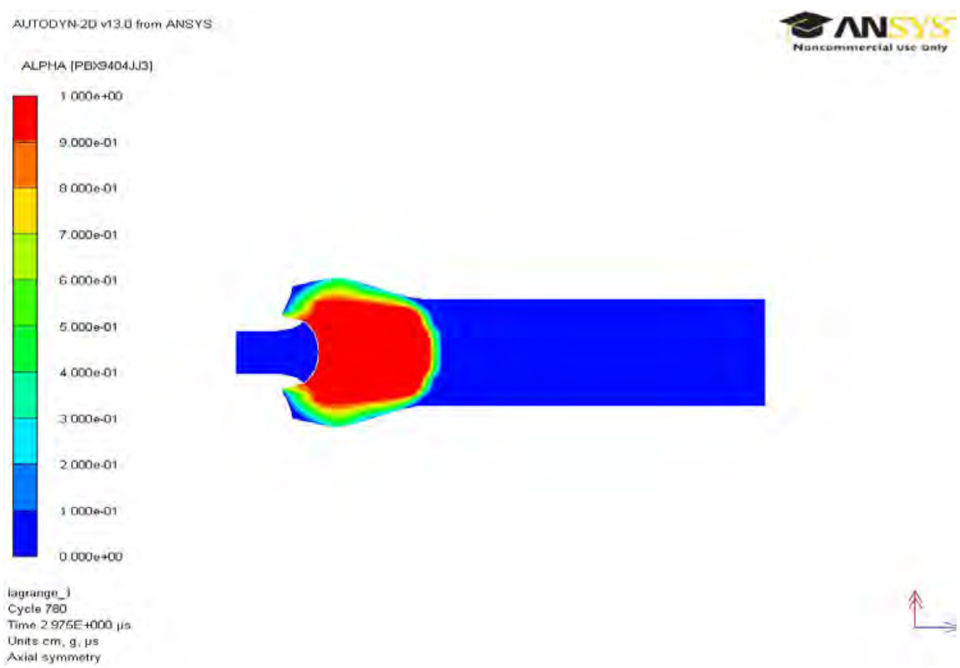

Figure 14: Use of the ALPHA variable to describe the detonation process. The detonation expands here from the left to the right and along the radial-direction. Simulation results obtained for a steel projectile with a diameter of 4 mm and a velocity of 1200 m/s impacting a bare block of explosive PBX 9404 at a zoning of 1 cell/mm.

[25] See Appendix B, subchapter C, part 10.

[26] See chapter III, subchapter C, part 2, section d).

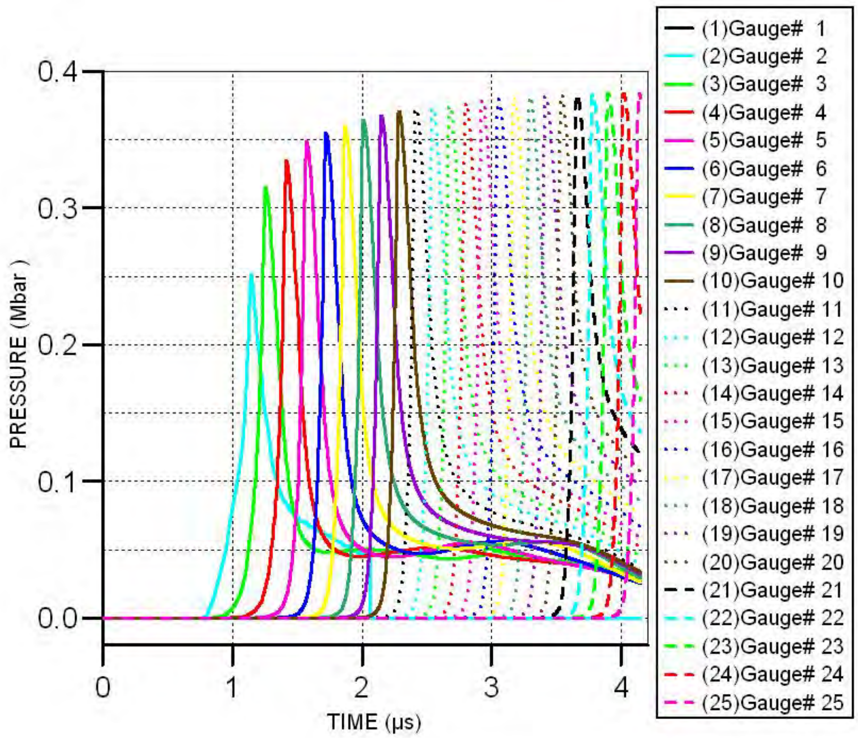

Figure 15: Example of a first-order detonation resulting from impact initiation. Increase of the pressure along the centerline as a function of the time. The reached steady state pressure after 4 µs is about 0.385 Mbar (Von Neumann Spike) and the detonation pressure is about 0.370 Mbar (Chapman Jouguet pressure). Simulation results obtained for a steel projectile with a diameter of 4 mm and a velocity of 1200 m/s impacting a bare block of explosive PBX 9404 at a zoning of 1 cell/mm. The gauge separation is 1 mm.

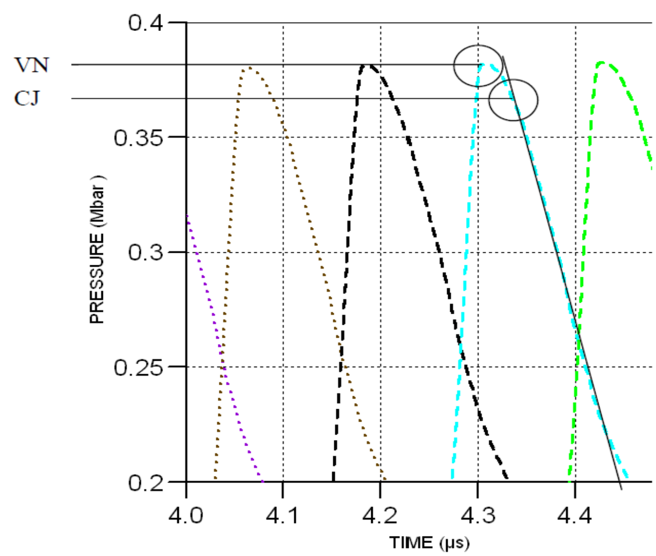

Figure 16: Zoom in figure 15 to show the CJ pressure (about 0.370 Mbar) and the VN spike (about 0.385 Mbar).

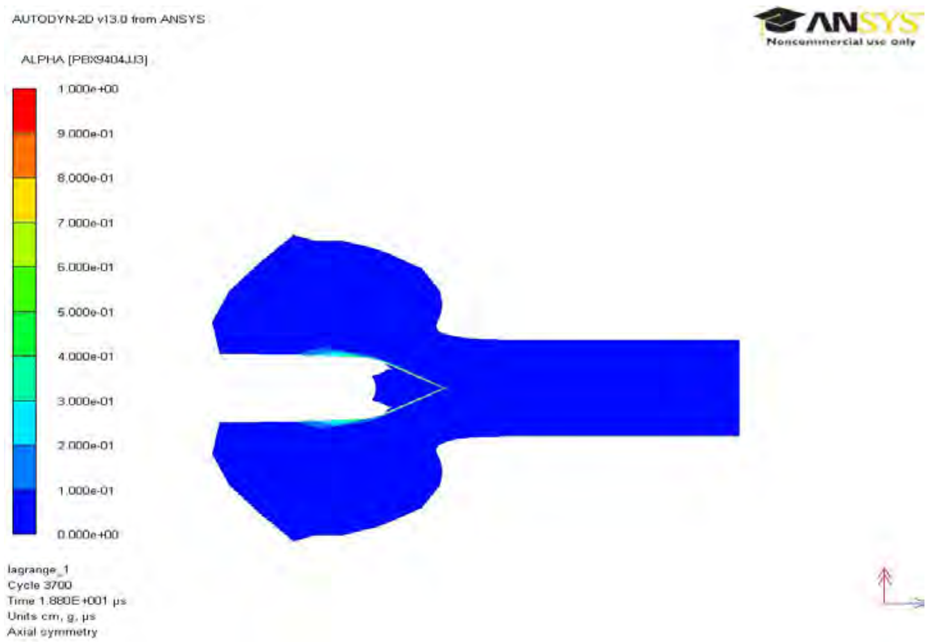

Figure 17: Use of the ALPHA variable to describe the detonation process. In this case, ALPHA is equal to 0. There is also no detonation. Simulation results obtained for a steel projectile with a diameter of 4 mm and a velocity of 1100 m/s impacting a bare block of explosive PBX 9404 at a zoning of 1 cell/mm.

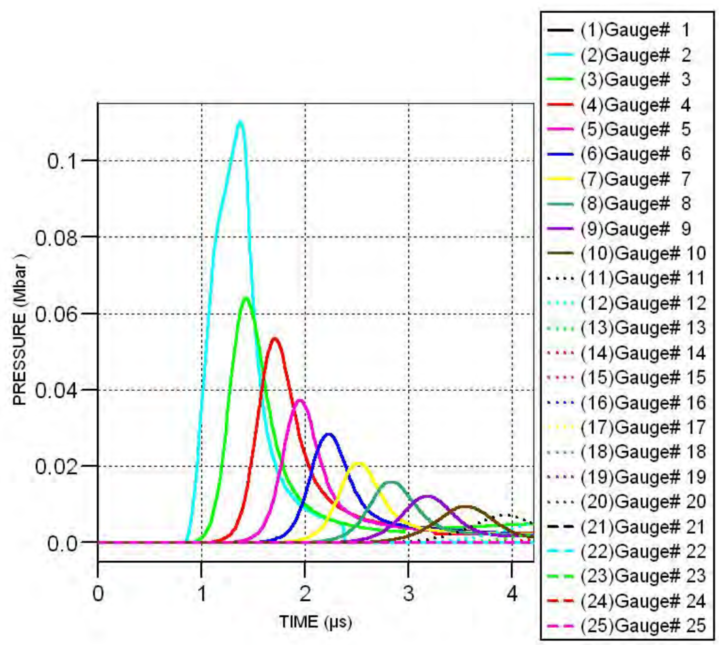

Figure 18: Example of non detonation. Diminution of the pressure along the centerline as a function of the time. In this case, the explosive is predicted not to detonate. The maximum pressure after 1.3 μs is about 0.115 Mbar (Von Neumann spike). Simulation results obtained for a steel projectile with a diameter of 4 mm and a velocity of 1100 m/s impacting a bare block of explosive PBX 9404 at a zoning of 1 cell/mm. The gauge separation is 1 mm.

B. EFFECT OF THE LENGTH ON IMPACT INITIATION

The effect of the length of the acceptor charge as well as the effect of the length of the projectile on the simulation results have also been tested. This check is important to see how the length of the acceptor charge and the length of the projectile can affect the initiation process of explosives and also affect the values of the initiation criterions.

Therefore, the Moulard experiment has been performed, first by changing the length of the acceptor charge and keeping the same length of the projectile (10 mm); and then by changing the length of the projectile and keeping the same length of the acceptor charge (50 mm). The tested lengths, so that the results have a significant meaning, have been chosen to cover a range going from 10% of the original value to 1000% of the original value. That means lengths of 5 mm, 10 mm, 50 mm, 100 mm and 500 mm for the acceptor charge and lengths of 1 mm, 5 mm, 10 mm, 20 mm and 100 mm for the projectile. If necessary, other lengths have been chosen to cover other sizes where some interesting effects could be expected. The gauges arrangement remains the same while changing the length of the projectile, but it has to be adjusted by increasing the length of the acceptor charge. This is due to the fact, that the total number of gauges cannot exceed 200. Assuming that the gauges still did not need to deliver very accurate information, the gauges have first been placed on the planar axes y = 1 mm, y = 2 mm, y = 3 mm, y = 4 mm, y = 5 mm and y = 7.5 mm and the remaining gauges have been placed along the centerline until at least one quarter of the explosive.

C. EFFECT OF THE ACCEPTOR CHARGE DIAMETER ON IMPACT INITIATION

One other effect on impact initiation could be due to width effects with regards to the acceptor charge. Checking this effect is also important to set up correctly the future simulations which will provide data concerning the v^2d and u^2d initiation criterions.

To check this effect, the Moulard experiment has been performed by changing the width of the acceptor charge. As already done with regards to the length effects on impact initiation, the widths have been chosen to cover a significant range, between about 20% and 1000% of the original value, which means values of 4 mm, 8 mm, 15 mm, 30 mm and 150 mm. The gauges disposal was adjusted along the y-axis to cover all the width of the acceptor charge.

D. EFFECT OF A BARRIER ON IMPACT INITIATION

The effect of a barrier in front of an acceptor charge has also to be checked to see whether a bare explosive can be considered like a covered explosive with regards to impact initiation or not, and how a barrier can potentially affect the impact initiation process. But before checking it, the ability of AUTODYN® to simulate impact initiation problems involving the presence of a barrier in front of the acceptor charge.

Therefore, a simulation with a 2 mm thick tantalum barrier has been performed and the simulation results have been compared with experimental results obtained in the literature [027, 029][27]. After that, the effect of the barrier thickness on impact initiation has been tested. For this purpose, a steel barrier with different thicknesses (2 mm, 2.5 mm and 5 mm) is built in front of the acceptor charge. The steel barrier is in each case directly in contact with the acceptor charge. The width of the steel barrier is the same as the width of the explosive, and the diameter of the projectile takes values between 2 mm and 10 mm with 2 mm steps. The fixed gauges are placed each 0.5 mm from the interface surface of the steel barrier till a quarter of the PBX 9404 acceptor charge along the centerline (y = 0 mm) as well as each 1 mm in the planes y = 1 mm, y = 2 mm, y = 3 mm, y = 4 mm, y = 6 mm and y = 7.5 mm. The zoning is still 2 cells/mm. Figure 19 shows the arrangement. The same experiment has then be done by using a 2 mm barrier made from aluminum and by using a 2 mm barrier made from tantalum to see the effect of the nature of the barrier.

[27] See Appendix C, subchapter A.

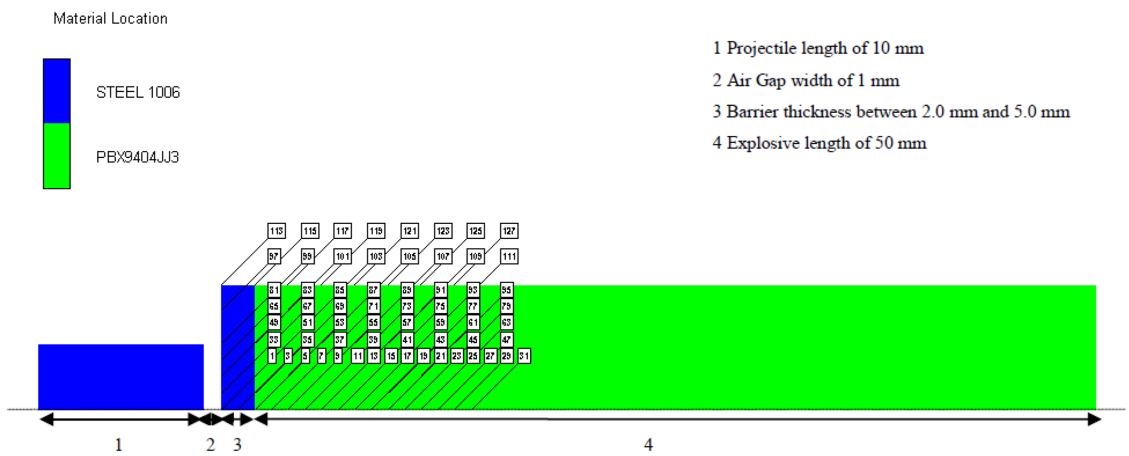

Figure 19: Arrangement used to show the effect of a barrier on impact initiation (only odd gauges are shown).

E. EFFECT OF A CONFINEMENT ON IMPACT INITIATION

As the effect of a barrier, the effect of the confinement of an acceptor charge with regards to impact initiation has been checked to see if confined explosive can be considered like a bare explosive with regards to impact initiation or not, and how a confinement can affect the initiation process.

Therefore, a first simulation has been set up by building a confinement all around a 15 mm wide and 50 mm long PBX 9404 acceptor charge. Confinement and acceptor are directly in contact. This confinement has a 2.5 mm thickness and is made, like the projectile is, of steel (STEEL 1006 in AUTODYN®). The projectile diameters were changed from 2 mm to 10 mm with 2 mm steps. The fixed gauges are placed each 0.5 mm from the interface surface of the steel barrier till a quarter of the PBX 9404 acceptor charge along the centerline (y = 0 mm) as well as each 1 mm in the planes y = 1 mm, y = 2 mm, y = 4 mm, y = 7.5 mm and in the steel plane y = 8.5 mm. The zoning is still 2 cells/mm. A second simulation, very similar to the first one, was also performed. That time, the same confinement as in the first simulation was set up, but the part of this confinement on the impact surface, which is actually a barrier, was removed. The impact surface of the acceptor charge is also bare. The gauges arrangement is the same as in the first simulation with the exception that it starts directly on the impact surface of the acceptor charge till a quarter of this charge in the same planes as before. These two arrangements are presented in figures 20 and 21:

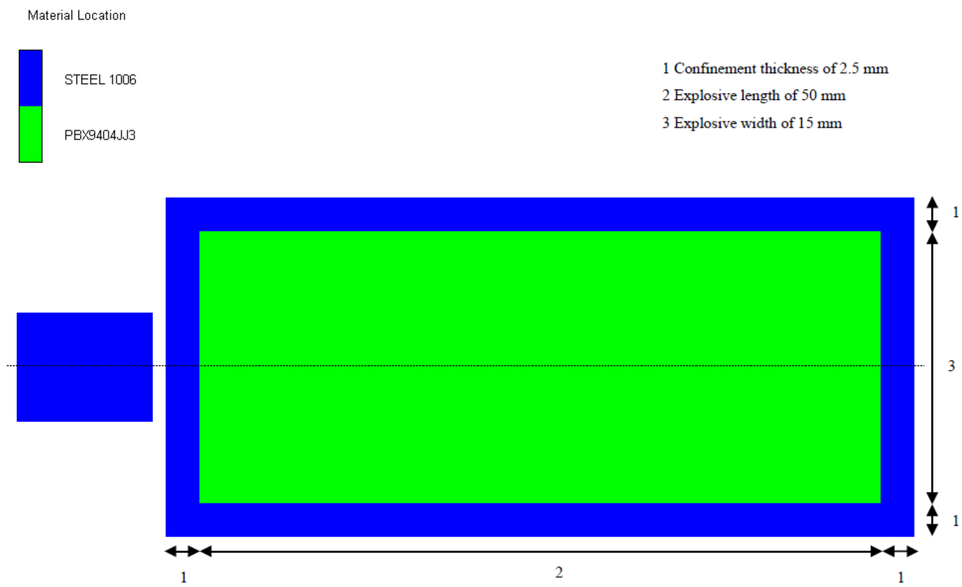

Figure 20: Arrangement used to show the influence of a total confinement on impact initiation.

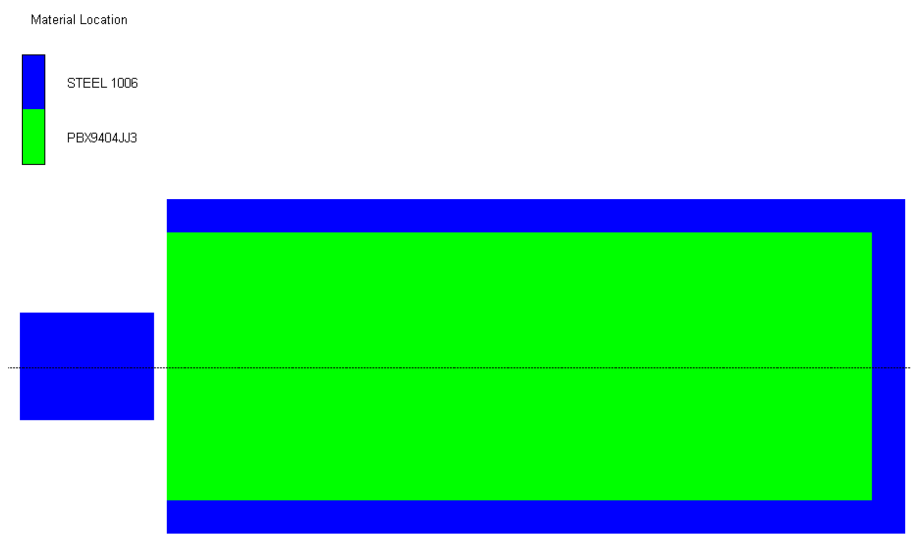

Figure 21: Arrangement used to show the influence of a confinement with a bare impact surface on impact initiation.

F. EFFECT OF AN AIR GAP BETWEEN BARRIER AND ACCEPTOR CHARGE ON IMPACT INITIATION

The effect of an air gap between a barrier and an acceptor charge has also been examined to check if the presence of an air gap makes the explosive easier to detonate than the absence of one, as Held related [006].

A similar arrangement as the one used in subchapter D has been utilized. The barrier, however, has no contact with the acceptor charge, but is separated from it by a 0.05 mm, 0.1 mm, 0.5 mm, 1 mm and at last 2 mm air gap. The thickness of the steel barrier is 2 mm. The fixed gauges are placed each 0.5 mm from the interface surface of the steel barrier till a quarter of the PBX 9404 acceptor charge along the centerline (y = 0 mm) as well as each 1 mm in the planes y = 1 mm, y = 2 mm, y = 3 mm, y = 4 mm, y = 6 mm and y = 7.5 mm. However, no gauges are placed in the air gap. The zoning is still 2 cells/mm. Figure 22 shows the arrangement:

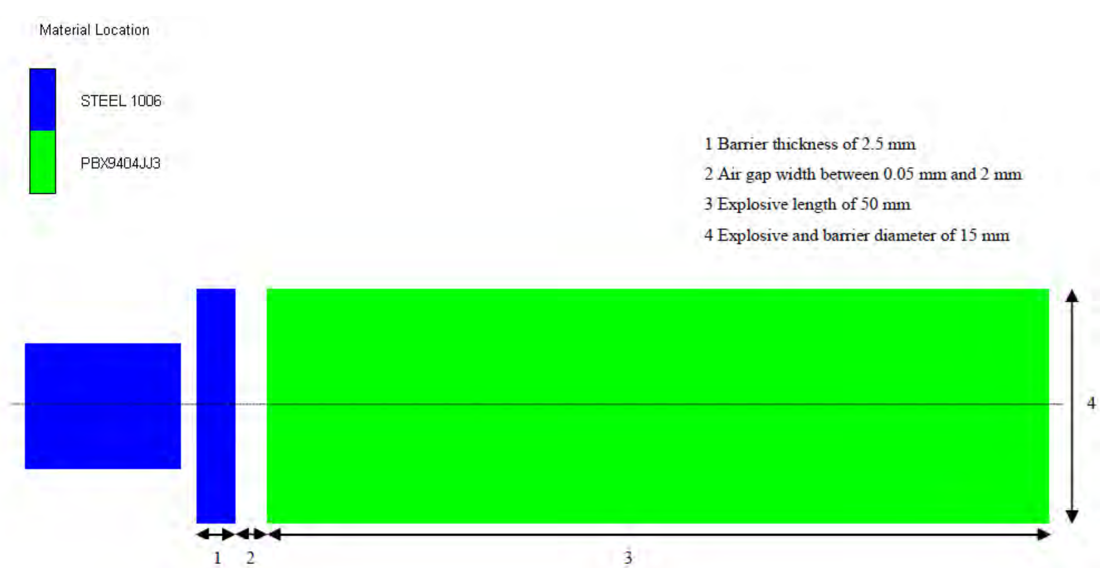

Figure 22: Arrangement used to show the influence of an air gap between a barrier and an acceptor charge.

G. STUDY OF OTHER EXPLOSIVES

The Moulard experiment, as already mentioned, has been performed for an acceptor charge made of PBX 9404 and a projectile made of steel. This experiment can be simulated for other explosives, with different sensitivities, in order to provide data results which will be used later to estimate the values of some initiation criterions, one of the most important points to be analyzed in this thesis. The results obtained in the preceding simulations of this work, i.e. influence of the lengths and of the widths of the explosive as well as the acceptor charge, have been taken into consideration for the computational setup.

In this way, similar experiments as the one performed by Moulard have been simulated by using acceptor charges[28] made of cast TNT, H6, Comp B. 65/35 and Octol 70/30. These explosives have been chosen because of their importance (nowadays or in the past) in the defense and civil industry, and because of their different sensitivities, which are covering a large range. The projectile is still made of steel. The materials properties are contained in Appendix B, part 1. The gauges disposal remains the same as in the Moulard experiment. In line with the observations done by former NPS students and with my personal experiences, the zoning has been chosen to 2 cells/mm.

H. EFFECT OF THE PROJECTILE MATERIAL ON IMPACT INITIATION

If the nature of the acceptor charge can be changed by performing the Moulard experiment, the nature of the projectile can be changed too, allowing further comparisons and providing more data to estimate the u^2d Held criterion, the Mader $\rho v^2 d$ criterion and the Chick $\sqrt{\rho}v^2d$, which depend on the densities of the projectile as well as on the densities of the explosive.

---

[28] Data for these explosives are in the AUTODYN® library. They are referred in the Appendix B, part 1.

Simulations have also been realized for projectile made of copper, aluminum and tungsten. These materials have been chosen because of their different densities, covering a range going from 2.70 g/cm^3 for aluminum to 18.10 g/cm^3 for tungsten[29]. The acceptor charge is still made of PBX 9404. The material properties are contained in Appendix B, part 2. The gauges arrangement remains the same as in the Moulard experiment and the zoning size is still 2 cells/mm.

I. V^{2}D AND U^{2}D HELD CRITERIONS

As already mentioned in Chapter II, the Held v^{2}d criterion ignores the effects of the Hugoniot characteristics of the projectile and explosive, which induces density and shock propagation. For the case of density alone, the Held u^{2}d seems useful. Estimating the values of these two criterions for different explosives and for different projectile materials should also give reliable information concerning the sensitivity of explosives. However, information got from the literature[30] have shown that these criterions may not be really constant but have a range of values. Furthermore, a comparison between the Held u^{2}d criterion, the Mader ρv^{2}d criterion and the Chick $\sqrt{\rho}$v^{2}d criterion done by Held to show what criterion gives values which are "the most stabile" for different projectile densities and diameters is not really consistent, because it involves only two particular examples [016]. These criterions have also to be estimated for different explosives and different projectile densities to check these statements.

The v^{2}d and u^{2}d Held criterions are defined as follow:

[29] The Hugoniot parameters of the tungsten-based alloy listed in AUTODYN® is not available in the literature. The theoretical results obtained in the thesis and concerning tungsten have also been calculated using a tungsten-based alloy with a density of 19.22 g/cm^3.

[30] See Chapter IV, subchapter C, part 4.

with Critical initiation velocity

... Critical initiation diameter

... Cratering velocity, with

and ρ_t ... Target (acceptor charge) density

ρ_p ... Projectile density

Other initiation criterions, which take as well the density of the target and the density of the projectile into consideration, have been formulated by Chick and Mader [016]. They are:

J. PRESSURE AT THE IMPACT SURFACE, RUN DISTANCES AND RAREFACTION EFFECTS

Pressure calculations at impact surfaces as well as run distance and rarefaction calculations are three very important tools which can be used to interpret different effects, like the effect of the length of the projectile on impact initiation[31], presented in this thesis. The pressure at the interfaces is also needed to estimate the values of a new criterion presented in later sections[32].

[31] See chapter VI and VII, subchapter B.

[32] See chapter VI, subchapter I.

1. Pressure at the impact surface

As already mentioned in chapter III, it is possible, using Hugoniot waves and Hugoniot parameters, to calculate the impact pressure P at different interfaces. Use of the equations presented in chapter III, subchapter D, part 1 for an interface steel/PBX 9404 and an interface steel/steel provides:

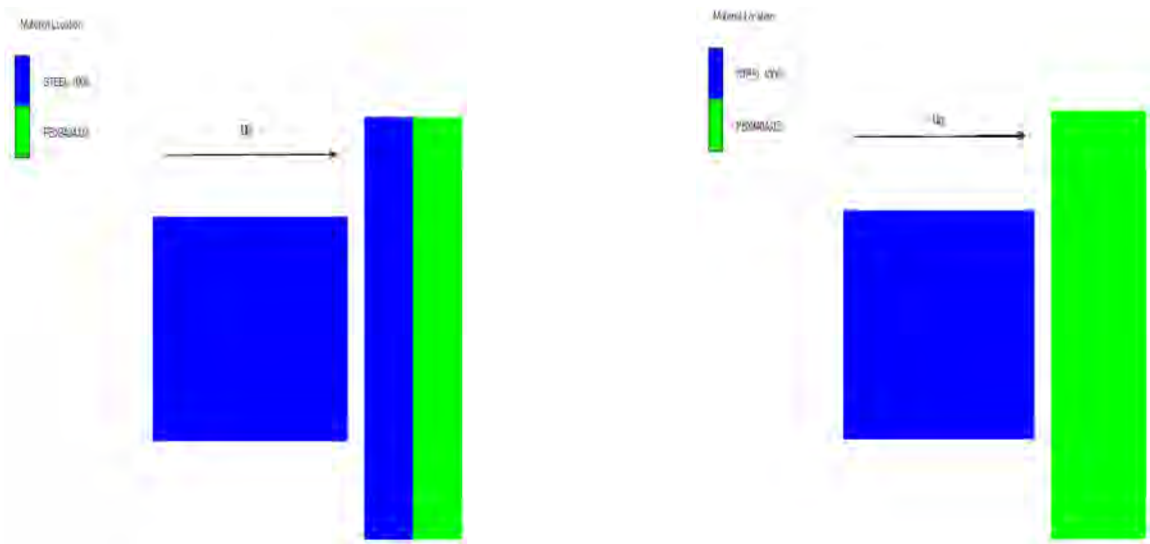

Figure 23: Interface steel/steel (left) and interface steel/PBX 9404 (right) just before the impact of a steel projectile with the velocity u_0.

$P_{Steel(projectile)} = P_{PBX9404}$ for the interface Steel/PBX 9404 and

$P_{Steel(projectile)} = P_{Steel(barrier)}$ for the interface Steel/Steel

with

$$P_{Steel(projectile)} = \rho_0 c_0(u_0-u) + \rho_0 s(u_0-u)$$

$$P_{Steel(barrier)} = \rho_0[c_0 u+su^2]$$

$$P_{PBX9404} = \rho_0[c_0 u+su^2]$$

with

P ... Pressure in Pa

ρ_0 ...Density in the unreacted explosive in $kg.m^{-3}$

c_0... Bulk sound speed in $m.s^{-1}$

s ... Constant dimensionless

u_0... Initial impact velocity in $m.s^{-1}$

u ... Particle velocity in $m.s^{-1}$

The Hugoniot values for Steel and PBX 9404, tabulated in table 51[33], are used below to estimate the particle velocity after the impact, which is later needed to estimate the impact pressure:

$$P = 7890[4569(u_0-u)+1.490(u_0-u)^2] = 1840[2310u+2.767u^2] \quad \text{(interface Steel/PBX 9404)}$$

$$P = 7890[4569(u_0-u)+1.490(u_0-u)^2] = 7890[4569u+1.490u^2] \quad \text{(interface Steel/Steel)}$$

The solution of these equations is:

for the interface Steel/PBX 9404, and

for the interface Steel/Steel.

The obtained particle velocity can after that be introduced in the Hugoniot wave equations to find the original impact pressure P at the interface. This calculation is valid for all explosives. The only differences are the constant obtained from the material properties[34]. This calculation should help us, on the one hand, to confirm the consistence of our simulation models and results with the theory by allowing impact pressures comparisons, and on the other hand, if necessary, to analyze some of the effects highlighted in this research project.

[33] See Appendix B, subchapter C.

[34] See Appendix B, subchapter C for the different Hugoniot values of the explosives and projectiles used in this thesis.

Comparisons with simulation data are possible, because these same impact pressures can as well be obtained by performing simulations in AUTODYN®. Therefore, the arrangement of subchapter A of this chapter, which has been arranged to replicate the Moulard experiment, has been used again. By deleting one of the fixed gauges present at the end of the centerline of the acceptor charge[35] and placing one moving gauge at the top of the projectile on the impact area, the impact pressure could be obtained on both sides of the interface.

2. Run distances

The calculations concerning run distances and presented in chapter III, subchapter C, part 2, section e) should help us, if necessary, to confirm the consistence of our simulation models and results with the theory by allowing run distances comparisons or it should support, like in chapter VII subchapter B, some assumptions formulated as a consequence of critical observations of the results obtained by the simulations.

Run distances can also be estimated without calculations. Indeed, if the knowledge of the initial impact pressure gives the possibility to calculate the run distance of an explosive, it is also possible to obtain this distance on a simple way, performing some simulations with AUTODYN®. Therefore, the arrangement of subchapter A of this chapter has been used again. The projectile diameter, however, has been fixed to three different values (3 mm, 6 mm and 10 mm) and the projectile has been assigned for each fixed diameter different velocities bigger than the threshold ones. Only three diameters, more or less equally partitioned in the study area, have been tested, because the results, according to the equation above, should be the same. For the purpose of this study, all the gauges that are not placed along the centerline were deleted. The zoning is now 4 cells/mm. That allows the possibility to place 1 gauge each 0.25 mm along the centerline to improve the

[35] Gauges at the end of the acceptor charge are not really needed for this simulation, and because of the limitation of 200 gauges, one gauge has to be removed before adding another one.

accuracy of the results[36]. By observing the emergence of a steady state value, the CJ pressure, by plotting the pressures as a function of the time for the different gauges along the centerline, it is possible to find the gauge by which this steady state value is reached. As a consequence, the knowledge of the position of this gauge[37] allows to find the run distance of the explosive under the impact initiation conditions which have been used.

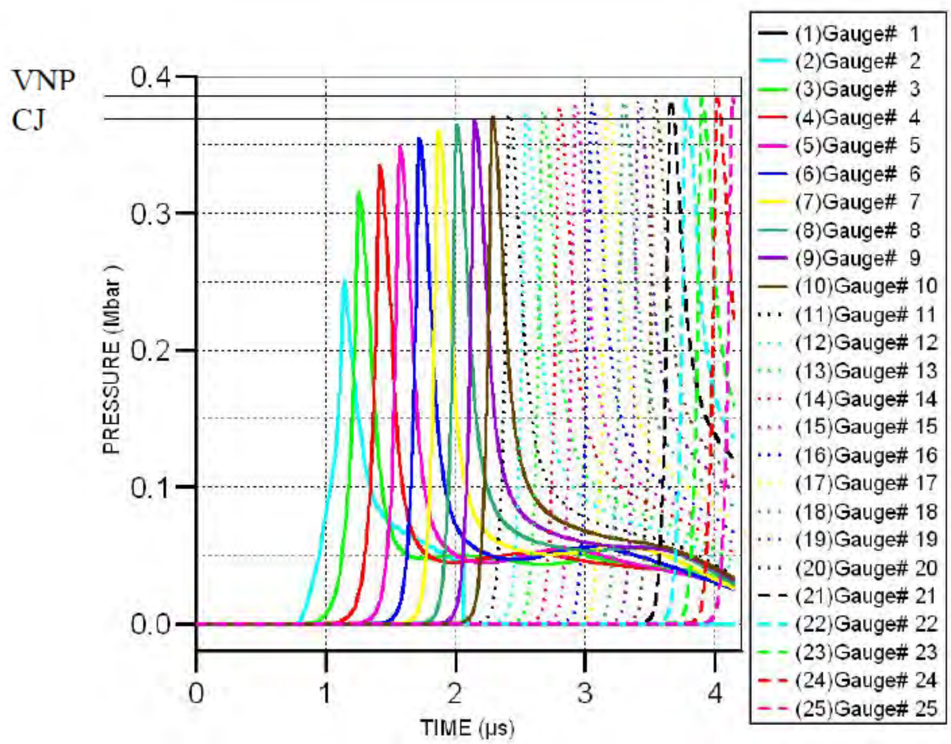

Figure 24: Estimation of the run distance by pressure analysis. The CJ pressure of 3.70 Mbar is first reached by the 19th gauge. By one gauge/mm, this means a run distance of 19 mm. Simulation results obtained for a steel projectile with a diameter of 4 mm and a velocity of 1200 m/s impacting a bare block of explosive PBX 9404 at a zoning of 1 cell/mm.

3. Rarefaction effects

---

[36] Gauges have in that case to be very accurate, because they do not give qualitative information but quantitative ones.

[37] There are 4 gauges/mm starting from the impact surface at the top of the acceptor charge and ending at the bottom of it.

Using the Hugoniot parameters for PBX 9404 and steel, the theoretical values of the distance x' over which the shock maintains constant peak pressure can be calculated for the explosive PBX 9404 and compared to the run distances for this same explosive. This comparison should show if rarefaction effects could have affect the results obtained in this thesis or not.

THIS PAGE INTENTIONALLY LEFT BLANK

VI. RESULTS

A. MOULARD EXPERIMENT FOR PBX 9404

The results obtained by simulating the Moulard experiment with AUTODYN®, described in the precedent chapter[38], are presented in this subchapter. They are graphically compared with the experimental values of Moulard.

1. Simulation with 1 cell/mm

The different Go/No Go threshold velocities have been noted down and plotted in figure 25 as a function of the projectile diameter. The values Moulard obtained in 1981 have also been plotted in the same figure. The values are available in Appendix C.

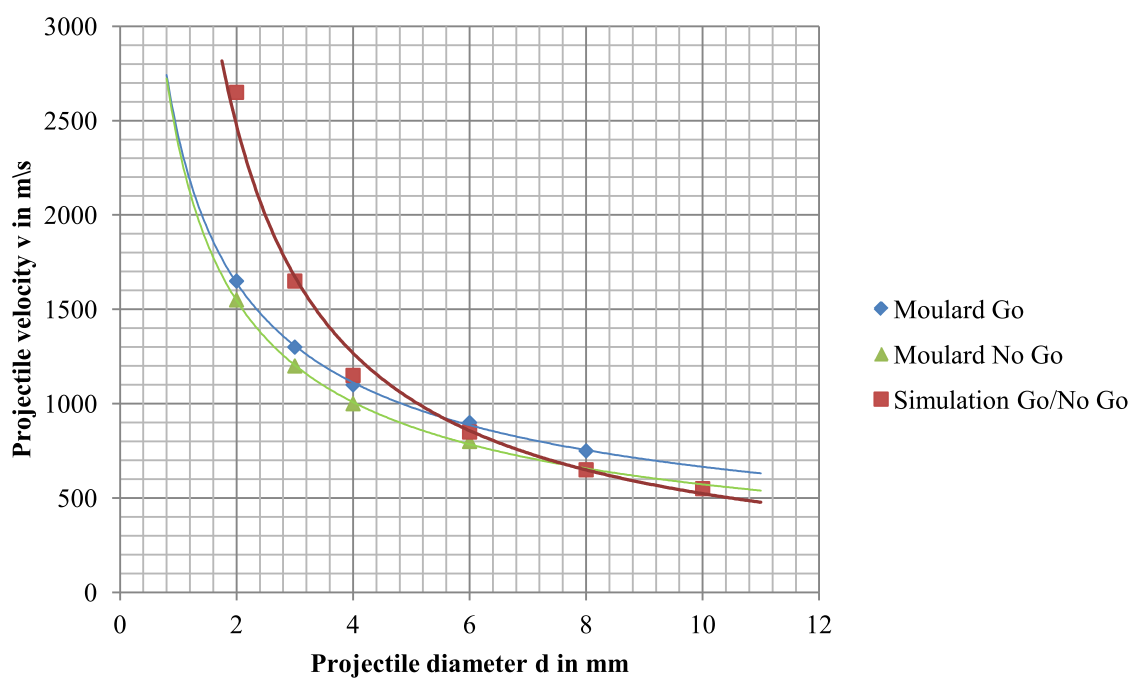

Figure 25: "Go/No Go" velocities as a function of the projectile diameter. Simulation results obtained for a steel projectile impacting a bare block of explosive PBX 9404 at a zoning of 1 cell/mm. Moulard experimental results obtained in the literature and tabulated in the Appendix B, part 1 [012].

[38] See chapter V, subchapter A.

The Von Neumann spike[39] is approximated to 0.385 Mbar, while the steady state Chapman Jouguet pressure is at 0.370 Mbar, which is consistent with the theory. The problem set up seems also, at first appearance, to be consistent.

A trend line has been plotted to give the tendency of the results for the study area. Therefore, the "power" model of the software Excel, which uses $x^{constant}$ functions, seemed to be best appropriated. All results obtained from the simulation, with exception of the results obtained for the 6 mm and 8 mm diameters, are not contained between the Go and No Go values of Moulard. The equations of the plots are:

$v = 2419*d^{-0.56}$ (Moulard experiment, Go)

$v = 2373*d^{-0.62}$ (Moulard experiment, No Go)

$v = 4833*d^{-0.97}$ (Simulation with 1 cell/mm)

The simulation results, as well as the Moulard experiment results, show that the requested projectile velocity to reach the detonation of the considered explosive decreases with the projectile diameter. The equations above give information about how fast it decreases and when a limit is reached. These equations have been discussed in the next chapter[40]. The trend, that a limit could be reached, can indeed already be seen in figure 24 for diameters larger than 10 mm.

2. Simulation with 2 cells/mm

As for the simulation with 1 cell/mm, the threshold Go/No Go velocities have been noted down and plotted in figure 26 with the results of the Moulard experiment. This values are available in the Appendix C. At 2 cells/mm, the resolution prediction should be closer to the experiment than with 1 cell/mm.

[39] See chapter III, subchapter B, part 2, section d).

[40] See chapter VII, subchapter A.

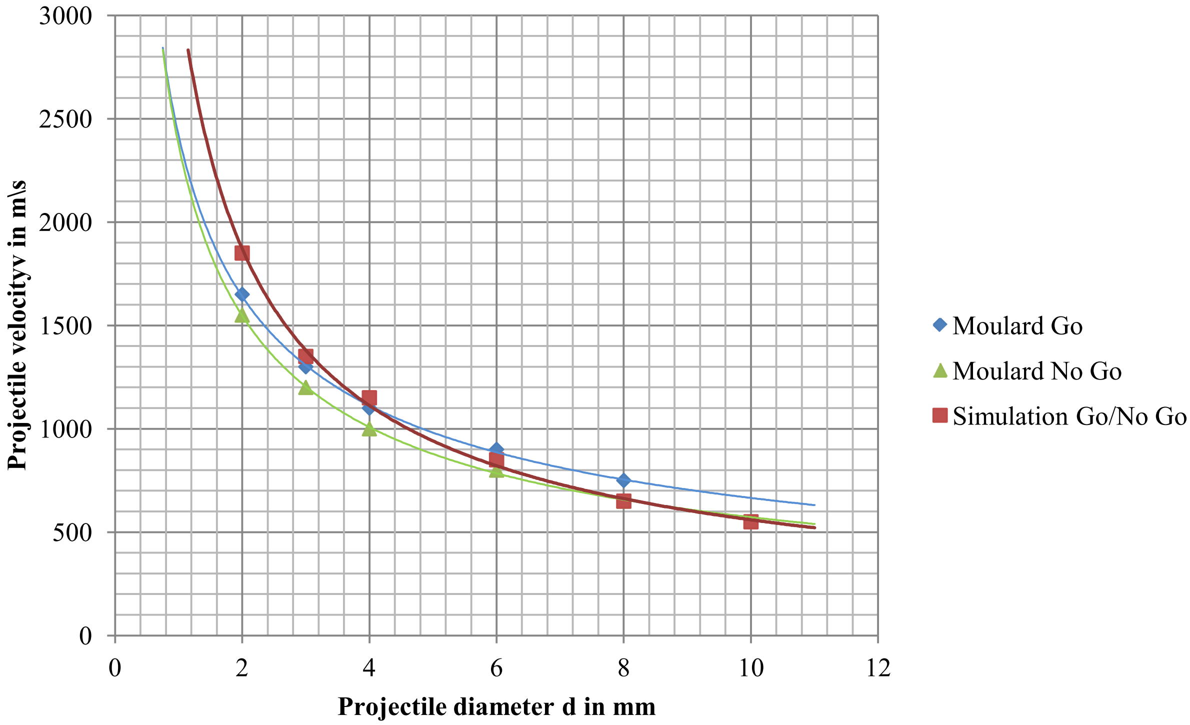

Figure 26: "Go/No Go" velocities as a function of the projectile diameter. Simulation results obtained for a steel projectile impacting a bare block of explosive PBX 9404 at a zoning of 2 cells/mm. Moulard experimental results obtained in the literature and tabulated in the Appendix B, part 1 [012].

That time, the Von Neumann Spikes are approximated to 0.425 Mbar. The Chapman Jouguet peaks, however, has the same steady state value of about 0.370 Mbar. With exception of the 2 mm and 3 mm diameters, all diameters are comprised between the Go and No Go values of Moulard, giving a quite more accurate model. The equation of the new plot is:

$$v = 3145 * d^{-0.75} \qquad \text{(Simulation with 2 cells/mm)}$$

3. Simulation with 4 cells/mm

At 4 cells/mm, the resolution prediction should be still more closer than with 2 cells/mm. Values are available in the Appendix C.

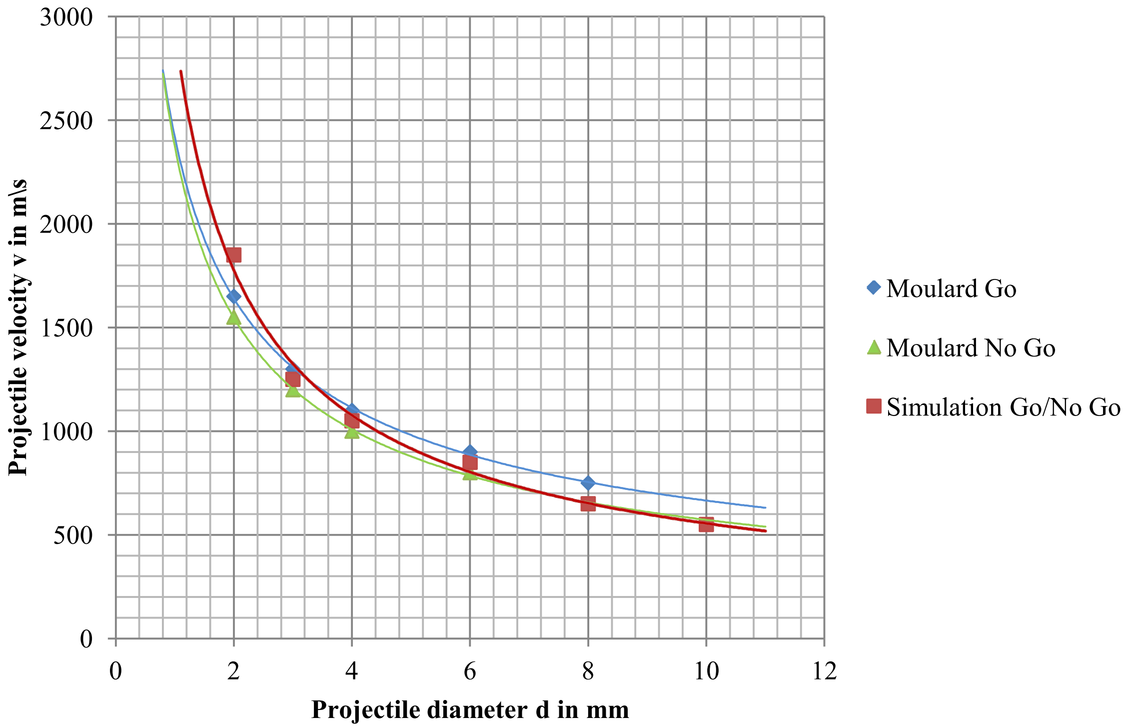

Figure 27: "Go/No Go" velocities as a function of the projectile diameter. Simulation results obtained for a steel projectile impacting a bare block of explosive PBX 9404 by a zoning of 4 cells/mm. Moulard experimental results obtained in the literature and tabulated in the Appendix B, part 1 [012].

That time, the Von Neumann Spikes took values of about 0.470 Mbar. The Chapman Jouguet peaks, however, has still the steady state value of about 0.370 Mbar. Only the 2 mm diameter is not comprised between the Go and No Go values of Moulard, giving an even better model as the one obtained for the simulation with a zoning of 2 cells/mm. The equation of the new plot is:

$$v = 2931 * d^{-0.72} \qquad \text{(Simulation with 4 cells/mm)}$$

B. EFFECT OF THE LENGTH ON IMPACT INITIATION

The simulations results issued from the arrangement described in the precedent chapter are presented below. They should help to show the potential effects of the length of the projectile and the length of the acceptor charge on impact initiation.

1. Effect of the length of the acceptor charge on impact initiation

The Go/No Go threshold velocities of a block of PBX 9404 with different lengths impacting by a steel projectile have been noted down in a table in the Appendix C and have all been plotted as a function of the projectile diameter in figure 28:

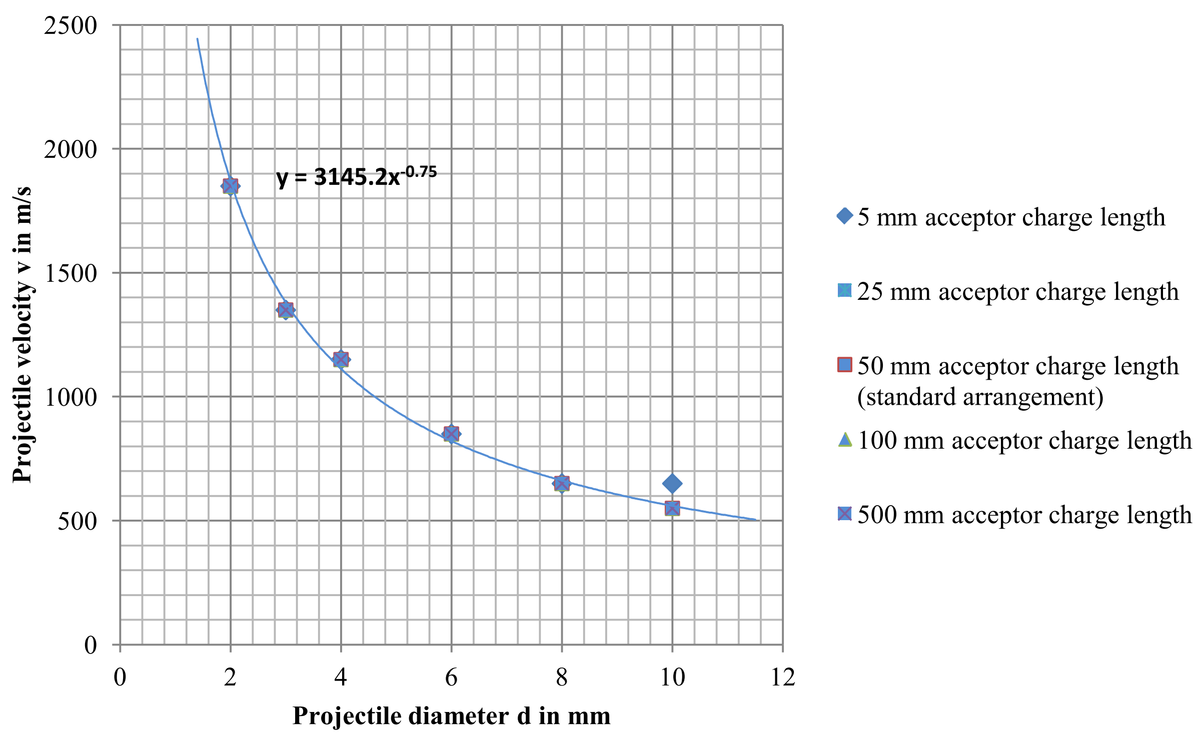

Figure 28: "Go/No Go" velocities as a function of the projectile diameter for different acceptor charge lengths. Simulation results obtained for a steel projectile impacting a bare block of explosive PBX 9404 at a zoning of 2 cells/mm.

It is important to notify, that the velocity needed to make the 5 mm long acceptor charge detonating by using a 10 mm projectile diameter is higher than for all other acceptor charge lengths impacting by the same projectile diameter (650 m/s vs. 550m/s). More about this will be discussed in chapter VII, subchapter D, part 1.

2. Effect of the length of the projectile on impact initiation

This time, these are the Go/No Go threshold velocities of a block of PBX 9404 with a constant length impacting by a steel projectile with different lengths which have been noted down in a table in the Appendix C and have all been plotted as a function of the projectile diameter in figure 29:

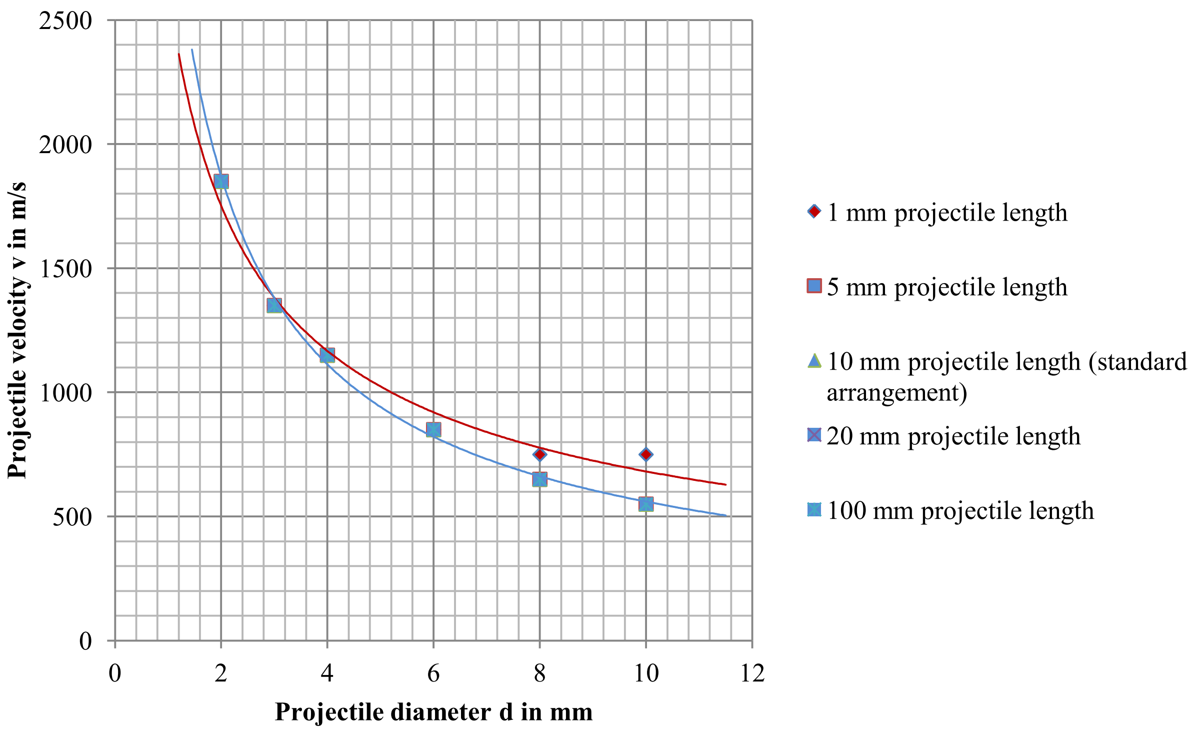

Figure 29: "Go/No Go" velocities as a function of the projectile diameter for different projectile lengths. Simulation results obtained for a steel projectile impacting a bare block of explosive PBX 9404 at a zoning of 2 cells/mm.

By the use of the "power" trend line, all the plots have the same trend, except the one for a 1 mm projectile length, the smallest length value of the serial. These trend differences occurred between the 5 mm projectile length and the 5 mm projectile length. That is why some more simulations for a 2 mm and 3 mm projectile length have been performed. They are plotted in figure 30 and the values are tabled in Appendix C.

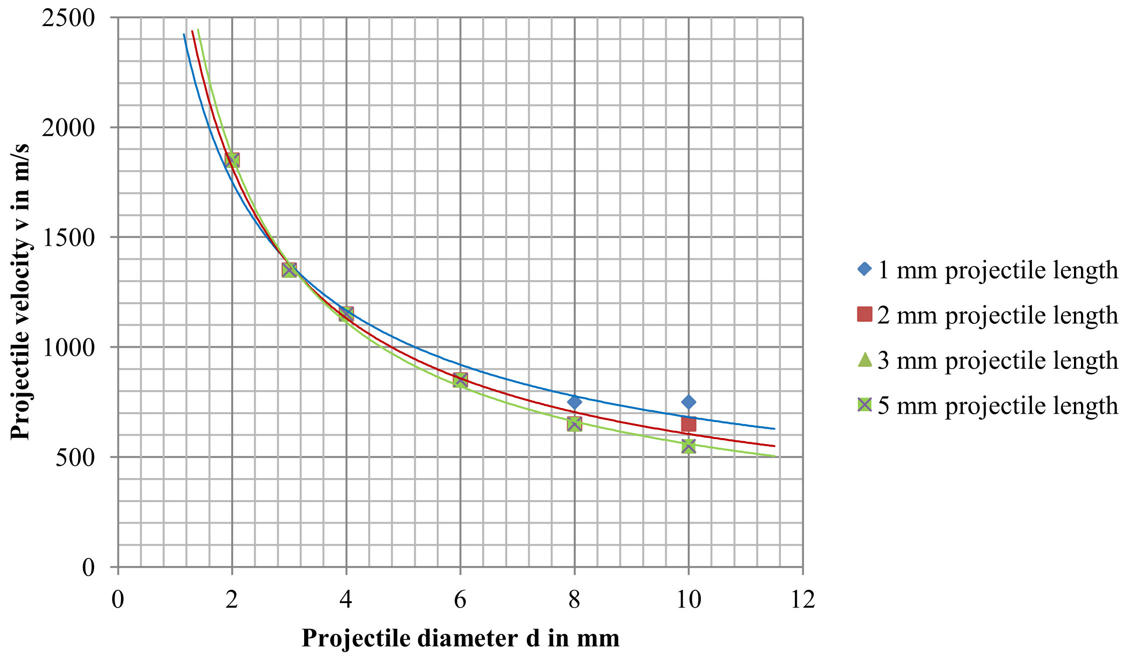

Figure 30: "Go/No Go" velocities as a function of the projectile diameter for small projectile lengths. Simulation results obtained for a steel projectile impacting a bare block of explosive PBX 9404 at a zoning of 2 cells/mm.

The 3 mm and the 5 mm projectile length plots have the same trend. The 1 mm and the 2 mm projectile length plots are different from each other and are both different from the 3 mm and 5 mm ones. The equations of all plots are contained in table 6:

Projectile length in mm	Equation of the plot
1	$v = 2630*d^{-0.59}$
2	$v = 2616*d^{-0.68}$
3	$v = 3145*d^{-0.75}$
5	$v = 3145*d^{-0.75}$
10	$v = 3145*d^{-0.75}$
20	$v = 3145*d^{-0.75}$
100	$v = 3145*d^{-0.75}$

Table 5: Equations of the plots of figure 29.

C. EFFECT OF THE ACCEPTOR CHARGE DIAMETER ON IMPACT INITIATION

The simulation results of the arrangement used to show the effect of the acceptor charge diameter on impact initiation and presented in the precedent chapter[41] are listed below.

The Go/No Go threshold velocities obtained for the impact of a block of PBX 9404 with different steel projectile diameters have been noted down in Appendix C and plotted as a function of the projectile diameter in figure 31:

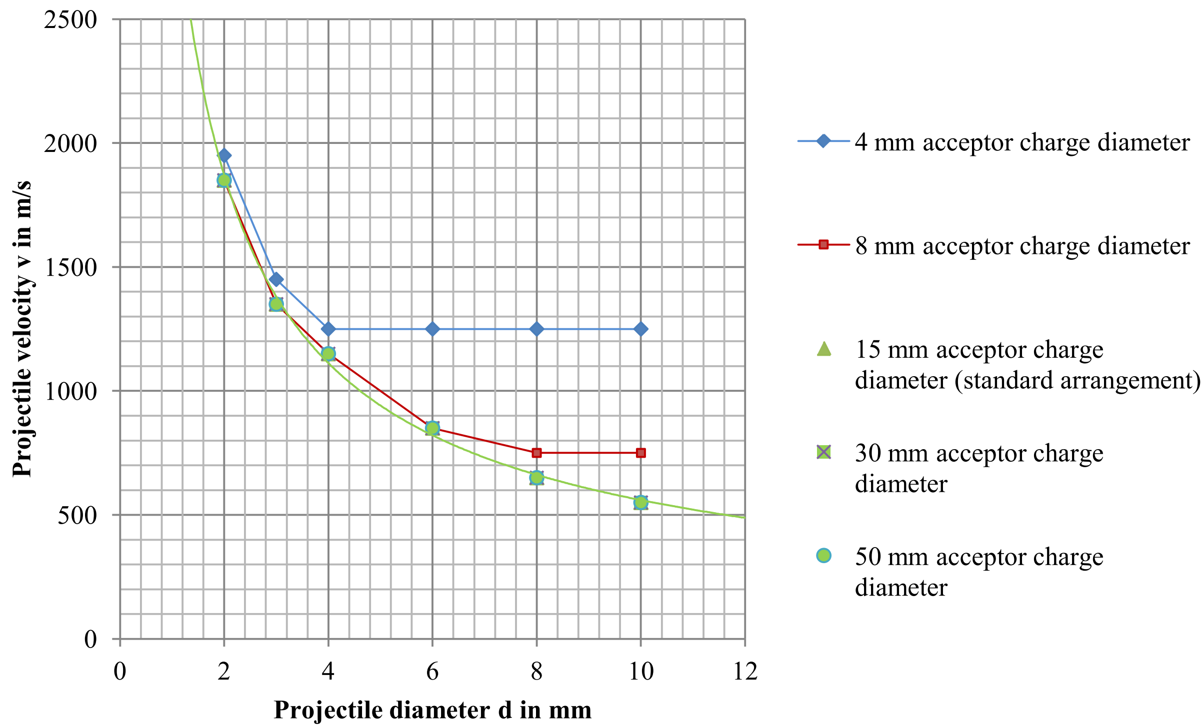

Figure 31: "Go/No Go" velocities as a function of the projectile diameter for different acceptor charge diameters. Simulation results obtained for a steel projectile impacting a bare block of explosive PBX 9404 at a zoning of 2 cells/mm.

The use of the "power" trend line was this time meaningful for the 15 mm, 30 mm and 50 mm acceptor charge diameters, but not for the 4 mm and 8 mm acceptor charge diameters, mainly because of the steady state value reached for the larger diameter. For

41

these two plots, no mathematics model has been used. The 15 mm, 30 mm and 50 mm acceptor charge diameter plots are identical. The 8 mm acceptor charge diameter plot is identical to the 15 mm, 30 mm and 50 mm acceptor charge diameter plots for projectile diameters smaller than 8 mm. For projectile diameters larger than 8 mm, a constant velocity of 750 m/s is reached. The 4 mm acceptor charge diameter plot is different from all other plots. The Go/No Go values for the three smallest projectile diameters are 100 m/s higher than the values of the other plots, and a constant velocity of 1250 m/s is reached for projectile diameters equal or larger than 4 mm. This will be discussed later[42].

D. EFFECT OF A BARRIER ON IMPACT INITIATION

The simulations results of the arrangements used to show the effect of a barrier on impact initiation and presented in the precedent chapter[43] are listed below.

1. Ability of AUTODYN® to simulate impact initiation problems involving covered explosives

The results of a similar simulation concerning the simulation of a steel projectile impact against a block of PBX 9404 protected by a 2 mm tantalum barrier and described in chapter V, subchapter D are tabulated in Appendix C and plotted in figure 32. These results are compared to the experimental results from Moulard [027] and James, Haskins and Cook [029], which have been obtained under similar conditions.

---

[42] See chapter VII, subchapter C.

[43] See chapter V, subchapter D.

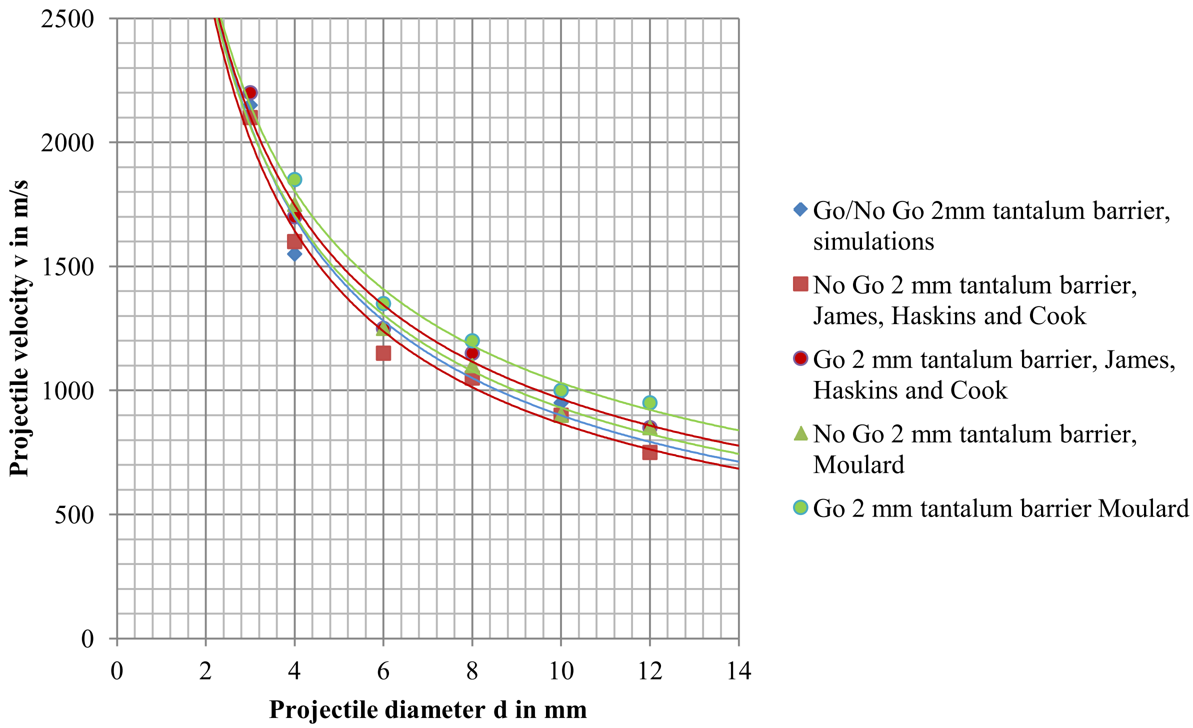

Figure 32: "Go/No Go" velocities as a function of the projectile diameter for a 2mm tantalum barrier. Simulation results obtained for a steel projectile impacting a covered (2 mm tantalum barrier) but unconfined block of explosive PBX 9404 at a zoning of 2 cells/mm. James, Haskins and Cook experimental results as well as Moulard experimental results obtained in the literature [027, 029] and tabulated in the Appendix C, subchapter A.

The "simulations" plot is comprised between the two "James, Haskins and Cook" experimental plots. The Moulard experimental values, however, are quite different, but still have the same trend. As it was already the case before, it was impossible to obtain consistent simulation results for the 2 mm projectile diameter concerning the 2 mm tantalum barrier, because of simulation errors in AUTODYN®. Results for the 2 mm projectile diameter haven't been noted down by Moulard. The differences between these plots will be discussed in later[44].

[44] See chapter VII, subchapter D, part 2.

2. Effect of the thickness of a barrier on impact initiation

The results concerning the Go/No Go threshold velocities of a block of PBX 9404 with different steel barrier thicknesses impacting by a steel projectile have been put together in figure 33. The corresponding values are tabled in Appendix C. The results for a bare block of PBX 9404 have been put in the same figure.

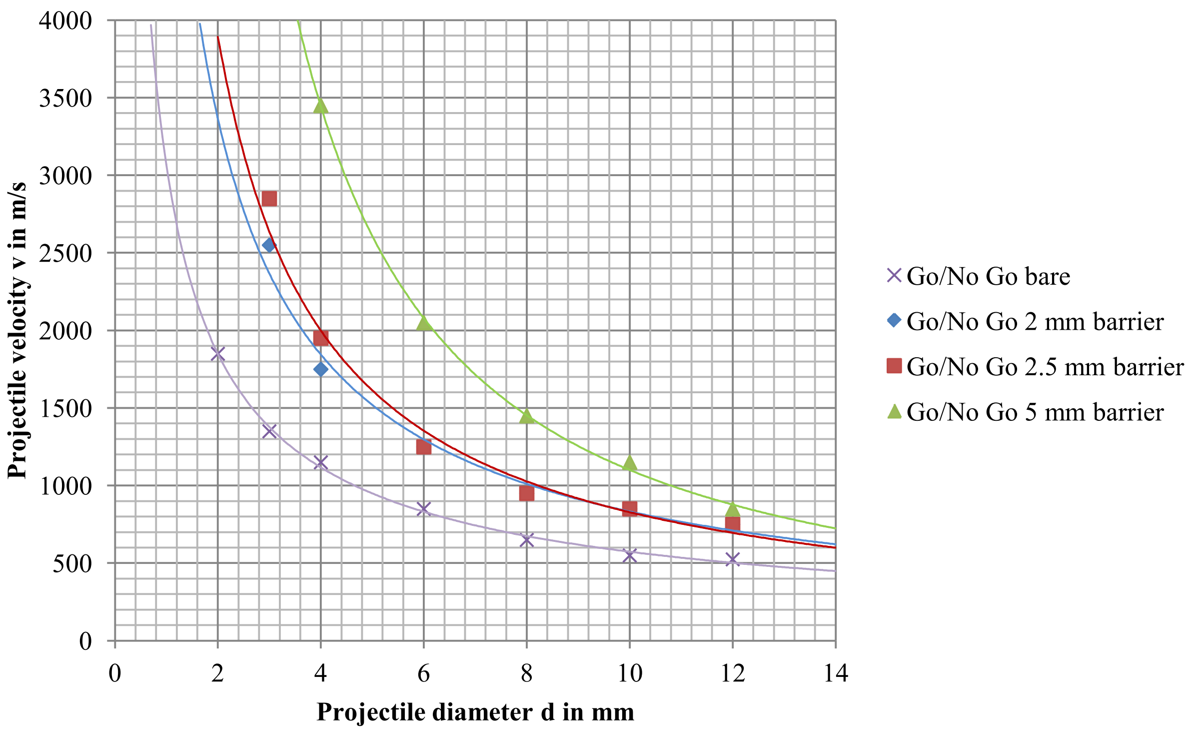

Figure 33: "Go/No Go" velocities as a function of the projectile diameter for different steel barrier thicknesses. Simulation results obtained for a steel projectile impacting a covered (steel barrier) but unconfined block of explosive PBX 9404 at a zoning of 2 cells/mm.

All plots, by using the "power" function, have different trends. It is impossible to obtain consistent simulation results for the 2 mm projectile diameter concerning the 2 mm, 2.5 mm and 5 mm barriers, and for the 3 mm projectile diameter concerning the 5 mm barrier. Indeed, AUTODYN® provided error messages. These diameters are obviously too small to allow reliable calculations with the AUTODYN® codes. This is due to this "critical diameter" phenomenon, mentioned among others by Zoellner [030].

The pressures along the centerline within the 5 mm steel barrier and just after the interface Steel/PBX 9404 within the explosive have been noted down in the Appendix C and plotted as a function of the distance from the impact side of the steel barrier in figure 34. The values come from a simulation provided for a projectile made of steel with a diameter of 10 mm and a velocity of 700 m/s impacting a covered (5 mm barrier) but unconfined block of explosive PBX 9404.

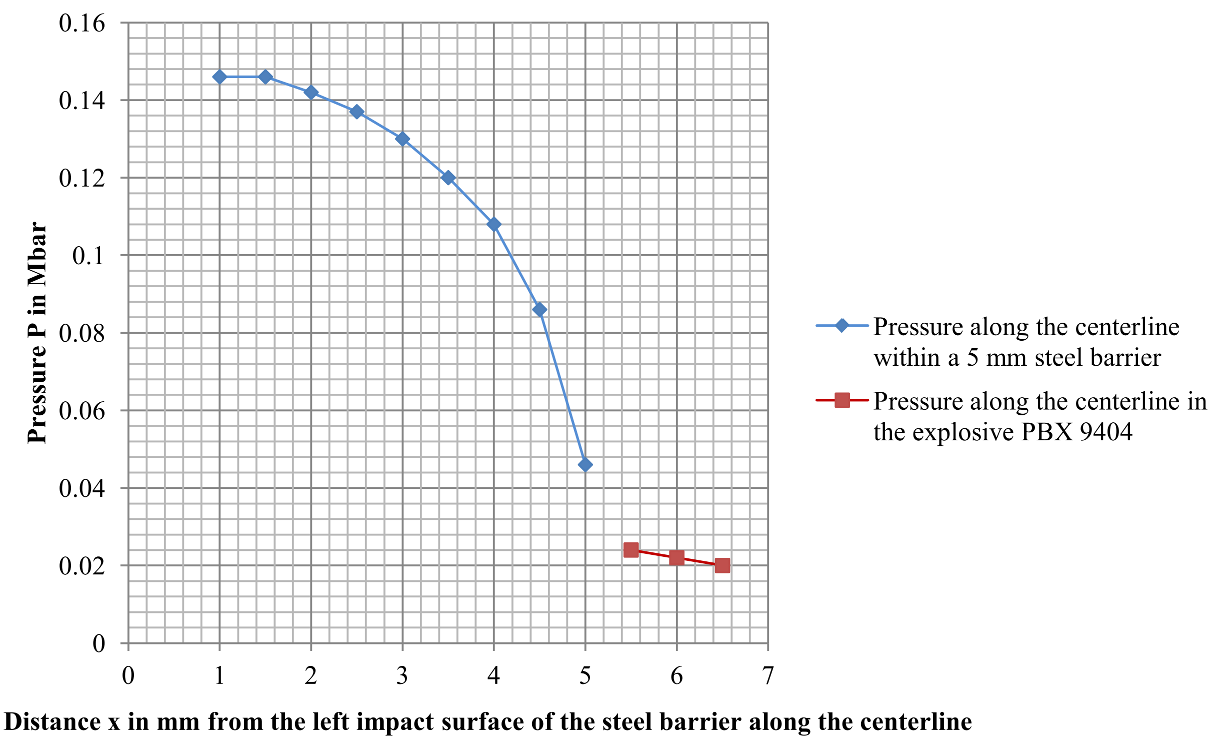

Figure 34: Pressure P along the centerline within a 5 mm steel barrier and in the block of explosive PBX 9404 as a function of the distance from the impact surface of the steel barrier along the centerline. Simulation results obtained for a 10 mm steel projectile diameter impacting a covered (5 mm steel barrier) but unconfined block of explosive PBX 9404 at 700 m/s at a zoning of 2 cells/mm.

The pressure decreases progressively with the distance from the impact surface of the steel barrier. The break which occurs between 5.0 and 5.5 mm is due to the interface Steel/PBX 9404[45]. The pressure decreases strongly at the interface and decreases after that linearly with the distance along the centerline.

[45] The cell by 5.0 mm is still in the steel, the cell by 5.5 mm is however in the explosive PBX 9404.

This plot helps us to justify why it is more difficult to initiate a covered explosive than a bare explosive. This will be shown in the next chapter[46].

3. Effect of the nature of a barrier on impact initiation

The results obtained for the same simulations with a 2 mm steel barrier, a 2 mm tantalum barrier and a 2 mm aluminum barrier are presented the Appendix C and plotted in figure 35.

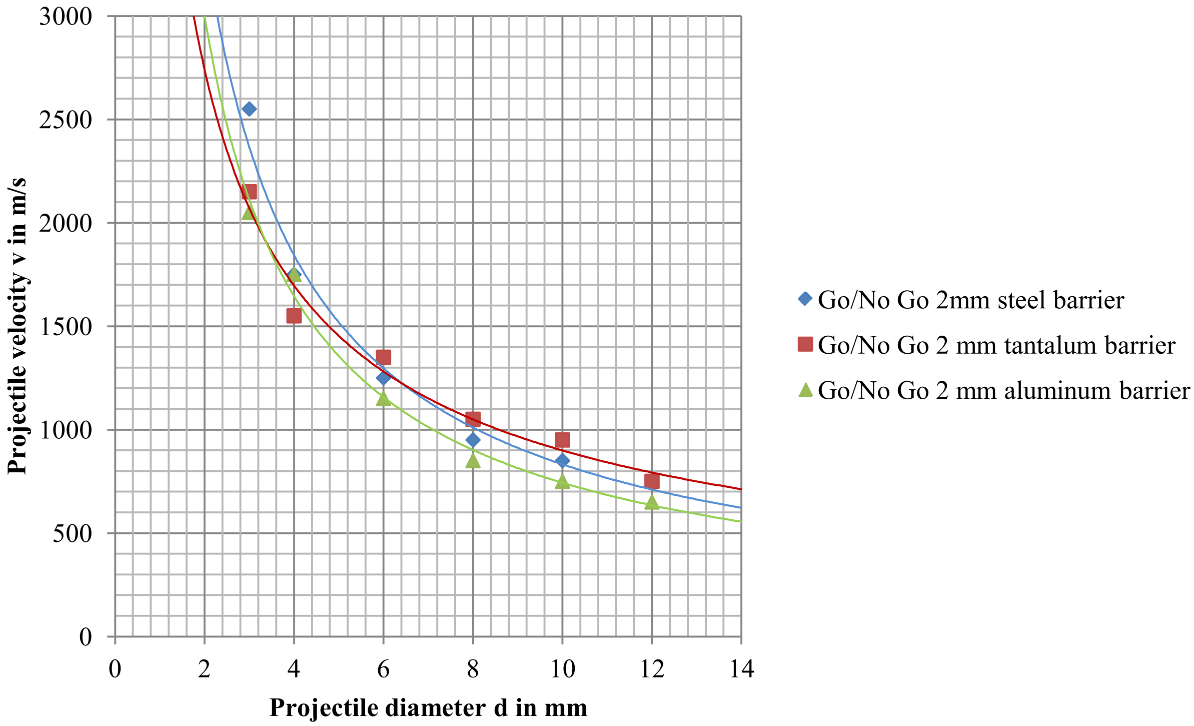

Figure 35: "Go/No Go" velocities as a function of the projectile diameter for different barrier materials. Simulation results obtained for a steel projectile impacting a covered (2 mm barrier) but unconfined block of explosive PBX 9404 at a zoning of 2 cells/mm.

Here too, all plots are different. No simulation results are available with regards to the 2 mm projectile diameter for the same raisons enounced above. These results will be discussed in the same chapter[47].

[46] See chapter VII, subchapter D, part 1.

E. EFFECT OF A CONFINEMENT ON IMPACT INITIATION

The simulations results of the arrangements used to show the effect of a confinement on impact initiation and presented in the precedent chapter[48] are listed below.

1. Simulation with a 2.5 mm thick confinement all around the explosive

The Go/No Go threshold velocities have been tabulated in Appendix C during the simulations and plotted as a function of the projectile diameter in figure 36. The original plot of the PBX 9404 bare explosive[49] has been plotted in the same figure to permit comparisons.

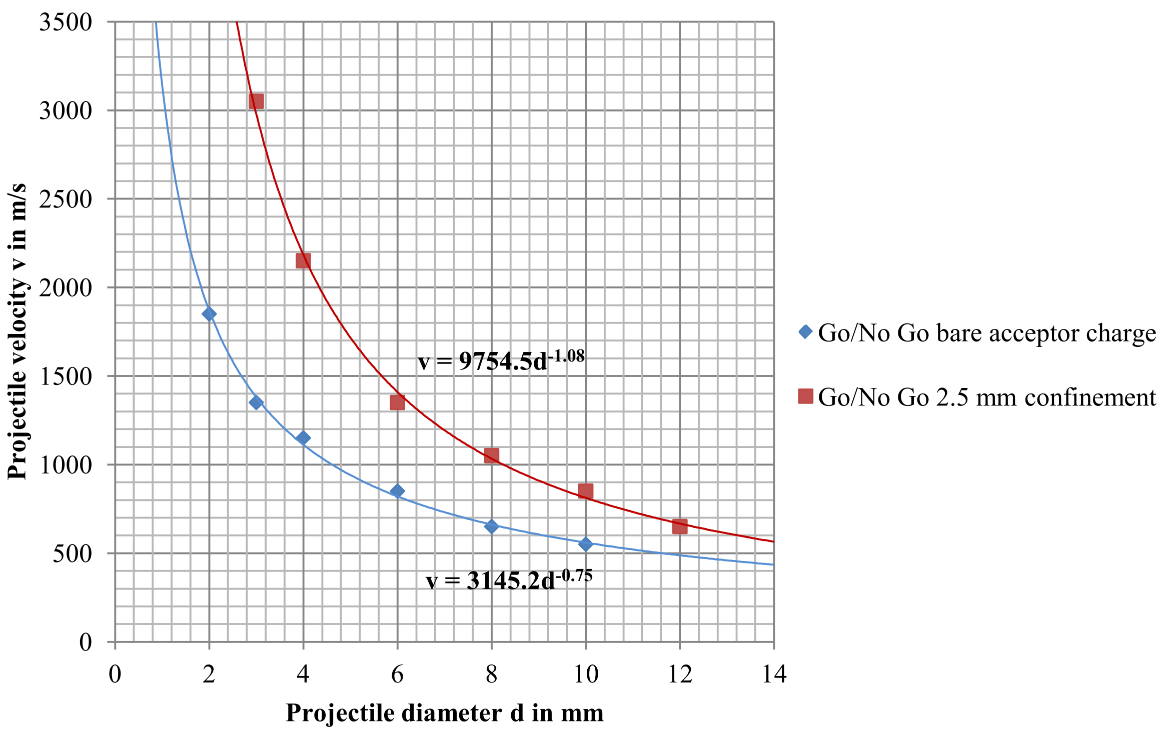

Figure 36: "Go/No Go" velocities as a function of the projectile diameter for a bare and a confined (2.5 mm steel confinement) acceptor charge. Simulation results obtained for a steel projectile impacting a block of explosive PBX 9404 at a zoning of 2 cells/mm.

[47] See chapter VII, subchapter D, part 3.

[48] See chapter V, subchapter E, part1.

[49] See figure chapter V, subchapter A, part 2.

According to these plots, bare acceptor charge and completely confined (covered and confined) acceptor charge do not have the same reaction with regards to impact initiation: the bare acceptor is much easier to initiate than the confined one. This effect will be analyzed in the next chapter[50].

2. Simulation with a 2.5 mm confinement but with a bare impact surface

Figure 37 shows the Go/No Go threshold velocities with regards to the initiation of a block of PBX 9404 for a 2.5 mm confinement with no barrier (bare impact surface) as a function of the projectile diameter as well as these values for the same completely bare acceptor charge. Detailed values are available in Appendix C.

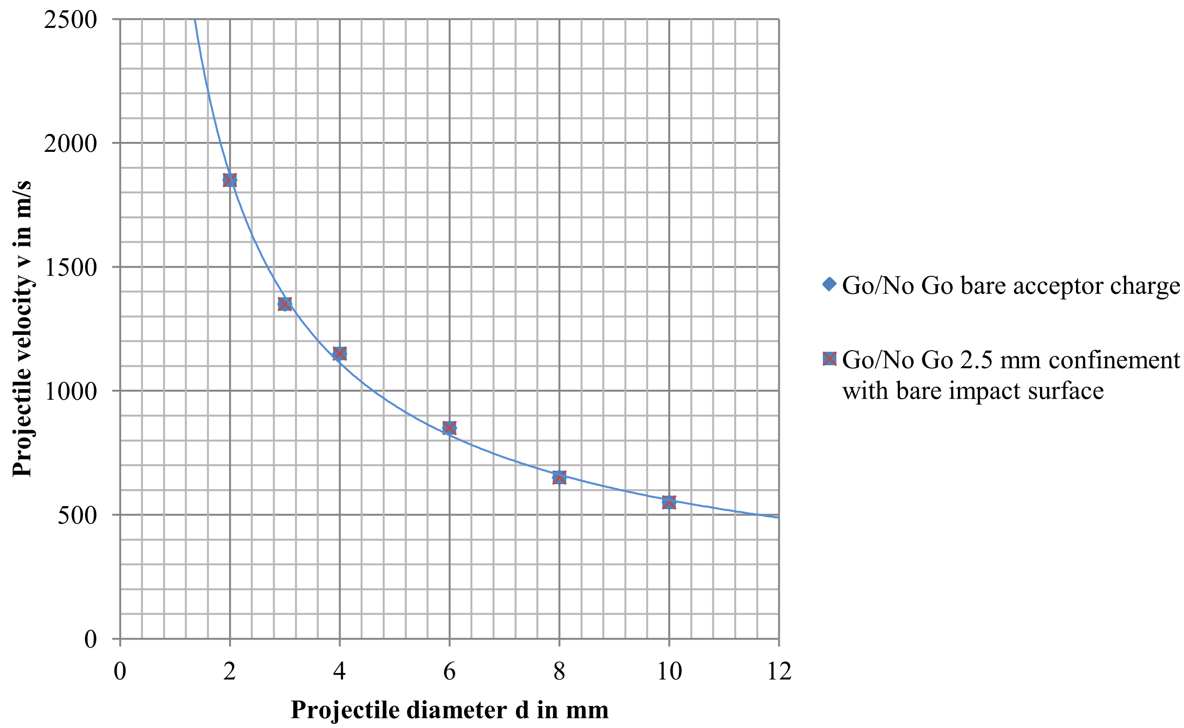

Figure 37: "Go/No Go" velocities as a function of the projectile diameter for a bare and a confined but uncovered (2.5 mm steel confinement with bare impact surface) acceptor charge. Simulation results obtained for a steel projectile impacting a block of explosive PBX 9404 at a zoning of 2 cells/mm.

---

[50] See chapter VII, subchapter E, part 1.

Both plots, by using the "power" trend line, have exactly the same trend. A confined but uncovered acceptor charge seems also to react on the same way to impact initiation than a bare acceptor charge.

F. EFFECT OF AN AIR GAP BETWEEN BARRIER AND ACCEPTOR CHARGE ON IMPACT INITIATION

The simulation results of the arrangement used to show the effect of an air gap placed between a barrier and an acceptor charge on impact initiation and presented in the precedent chapter[51] are presented below. These results will be discussed in the next chapter.

The results obtained by simulating an impact initiation on a block of PBX 9404 protected by a 2 mm steel barrier separated from the block by an air gap with different widths have been plotted in figure 38. Values are tabled in the Appendix C. They can be compared to the results for a block of PBX 9404 protected by a 2 mm barrier directly in contact with it, which have been also plotted.

[51] See chapter V, subchapter F.

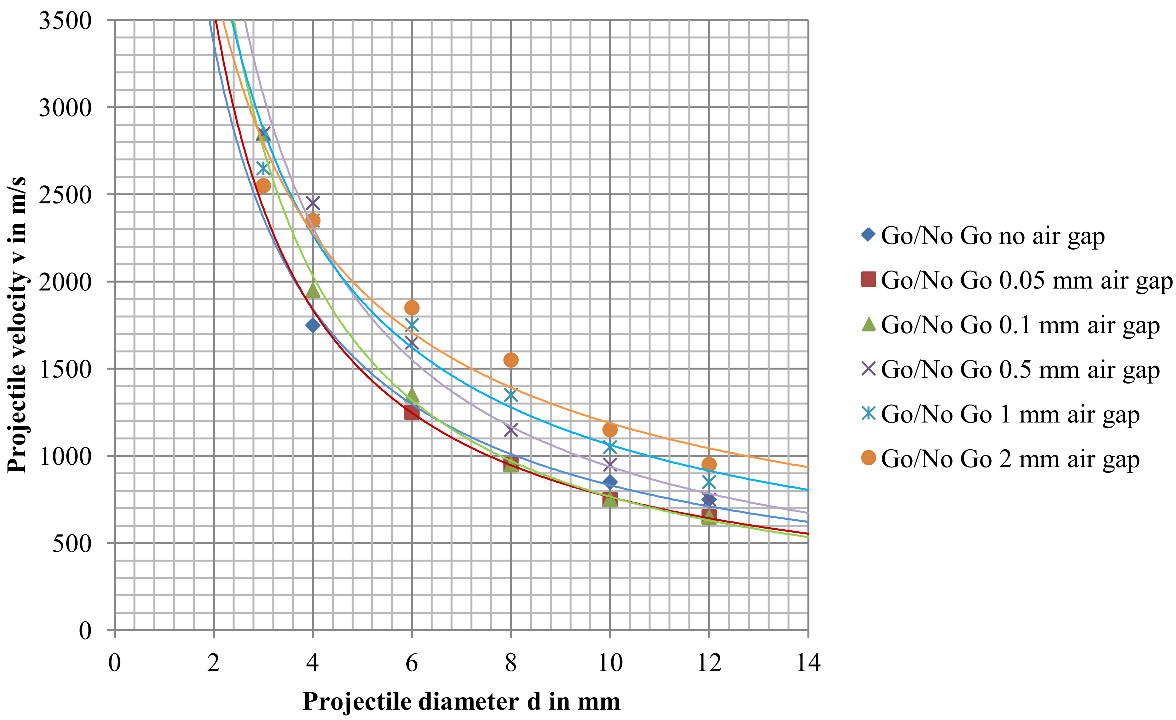

Figure 38: "Go/No Go" velocities as a function of the projectile diameter for different air gap widths separating the acceptor charge from the 2.5 mm steel barrier. Simulation results obtained for a steel projectile impacting a block of explosive PBX 9404 by a zoning of 2 cells/mm.

All plots doubtlessly have, by using the "power" function, different trends, but some of them are very similar. It is the case of the "no air gap" and "0.05 mm air gap" plots with regards to the smaller diameters, and of the "0.05 mm air gap" and "0.1 mm air gap" for the larger diameters. Their equations are given in table 9. As before, consistent simulations for a 2 mm projectile diameter were impossible.

Compared to the plot with a 2 mm barrier directly in contact with the block of explosive PBX 9404, the plots concerning the 0.5 mm, 1 mm and 2 mm air gap show the general trend, despite small disparities, that increasing the width of the air gap increases the Go/No Go threshold velocities needed to make this block of explosive detonating. However, small air gaps, apparently less than 0.1 mm wide, if they seem to afford the same effect for small projectile diameters (less than 4 mm for the 0.05 mm air gap, less than 6 mm for the 0.1 mm air gap), have the contrary effect on larger diameters (respectively more than 4 mm and 6 mm). It seems indeed easier to initiate a block of PBX 9404 for a large projectile diameter if there is a very small air gap between barrier and acceptor charge[52].

G. STUDY OF OTHER EXPLOSIVES

The explosives TNT, H6, Comp. B (65/35) and Octol (70/30) have been impacted as described in the precedent chapter[53] and the results have been plotted in this section.

1. Simulation with TNT

The simulations have been performed for TNT as acceptor charge, and the threshold Go/No Go velocities have been noted down and plotted as a function of the projectile diameter in figure 39. The detailed values can be seen in the Appendix C.

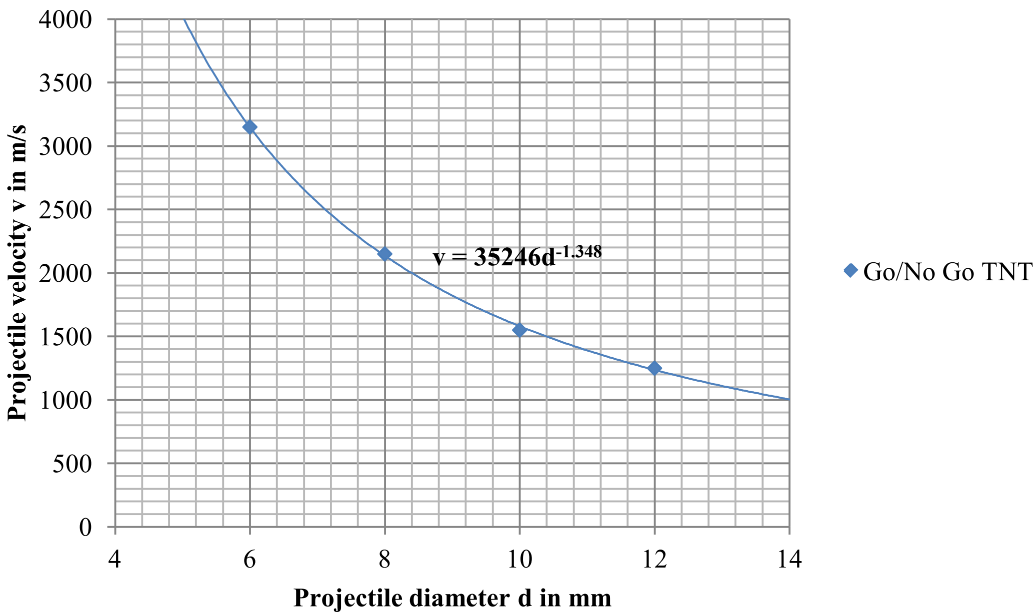

Figure 39: "Go/No Go" velocities as a function of the projectile diameter. Simulation results obtained for a steel projectile impacting a bare block of explosive TNT by a zoning of 2 cells/mm.

52 With regards to a 12 mm diameter projectile, a velocity of at least 650 m/s is needed with a small air gap (less than 0.1 mm) vs. a velocity of at least 750 m/s with no air gap.

53 See chapter V, subchapter G.

The detonation value of cast TNT is about 0.210 Mbar. It is consistent with the results from the simulation. However, it was impossible to obtain a detonation with projectiles which had a diameter smaller than 6 mm. A similar effect has already been observed by other scientists like Zoellner [030] .

2. Simulation with H6

The simulations have been performed for H6 as acceptor charge, and the threshold Go/No Go velocities have been noted down and plotted as a function of the projectile diameter in figure 40. The detailed values can be seen in the Appendix C.

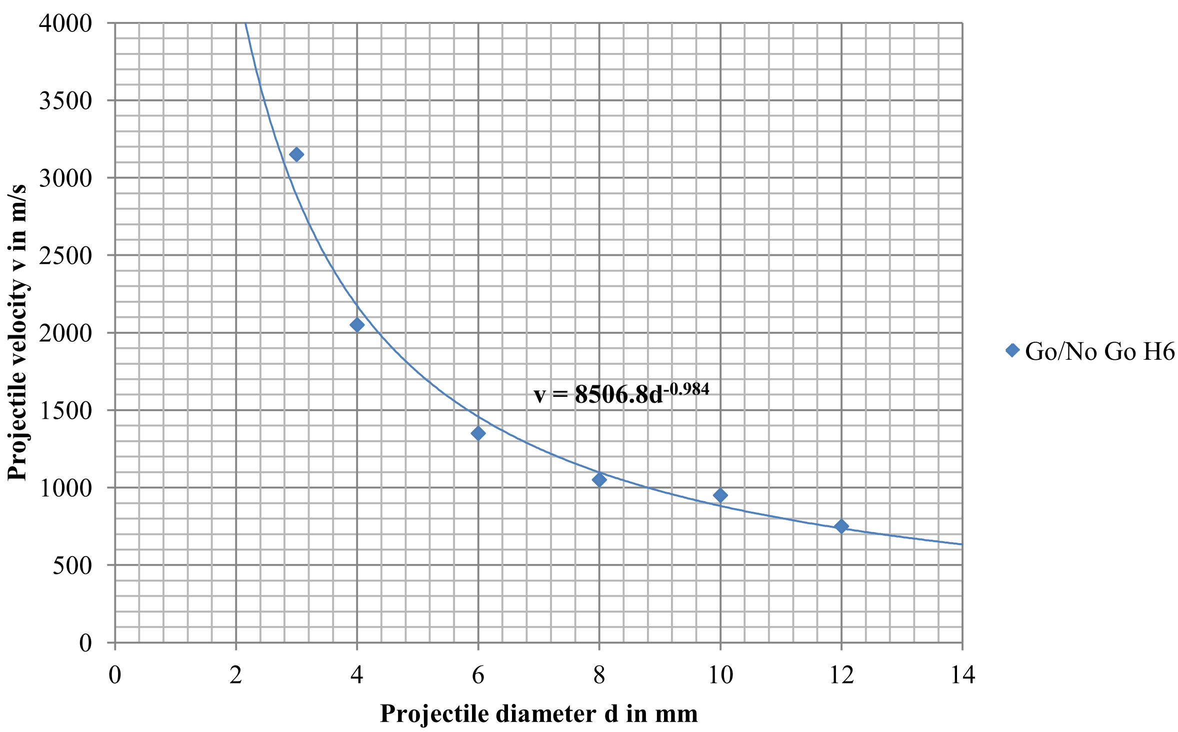

Figure 40: "Go/No Go" velocities as a function of the projectile diameter. Simulation results obtained for a steel projectile impacting a bare block of explosive H6 by a zoning of 2 cells/mm.

The detonation value of H6 is about 0.245 Mbar. It is consistent with the results from the simulation. However, it was impossible to obtain a detonation with projectiles which had a diameter smaller than, this time, 3 mm.

3. Simulation with Comp B.

The simulations have been performed for Comp B. (65/35) as acceptor charge, and the threshold Go/No Go velocities have been noted down and plotted as a function of the projectile diameter in figure 41. The detailed values can be seen in the Appendix C.

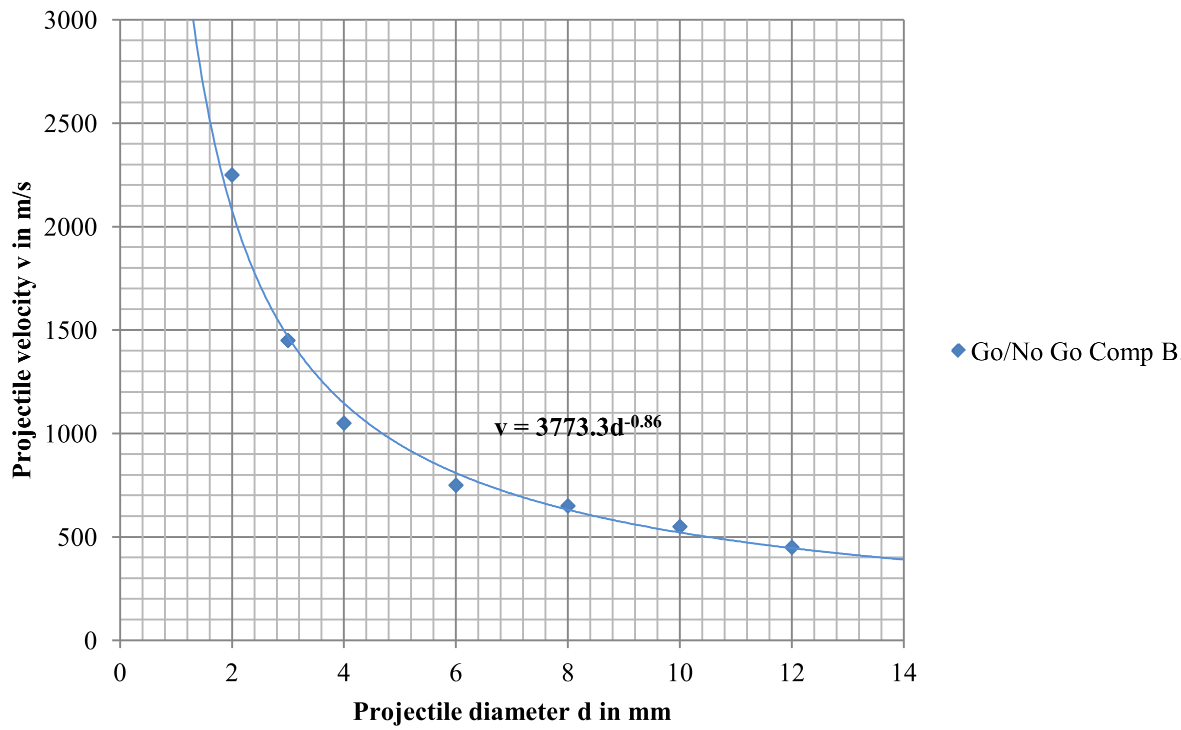

Figure 41: "Go/No Go" velocities as a function of the projectile diameter. Simulation results obtained for a steel projectile impacting a bare block of explosive Comp. B by a zoning of 2 cells/mm.

The detonation value of Comp B. (65/35) is about 0.295 Mbar. It is consistent with the results from the simulation. This time, there is no more restriction concerning the projectile diameter.

4. Simulation with Octol

The simulations have been performed from now on for Octol (70/30) as acceptor charge, and the threshold Go/No Go velocities have been noted down and plotted as a function of the projectile diameter in figure 42. Values can be seen in the Appendix C.

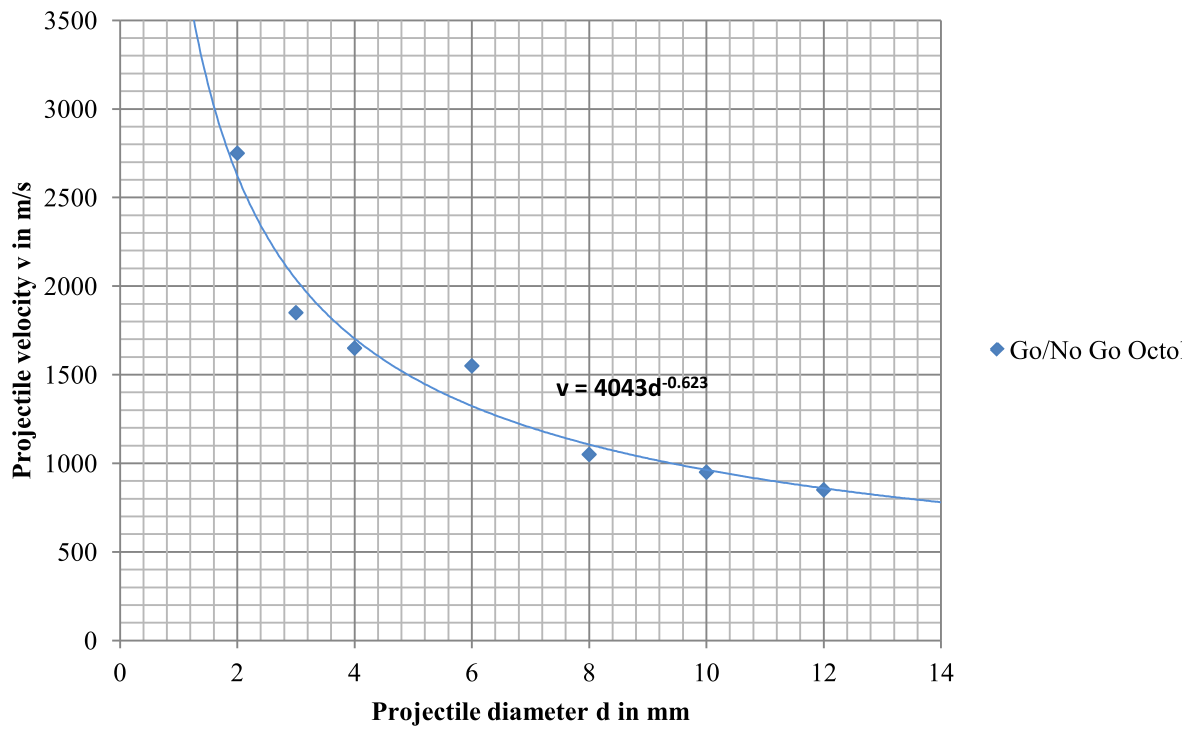

Figure 42: "Go/No Go" velocities as a function of the projectile diameter. Simulation results obtained for a steel projectile impacting a bare block of explosive Octol by a zoning of 2 cells/mm.

The detonation value of Octol (70/30) is about 0.320 Mbar. It is consistent with the results from the simulation. Here as well, there is no restriction concerning the projectile diameter.

H. EFFECT OF THE PROJECTILE MATERIAL ON IMPACT INITIATION

The block of PBX 9404 has been impacted by different projectiles, copper, aluminum and tungsten, according to the description done in the precedent chapter[54]. The results have been plotted below and will be used and discussed later[55].

[54] See chapter V, subchapter H.

[55] See chapter VII, subchapter H.

1. Simulation with Copper

The simulations have been performed by using copper as a projectile material. The Go/No Go threshold velocities are reported in Appendix C and plotted as a function of the projectile diameter in figure 43.

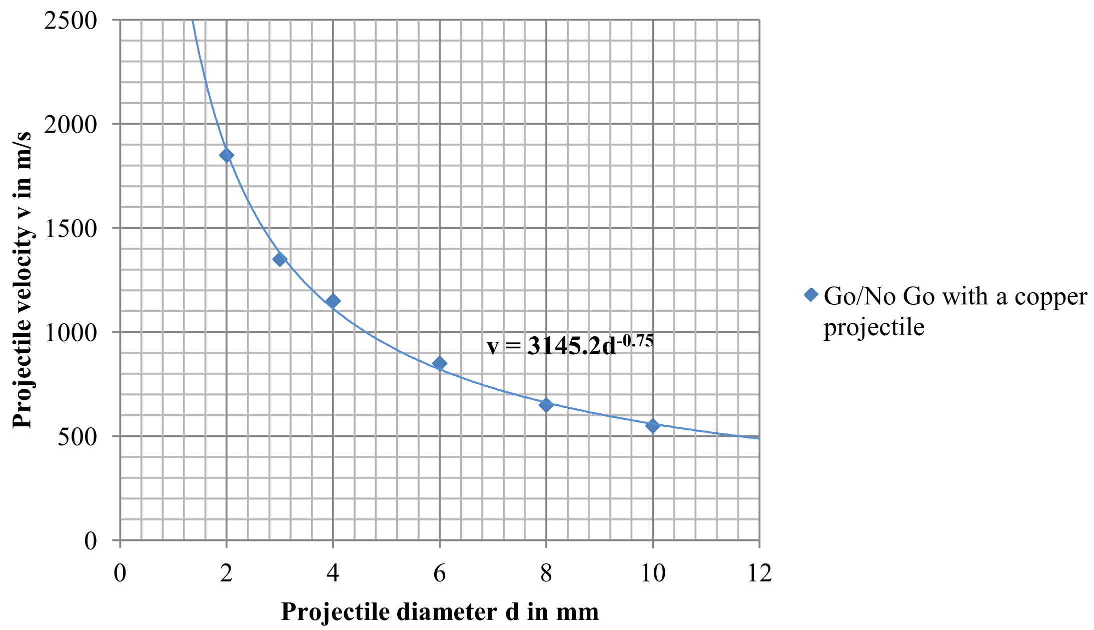

Figure 43: "Go/No Go" velocities as a function of the projectile diameter. Simulation results obtained for a copper projectile impacting a bare block of explosive PBX 9404 by a zoning of 2 cells/mm.

2. Simulation with Aluminum

The Go/No Go threshold velocities for an aluminum projectile are tabulated in Appendix C and plotted as a function of the projectile diameter in figure 44.

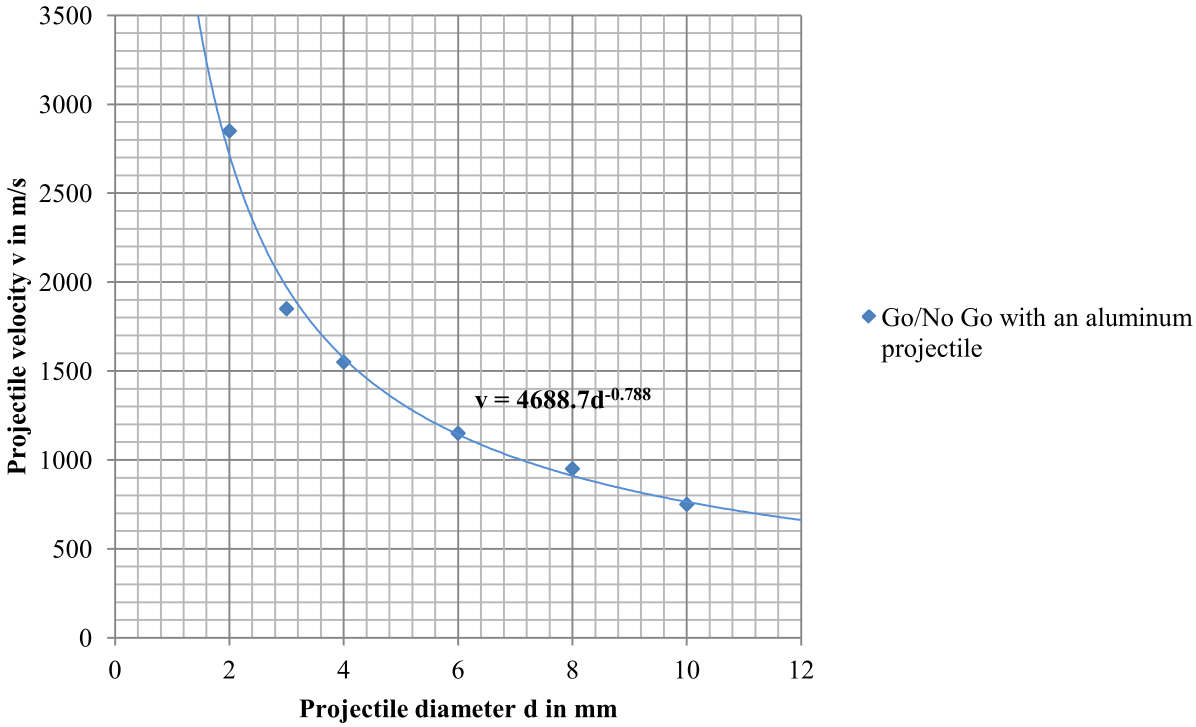

Figure 44: "Go/No Go" velocities as a function of the projectile diameter. Simulation results obtained for an aluminum projectile impacting a bare block of explosive PBX 9404 by a zoning of 2 cells/mm.

3. Simulation with Tungsten

That time, the Go/No Go threshold velocities for a tungsten projectile have been taken down in a table in the Appendix C and plotted as a function of the projectile diameter in figure 45.

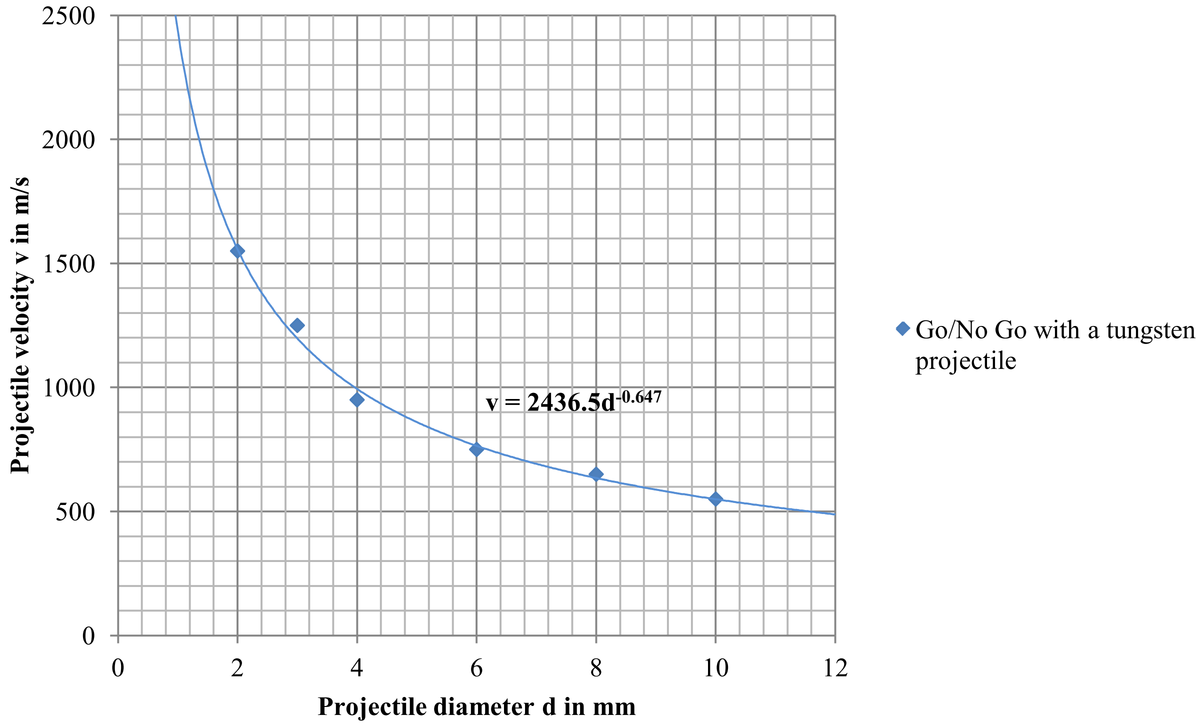

Figure 45: "Go/No Go" velocities as a function of the projectile diameter. Simulation results obtained for a tungsten projectile impacting a bare block of explosive PBX 9404 by a zoning of 2 cells/mm.

I. V²D AND U²D HELD CRITERIONS

The Go/No Go threshold velocities which have been noted down in the subchapters A, G and H of chapter VI from the simulations in AUTODYN® with a zoning of 2 cells/mm, have been used in this subchapter to estimate the values of the initiation criterions found by Held[56] or colleagues[57]. The results are contained in tables 6 to 15 and figure 46 to 47.

[56] See chapter II and chapter V, subchapter A.

[57] See chapter V, subchapter A.

1. Explosive PBX 9404 , different projectiles

a) v^2d Held criterion

Projectile diameter vs. Projectile material	Steel	Copper	Aluminum	Tungsten
2 mm	6.85	6.85	16.25	4.81
3 mm	5.47	5.47	10.27	4.69
4 mm	5.29	5.29	9.61	3.61
6 mm	4.34	4.34	7.94	3.38
8 mm	3.38	3.38	7.22	3.38
10 mm	3.03	3.03	5.63	3.03

Table 6: Values of v^2d ($mm^3/\mu s^2$) for the explosive PBX 9404 and steel, copper, aluminum and tungsten projectiles. Results calculated from simulation results obtained in chapter VI, subchapter H.

The values of v^2d concerning PBX 9404 are for each projectile material not constant in the "vertical", that means not constant for the different diameters of the same projectile material. In the "horizontal", that means for the different projectile materials of a same diameter, the values of steel and copper are the same. The values of tungsten are smaller, the values of aluminum are quite larger.

b) u^2d Held criterion

Projectile diameter vs. Projectile material	Steel	Copper	Aluminum	Tungsten
2 mm	3.11	3.23	4.88	2.76
3 mm	2.49	2.58	3.08	2.69
4 mm	2.41	2.50	2.89	2.07
6 mm	1.97	2.05	2.38	1.94
8 mm	1.54	1.60	2.17	1.94
10 mm	1.38	1.43	1.69	1.74

Table 7: Values of u^2d ($mm^3/\mu s^2$) for the explosive PBX 9404 and steel, copper, aluminum and tungsten projectiles. Results calculated from simulation results obtained in chapter VI, subchapter H.

The values of u^2d in the "vertical" are still quite different, but the values in the horizontal seem to be much closer. This point will be performed in the discussion part in the next chapter[58].

The u^2d Held criterion, which has been given by Held as the best initiation criterion with regards to impact initiation with different projectile densities [016], has also been plotted in a log/log chart in figure 45 and in a normal chart in figure 46:

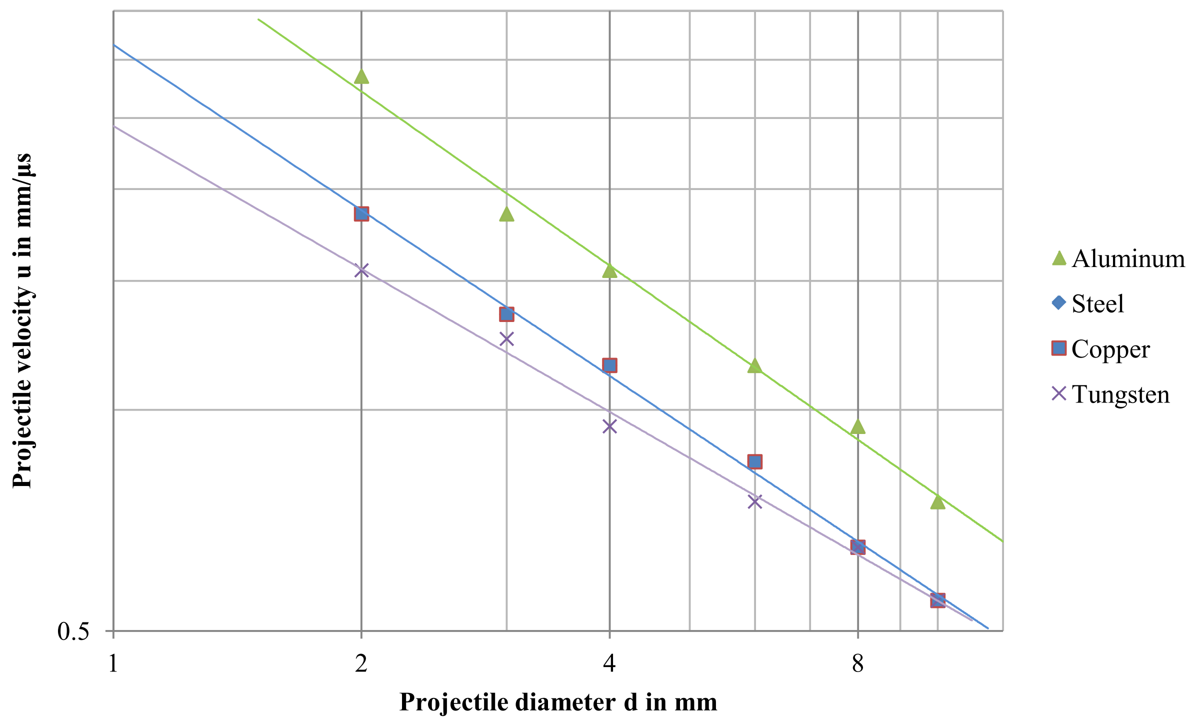

Figure 46: u^2d criterion ($mm^3/\mu s^2$) given in a log/log chart showing the projectile "Go/No Go" velocities as a function of the projectile diameter for different projectile materials. Simulation results obtained for a projectile impacting a bare block of explosive PBX 9404 by a zoning of 2 cells/mm. The legend is ordered with regards to the material densities going from the lowest (aluminum) to the highest (tungsten).

The lines in figure 45 are not parallel and have a slope different from 2, as the equations below show.

[58] See chapter VII, subchapter I.

Projectile	Equation
Aluminum	$v = 4.7*d^{-0.79}$
Steel	$v = 3.1*d^{-0.75}$
Copper	$v = 3.1*d^{-0.75}$
Tungsten	$v = 2.4*d^{-0.65}$

Table 8: Equations of the plots in figure 45.

This confirms the fact that the u^2d Held criterion is not constant.

c) $\rho v^2 d$ Mader criterion

Projectile diameter vs. Projectile material	Steel	Copper	Aluminum	Tungsten
2 mm	54.05	61.13	44.02	86.97
3 mm	43.17	48.82	27.82	84.84
4 mm	41.77	47.24	26.04	65.34
6 mm	34.23	38.71	21.50	61.09
8 mm	26.69	30.18	19.57	61.18
10 mm	23.89	27.01	15.24	54.75

Table 9: Values of $\rho v^2 d$ ($g/cm^3.mm^3/\mu s^2$) for the explosive PBX 9404 and steel, copper, aluminum and tungsten projectiles. Results calculated from simulation results obtained in chapter VI, subchapter H.

The $\rho v^2 d$ values are not constant too. Discussion about it will take place in the next chapter[59].

[59] See chapter VII, subchapter I.

d) $\sqrt{\rho v^2 d}$ Chick criterion

Projectile diameter vs. Projectile material	Steel	Copper	Aluminum	Tungsten
2 mm	19.23	20.45	26.74	20.44
3 mm	15.36	16.34	16.90	19.94
4 mm	14.86	15.81	15.82	15.36
6 mm	12.18	12.95	13.06	14.36
8 mm	9.50	10.10	11.89	14.38
10 mm	8.50	9.04	9.26	12.87

Table 10: Values of $\sqrt{\rho v^2 d}$ ($\sqrt{(g/cm^3)}.mm^3/\mu s^2$) for the explosive PBX 9404 and steel, copper, aluminum and tungsten projectiles. Results calculated from simulation results obtained in chapter VI, subchapter H.

Similar to the $\rho v^2 d$ values, the $\sqrt{\rho v^2 d}$ values are also different. Differences in the values will be discussed later[60].

2. Steel projectile, different explosives

a) $v^2 d$ Held criterion

Projectile diameter vs. Explosive material	TNT	H6	Comp.B	Octol	PBX9404
2 mm	/	/	10.13	15.13	6.85
3 mm	/	29.77	6.31	10.27	5.47
4 mm	/	16.81	4.41	10.89	5.29
6 mm	59.54	10.94	3.38	14.42	4.34
8 mm	36.98	8.82	3.38	8.82	3.38
10 mm	24.03	9.03	3.03	9.03	3.03
12 mm	18.75	6.75	2.43	8.67	3.31

Table 11: Values of $v^2 d$ ($mm^3/\mu s^2$) for different explosives and a steel projectile. Results calculated from simulation results obtained in chapter VI, subchapter G.

The values of $v^2 d$ seem also not to be constant for the other explosives tested here. The $v^2 d$ Held criterion has been plotted in a log/log chart in figure 47. It has also been plotted as a function of the projectile diameter in figure 48.

60 See chapter VII, subchapter I.

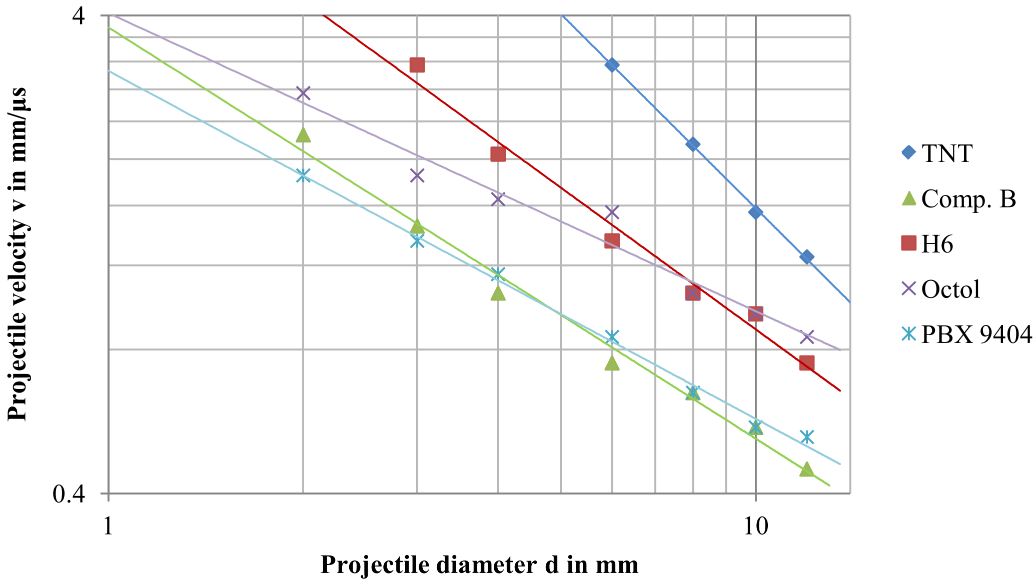

Figure 47: v^2d criterion ($mm^3/\mu s^2$) given in a log/log chart showing the projectile "Go/No Go" velocities as a function of the projectile diameter for different projectile materials. Simulation results obtained for a steel projectile impacting a bare block of explosive PBX 9404 by a zoning of 2 cells/mm. The legend is ordered with regards to the explosive densities, going from the lowest (TNT) to the highest (PBX 9404).

The lines in figure 45 are not parallel and have a slope different from 2, as the equations below show.

Explosive	Equation
TNT	$v = 35.3*d^{-1.35}$
Comp. B	$v = 3.8*d^{-0.86}$
H6	$v = 8.5*d^{-0.98}$
Octol	$v = 4.0*d^{-0.62}$
PBX 9404	$v = 3.1*d^{-0.73}$

Table 12: Equations of the plots of figure 47.

This confirms the fact that the v^2d Held criterion is not constant.

b) u^2d Held criterion

Projectile diameter vs. Explosive material	TNT	H6	Comp.B	Octol	PBX9404
2 mm	/	/	4.71	6.92	3.11
3 mm	/	13.76	2.93	4.70	2.49
4 mm	/	7.77	2.05	4.99	2.41
6 mm	28.15	5.06	1.57	6.60	1.97
8 mm	17.48	4.08	1.57	4.04	1.54
10 mm	11.36	4.17	1.41	4.13	1.38
12 mm	8.86	3.12	1.13	3.97	1.50

Table 13: Values of u^2d ($mm^3/\mu s^2$) for different explosives and a steel projectile. Results calculated from simulation results obtained in chapter VI, subchapter G.

The values of u^2d are different for each explosive (in the vertical) and quite different for the different diameters of a same explosive. Further discussions will take place later[61].

c) ρv^2d Mader criterion

Projectile diameter vs. Explosive material	TNT	H6	Comp.B	Octol	PBX9404
2 mm	/	/	79.95	119.4	54.05
3 mm	/	235.0	49.80	81.07	43.17
4 mm	/	132.7	34.82	85.99	41.77
6 mm	470.1	86.34	26.65	113.8	34.23
8 mm	292.0	69.64	26.69	69.64	26.69
10 mm	189.7	71.26	23.89	71.26	23.89
12 mm	148.1	53.30	19.19	68.46	26.11

Table 14: Values of ρv^2d ($g/cm^3.mm^3/\mu s^2$) for different explosives and a steel projectile. Results calculated from simulation results obtained in chapter VI, subchapter G.

Like the u^2d values, the values of ρv^2d are also quite different. Further discussions will take place later[62].

---

61 See chapter VII, subchapter I.

62 See chapter VII, subchapter I.

d) $\sqrt{\rho v^2 d}$ Chick criterion

Projectile diameter vs. Explosive material	TNT	H6	Comp.B	Octol	PBX9404
2 mm	/	/	28.45	42.50	19.23
3 mm	/	83.65	17.72	28.85	15.36
4 mm	/	47.24	12.39	30.60	14.86
6 mm	167.3	30.73	9.48	40.51	12.18
8 mm	103.9	24.78	9.50	24.78	9.50
10 mm	67.51	25.36	8.50	25.36	8.50
12 mm	52.69	18.97	6.83	24.36	9.29

Table 15: Values of $\sqrt{\rho v^2 d}$ ($\sqrt{(g/cm^3)}.mm^3/\mu s^2$) for different explosives and a steel projectile. Results calculated from simulation results obtained in chapter VI, subchapter G.

The similar results obtained here for the $\sqrt{\rho v^2 d}$ criterion will also be discussed later[63].

3. Introduction of a new criterion for bare explosive impact: the Pd energy criterion

The ranges of values found by the four criterions presented and calculated for different explosives and different projectiles below have shown the necessity to develop a new criterion, combining the impact velocity with the projectile diameter, while giving a physical signification to these initiation criterions, that includes the Hugoniot characteristics of both explosive and projectile. In esse, the objective is to take into account the behavior of the materials at impact, including density and shock.

The values of the Pd energy criterion have been calculated using the Hugoniot parameters, the Go/No Go threshold velocities collected in the literature in the one hand as well as the Go/No Go threshold velocities obtained in precedent simulations[64] on the other hand, and the projectile diameter. They are tabulated in tables 16 to 22.

[63] See chapter VII, subchapter I.

[64] See chapter VI, subchapter A, G and H.

a) Experimental values for PBX 9404 and a steel projectile estimated from the literature

Scientist		Moulard [027]		Weingart [026]		LeRoy Green [028]		Cook [029]	
	d mm	P GPa	P*d cal/cm^2	P GPa	P*d cal/cm^2	P GPa	P*d cal/cm^2	P GPa	P*d cal/cm^2
	2	13.1	626	10.4	497	18.5	884	9.4	449
	3	9.4	673	8.4	602	10.4	745	7.5	537
	4	7.5	716	7	669	8.4	802	6.6	630
	6	5.8	831	5.3	759	6.2	888	5.3	759
	8	4.5	860	4.5	860	5.3	1013	4.5	860
	10	3.4	812	3.8	907	4.5	1075	4.2	1003

Table 16: Values of Pd for the explosive PBX 9404 and a steel projectile. Results obtained in the literature [026, 027, 028, 029].

The results obtained with AUTODYN® under similar conditions (steel projectile, block of explosive PBX 9404) are presented below for comparison purposes:

Steel (simulations)	
P (GPa)	P*d (cal/cm^2)
16	764
10.4	745
8.4	802
5.8	831
4.2	802
3.4	812

Table 17: Simulation results concerning Pd and obtained in chapter VI, subchapter A, part 2 for a steel projectile impacting a bare block of PBX 9404

Average and deviation have been calculated and tabled in table 18.

	Moulard	Weingart	Le Roy	Cook	Bouvenot (simulations)
Average P*d (cal/cm^2)	753	716	901	706	793
Deviation P*d (cal/cm^2)	95	157	124	207	32

Table 18: Average and deviation of table 15.

The results obtained from experimental results found in the literature are all consistent with the ones obtained through the simulations. The average value of all experimental results is 769 cal/cm^2. This value is nearly identical to the simulation average value of 793. The Pd criterion seems also to be a consistent criterion.

b) Simulation values for PBX 9404 and different projectile materials

Projectile		**Aluminum**		**Steel**		**Copper**		**Tungsten**	
	d mm	P GPa	P*d cal/cm^2	P GPa	P*d cal/cm^2	P GPa	P*d cal/cm^2	P GPa	P*d cal/cm^2
	2	21	1003	16	764	15.9	759	15.2	726
	3	11.7	838	10.4	745	10.4	745	11.2	802
	4	9.3	888	8.4	802	8.4	802	7.8	745
	6	6.4	917	5.8	831	5.7	817	5.7	817
	8	5.1	974	4.2	802	4.1	783	4.8	917
	10	3.9	931	3.4	812	3.4	812	3.9	931

Table 19: Values of Pd for the explosive PBX 9404 and steel, copper, aluminum and tungsten projectiles. Results calculated from simulation results obtained in chapter VI, subchapter H.

	Aluminum	Steel	Copper	Tungsten
Average P*d (cal/cm^2)	925	793	786	823
Deviation P*d (cal/cm^2)	59	32	29	85

Table 20: Average and deviation of table 18.

The values obtained here for the four different projectile materials and PBX 9404 are still not constant, but the ranges seem to be quite smaller than the ones obtained for the v^2d, $\rho v^2 d$ and the $\sqrt{\rho} v^2 d$ criterions with the same explosive and the same projectiles. This point will be further analyzed in the next chapter[65].

These results have been furthermore plotted in a chart giving the pressure P as a function of one over the projectile diameter:

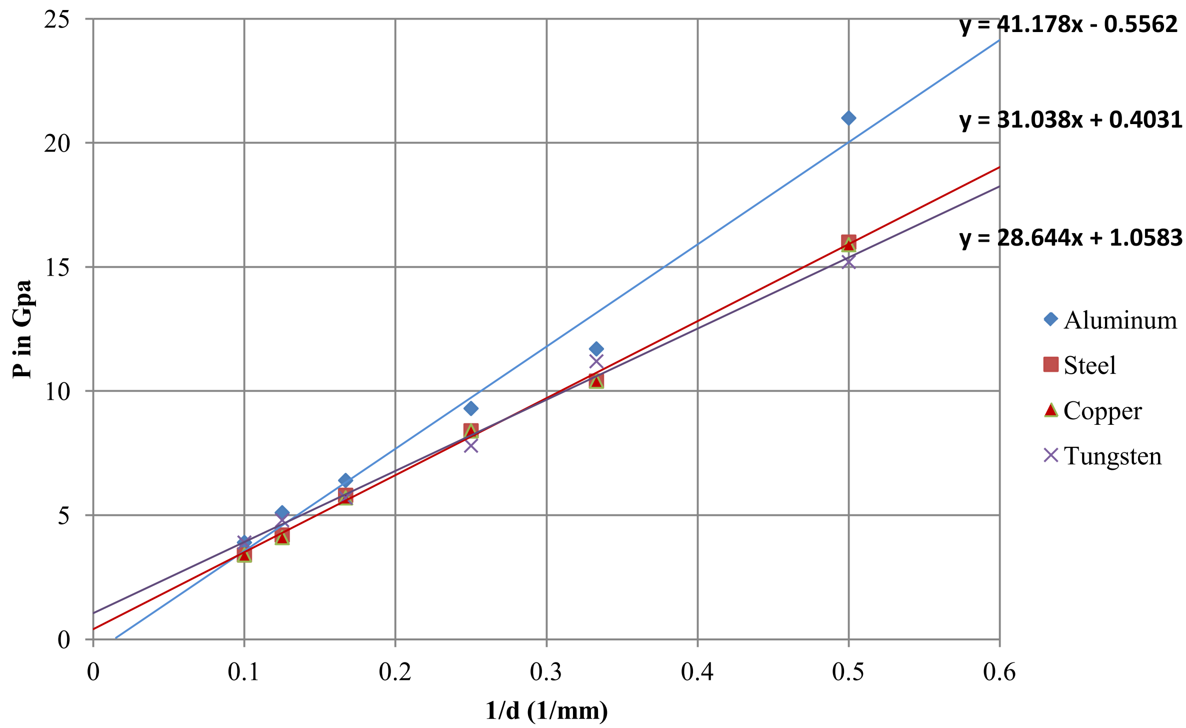

Figure 48: Pressure P as a function of one over the projectile diameter for a block of explosive PBX 9404 impacting by different projectiles. Results obtained in table 19.

The lines of copper and aluminum are identical, confirming the Held's assumption that these two materials can be treated together. The line of tungsten is very close to them. The results concerning aluminum are however different, but this is due to the extreme volatility which affects the smaller diameters (smaller than 4 mm). Slopes (close between the different materials) and values of the intersection with the y-axis (close to 0) of these four lines confirm the "relatively constancy" of this criterion.

65 See chapter VII, subchapter I.

c) Simulation results for other explosives and a steel projectile

Projectile		**TNT**		**H6**		**Comp. B**		**Octol**	
	d mm	P GPa	P*d cal/cm^2	P GPa	P*d cal/cm^2	P GPa	P*d cal/cm^2	P GPa	P*d cal/cm^2
	2	/	/	/	/	21.0	1002	29.2	1395
	3	/	/	31.1	2228	10.6	763	16.2	1161
	4	/	/	16.9	1615	6.5	628	13.8	1318
	6	29.2	4185	9.7	1390	4.0	580	12.6	1805
	8	16.7	3194	7.1	1351	3.4	649	7.4	1414
	10	10.6	2534	6.3	1493	2.6	631	6.4	1528
	12	8.0	2283	4.7	1353	2.0	581	5.6	1596

Table 21: Values of Pd for different explosives and a steel projectile. Results calculated from simulation results obtained in chapter VI, subchapter H.

	TNT	**H6**	**Comp. B**	**Octol**
Average P*d (cal/cm^2)	3049	1572	691	1460
Deviation P*d (cal/cm^2)	849	337	150	208

Table 22: Average and deviation of table 20.

These results have been furthermore plotted in a chart giving the pressure P as a function of one over the projectile diameter.

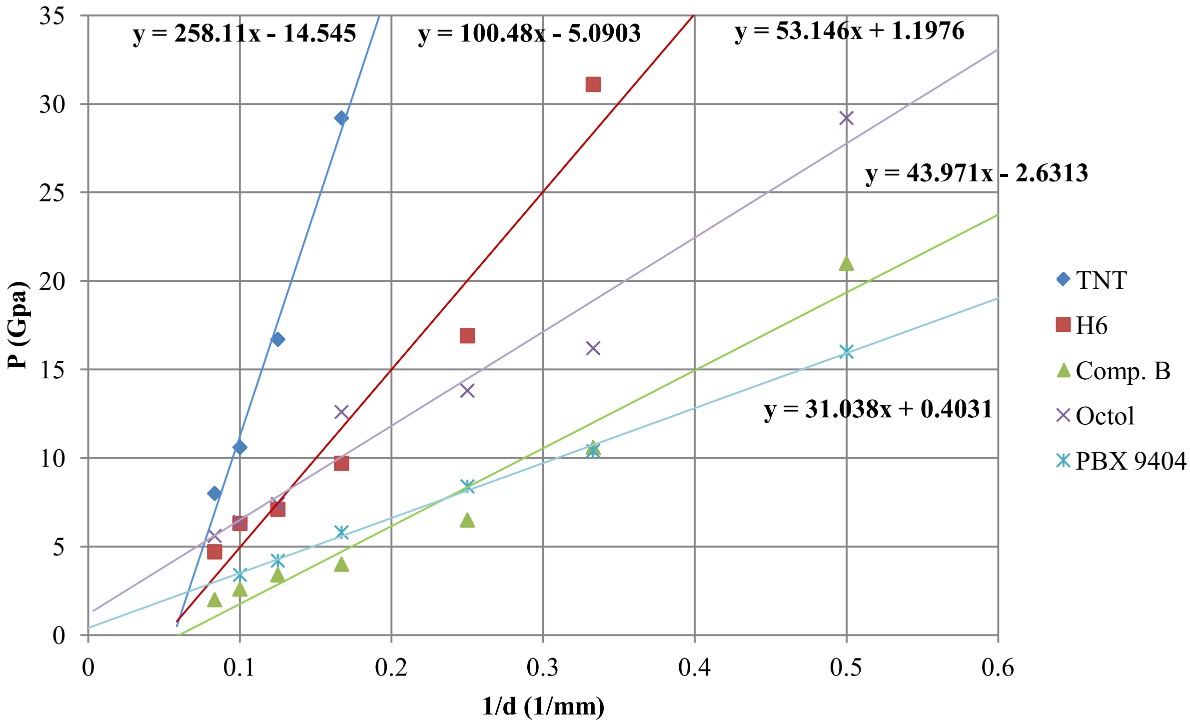

Figure 48 bis: P as a function of one over the projectile diameter for a block of explosive PBX 9404 impacting by different projectiles. Results obtained in table 21.

Results of tables 21 and 22 show some disparities between the different diameters of a same explosive. More about that is discussed in chapter VII, subchapter I. The graphical representation, however, gives already some information about it. First, all slopes are different, which means that each "ideal" Pd value of each explosive is different. From very insensitive explosives to very sensitive explosives, according to these plots: TNT, H6, Octol, Comp. B and PBX 9404. Furthermore, a value going against 0 of the intersection of the plot line with the y-axis means that the values of Pd are relatively constant. In that way, PBX 9404 and Octol show a very good behavior. After that come Comp. B, H6 and TNT which show more disparities. These disparities are quntified in next chapter.

J. PRESSURE AT THE IMPACT SURFACE, RUN DISTANCES AND RAREFACTION EFFECTS

The data concerning the pressures at the interfaces steel/steel and steel/PBX 9404, as well as the run distances and the rarefaction effects into the explosive PBX 9404 have been calculated or estimated in this part and compared to the results furnished by AUTODYN® in order to confirm again the ability of AUTODYN® to simulate with a great accuracy the impact initiation problems, and will be used to analyze some of the effects discussed in the next chapter.

1. Pressure at the impact surface

The theoretical pressures at the impact surface for the interfaces Steel/Steel and Steel/PBX 9404 have been calculated and plotted in figure 49 and 50 as a function of the projectile velocity. The same pressures have been estimated from the fixed and moving gauges respectively on the impact surface of the projectile and on the impact surface of the acceptor charge. This should verify and validate the use of Hugoniot analysis They have been plotted in the same figure. Numerical values are available in the Appendix C.

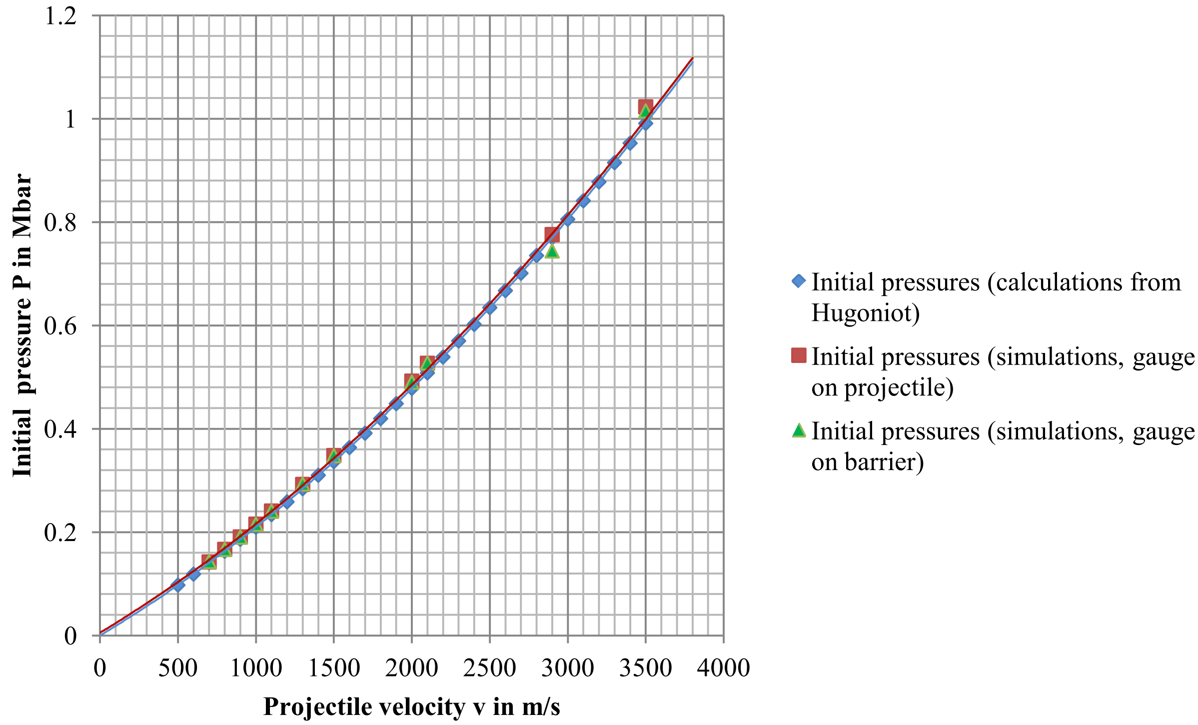

Figure 49: Impact pressure obtained at the interface steel/steel obtained from calculations or simulations with gauges on projectile and explosive as a function of the projectile velocity for a covered (2.5 mm steel barrier) acceptor charge. Simulation results obtained for a steel projectile impacting a block of explosive PBX 9404 at a zoning of 4 cells/mm.

The three plots have exactly the same trend. It is to notice, that this time, the "polynomial" (order 2) trend line is better adapted than the "power" one for the establishment of a mathematics model.

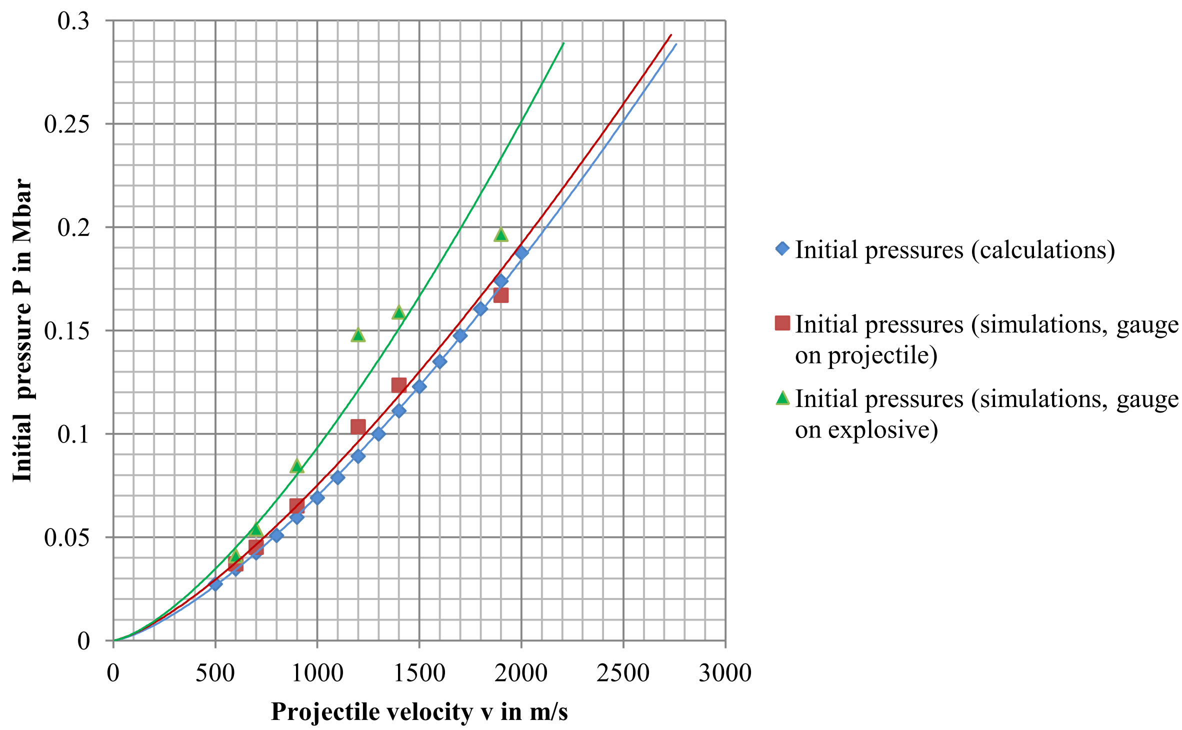

Figure 50: Impact pressure obtained at the interface steel/PBX 9404 obtained from calculations or simulations with gauges on projectile and explosive as a function of the projectile velocity for a bare acceptor charge. Simulation results obtained for a steel projectile impacting a bare block of explosive PBX 9404 at a zoning of 4 cells/mm.

In that case, the plot obtained through the calculations, which is of course the same as before, is similar to the plot obtained through the pressure values recorded by the gauge on the impact surface of the projectile. Small differences are perceptible, and these differences seem to remain the same for all the velocities of the study area. The plot obtained through the pressure values recorded by the gauge placed on the impact side of the acceptor charge, however, shows large differences with the two other plots. These differences, relatively small for small projectile velocities, become always larger by increasing the projectile velocities. This is due to the fact, that the explosive is detonating, affecting in that way the results of the gauge on the explosive[66].

66 See chapter VII, subchapter J, part 1.

2. Run distances

The theoretical run distances x for the explosive PBX 9404 have been plotted, according to the equations obtained in chapter V, subchapter J, in figure 51 as a function of the initial impact pressure P and in figure 52 as a function of the impact velocity[67] v.

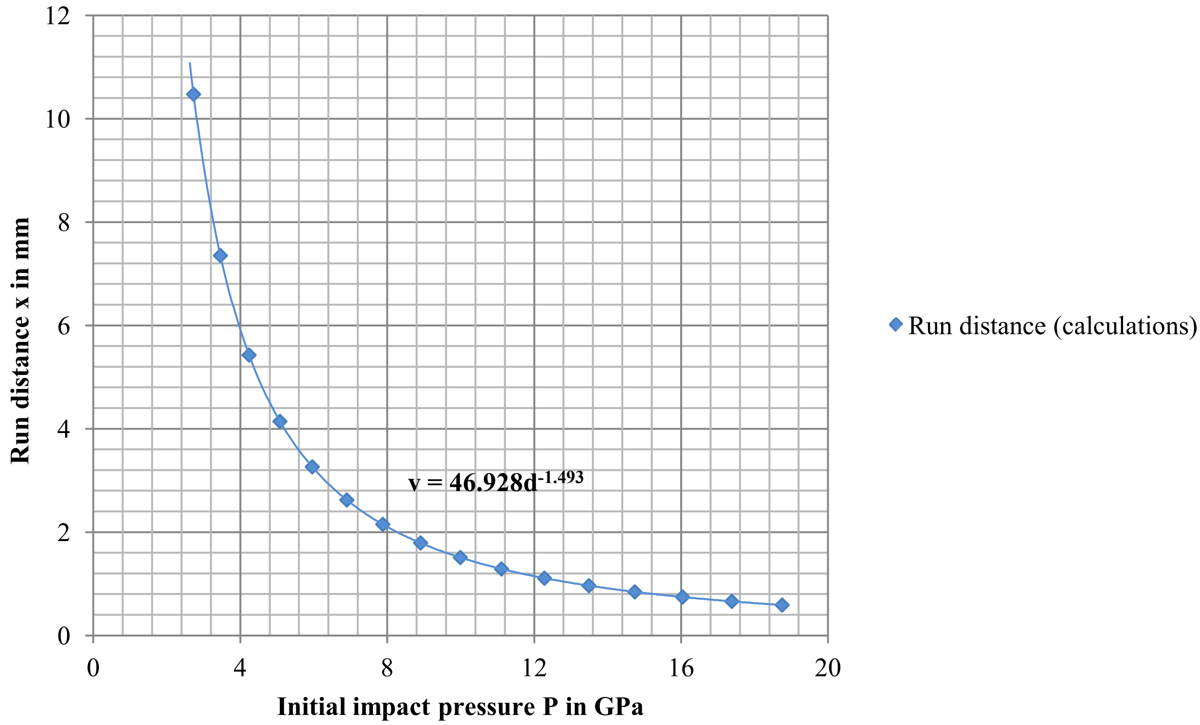

Figure 51: Run distance as a function of the initial impact pressure. Calculation results obtained for a steel projectile impacting a block of explosive PBX 9404 from Popalato.

According to this plot, the run distance decreases with the augmentation of the initial impact pressure. The description of the behavior is perfectly given by a "power" trend line whose equation is on the chart.

[67] This impact velocity corresponds to the projectile velocity.

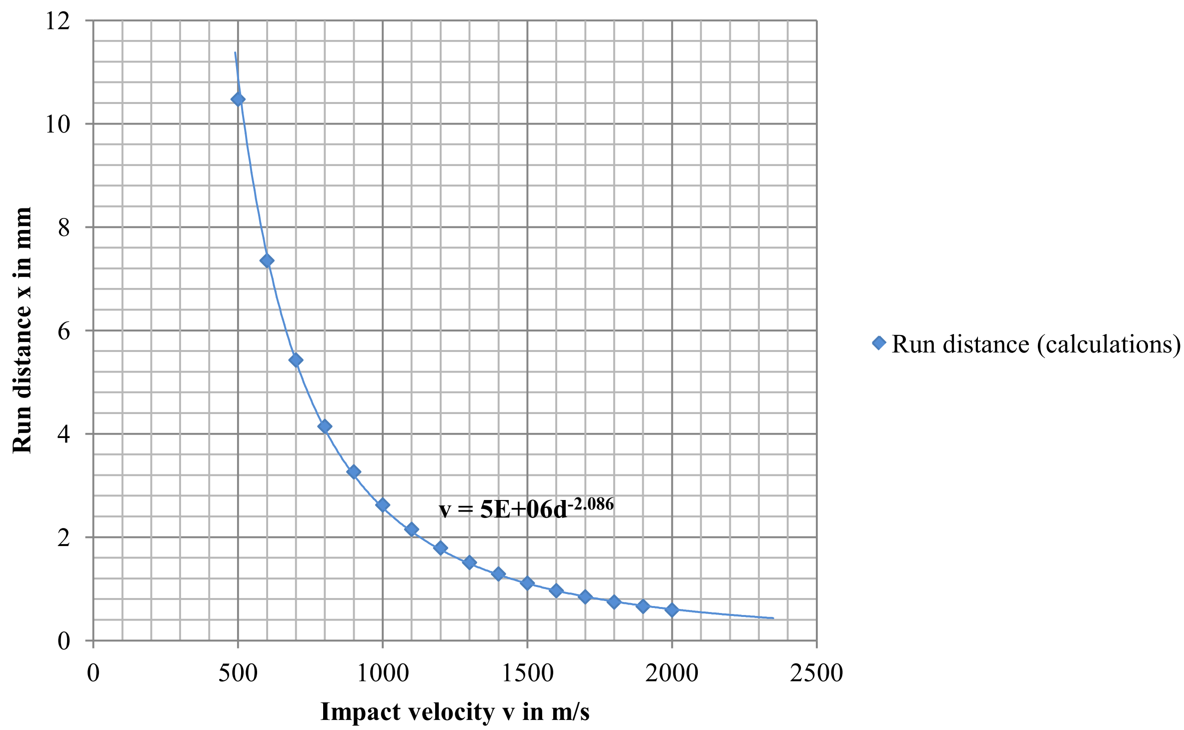

Figure 52: Run distance as a function of the impact velocity. Calculation results obtained for a steel projectile impacting a block of explosive PBX 9404 from Popalato.

According to this plot, the run distance also decreases with the augmentation of the impact velocity. This behavior, however, is better given by an exponential function, whose equation is present next to the plot.

The simulation results from the arrangement described in subchapter A, part 3 of chapter V have been plotted in figure 53. So have been the theoretical results presented above. By plotting the results, the Go/No Go threshold values of PBX 9404[68] have to be taken into consideration for each projectile diameter, so that a delimitation between the "physical correct" and "physical incorrect" results can be fixed. "Physical correct" means that the run distances are consistent with the Go/No Go threshold velocities observed in the precedent simulations, while "physical incorrect" means that these values cannot exist in the reality. Only the "physical correct" results have been plotted:

68 These values have been obtained in chapter VI, subchapter A, part 3.

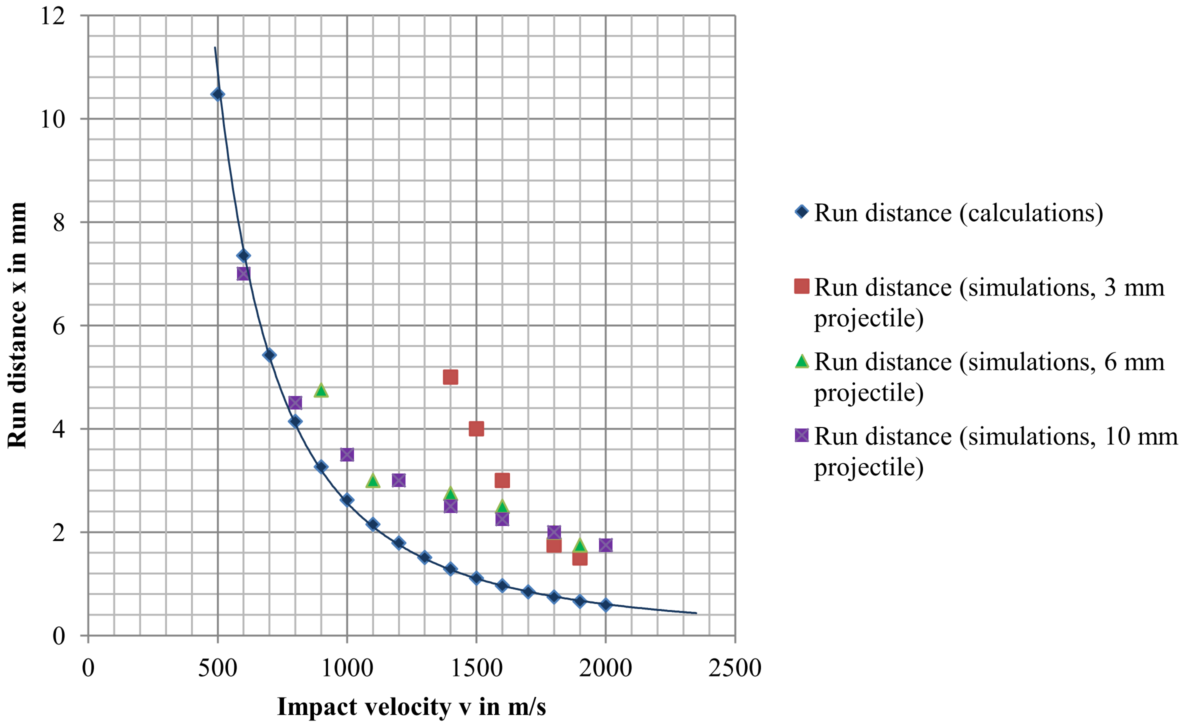

Figure 53: Run distance as a function of the impact velocity for different projectile diameters. Simulation and calculation results obtained for a steel projectile impacting a bare block of explosive PBX 9404 by a zoning of 4 cells/mm.

The plots are all different. The differences are one more time more important for the smaller diameters than for the larger ones. If the plots for the 6 mm and 10 mm projectile simulations seem to be relatively close from the theoretical results, the plot for the 3 mm projectile shows much more important differences which trend to be attenuated by the larger diameters.

3. Rarefaction effects

The distances x' over which the shock maintains constant peak pressure have been calculated[69] for the three "small" steel projectile lengths tested in this thesis[70] (1 mm, 2 mm and 3 mm) impacting a block of bare PBX 9404 and plotted as a function of the

[69] See equation in chapter III, subchapter D, part 3.

[70] See Results in chapter VI, subchapter D, part 2.

projectile velocity in figure 54. The results obtained for the run distances x[71] obtained by the calculations and by the simulations concerning the 6 mm and the 10 mm projectile diameters have been plotted in the same chart to estimate the cases in which the run distances x are larger than the distance x' to point up the situations where the rarefaction effects could influence the initiation and the detonation process. This will be discussed later[72].

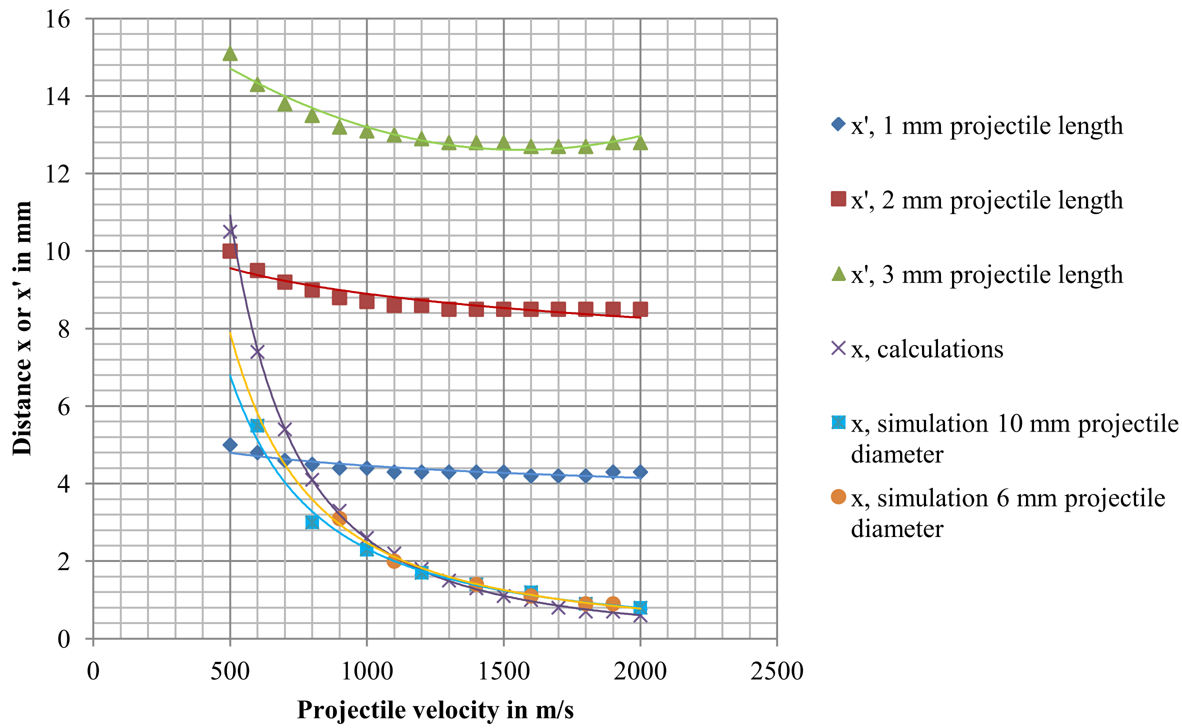

Figure 54: Distances x and x' as a function of the projectile velocity. Simulation and calculation results obtained for a steel projectile impacting a bare block of explosive PBX 9404 by a zoning of 4 cells/mm.

[71] See part 2 of this subchapter.

[72] See chapter VII, subchapter J, part 3

THIS PAGE INTENTIONALLY LEFT BLANK

VII. DISCUSSION OF RESULTS AND NECESSARY ASSUMPTIONS AND POTENTIAL IMPLICATIONS

The discussion of results and the necessary assumptions which are presented in this chapter confirm on the one hand the ability of AUTODYN® to be used as a very accurate software for simulating impact initiation problems for bare and covered explosives (subchapter A and D), and, on the other hand, to set up the computational technique (subchapter A, B, C, D and E) and to obtain data (subchapter G and H) which are needed to analyze some of the statements formulated by Held (subchapter B, D, E and F), especially the ones concerning the initiation criterions (subchapter I). To analyze these statements, "analysis tools" are used (subchapter J).

A. MOULARD EXPERIMENT FOR PBX 9404

The charts which have been plotted under subchapter A of chapter VI have all been put together in the same figure to allow a visual comparison between the different zonings and to help making some statements about the results of these simulations. Experimental results obtained by three other scientists, Weingart, Le Roy Green and James under similar conditions[73] have been put in the figure too.

[73] See chapter IV, subchapter C, part 4.

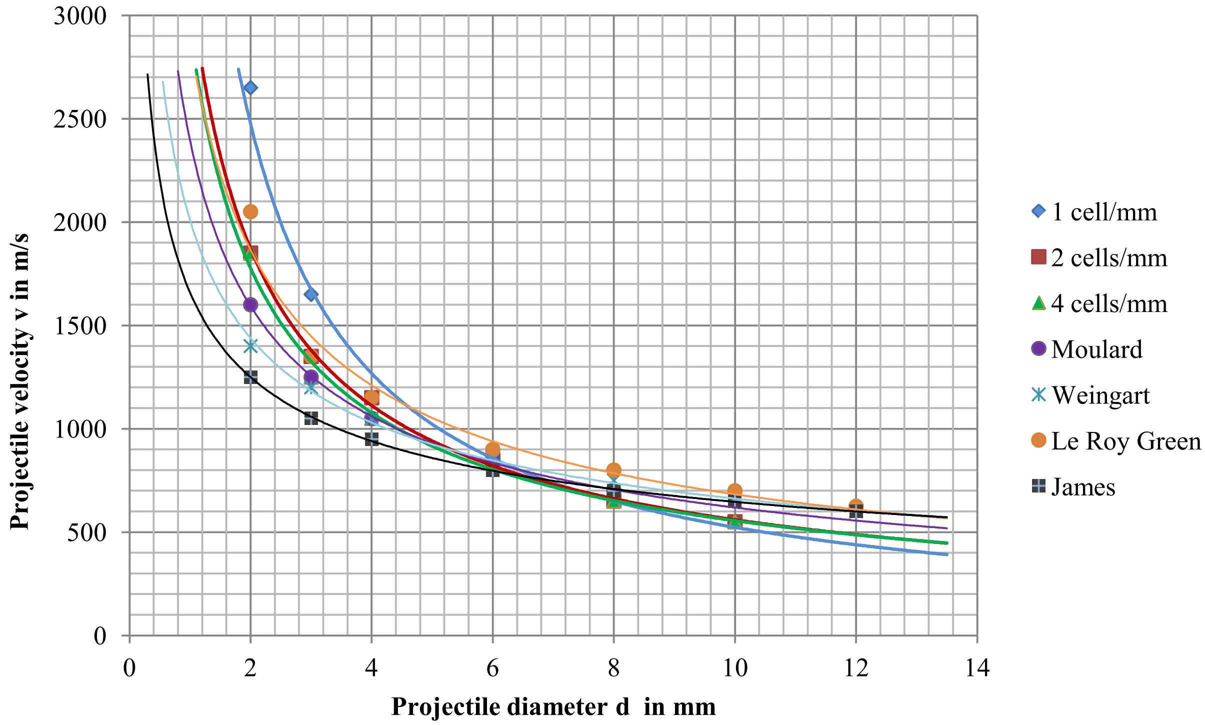

Figure 55: "Go/No Go" velocities as a function of the projectile diameter. Simulation results obtained for a steel projectile impacting a bare block of explosive PBX 9404 by a zoning of 1 cell/mm, 2 cells/mm and 4 cells/mm. Moulard, Weingart, LeRoy Green and James experimental results obtained in the literature [026, 027, 028, 029].

First, it is to notify, that the three simulations with different zoning are all relatively consistent with the results obtained by Moulard, Weingart, Le Roy Green and James, giving similar values, despite some disparities. The most important disparities are between the simulation results and the experimental results of Weingart, LeRoy Green and James. These experimental have been obtained under similar conditions (steel flat nosed projectile and block of PBX 9404), but the exact description is not known. These experimental results can also not be compared one to one. On the contrary, it is possible to compare these simulation results one to one with the Moulard experimental results, and the simulation with 2 cells/mm and 4 cells/mm show a very good match.

That means that AUTODYN® seems to be able to simulate impact initiation experiments with a good accuracy, making its use meaningful for this thesis, and the plots show clearly that that the zoning has an influence on the simulation results. Comparisons with the experimental results supplies: the finer, the more accurate.

Observing the equations of the plots presented in chapter VI, subchapter A, provide an interesting phenomenon: with a finer zoning, the equation of the plot seems to get closer and closer of the form $v = a*d^{-1/2}$, where a is a constant. This trend would confirm the idea of the existence of a more or less constant value of v^2d.

Nevertheless, the results given by the simulations with 2 cells/mm and 4 cells/mm are nearly identical. There are only very small differences for the smaller diameters, which behavior is anyway very volatile. It would also not be very meaningful to improve the accuracy of the zoning: it would only increase the simulation time without giving better results. That's the reason why a zoning of 2 cells/mm has been chosen for nearly all the other simulations[74].

B. EFFECT OF THE LENGTH ON IMPACT INITIATION

The effect of the length of the acceptor charge as well as the effect of the length of the projectile on impact initiation which have been tested before are analyzed below.

1. Effect of the length of the acceptor charge on impact initiation

According to the results plotted in figure 28[75], which cover a large range of lengths, it seems that the length of the acceptor charge has a very limited influence on impact initiation.

Limited, because one interesting effect has to be presented: as already mentioned[76], the impact velocity which was necessary to initiate the 5 mm long acceptor charge by using a

[74] The zoning has just been increased in case of need of more accuracy for special reasons.

[75] See chapter VI, subchapter B, part 1.

10 mm diameter projectile was surprisingly not 550 m/s, but 650 m/s, 100 m/s above the value expected[77]. With regards to a 10 mm diameter projectile, the threshold velocity value for which a detonation within 5 mm (the length of the acceptor charge in that case) still occurs is 600 m/s. This value is got from figure 53[78], which gives the run distance x in mm for the explosive PBX 9404 as a function of the impact velocity of steel a projectile with different diameters.

In other words, it could be that the acceptor charge is not long enough to allow detonation for a certain range of velocities, which are normally the threshold velocities concerning impact initiation with regards to projectile diameters.

As a consequence, it seems that the length of the acceptor charge has no influence on impact initiation, as long as the acceptor charge is longer than the run distances which are normally needed to obtain detonation. Knowing these run distances is also a necessity for setting up correctly the impact initiation problems.

2. Effect of the length of the projectile on impact initiation

According to the results plotted in figures 29 and 30, which as for part 1 of this subchapter cover a large range of lengths, it seems that the length of the projectile has no influence on impact initiation for a ratio "projectile diameter/projectile length" smaller than four. However, for a ratio larger than four, some differences occur. This could be due to some rarefaction effects which could occur by small projectile lengths. This effect has been checked in chapter VII, subchapter J, part 3. Results are conclusive.

As a consequence, the length of the projectile seems to have no influence on impact initiation, as long as the projectile is long enough compared to its diameter. A threshold

---

[76] See chapter VI, subchapter D, part 1.

[77] This value was expected because of precedent results. See chapter VI, subchapter A, part 2.

[78] See Chapter VI, subchapter J, part 2.

value is given by the ratio "projectile diameter/projectile length". The value found in this study is four. Below this value, rarefaction effects can occur and affect the detonation process. Knowledge concerning run distances and rarefaction effects studies are also needed before setting up impact initiation problems.

C. EFFECT OF THE ACCEPTOR CHARGE DIAMETER ON IMPACT INITIATION

The effect of the acceptor charge diameter on impact initiation, which have been tested before, are analyzed below.

According to the results presented in chapter VI, subchapter E, it seems that the acceptor charge diameter has absolutely no influence on impact initiation as long as the acceptor charge diameter is larger or equal to the projectile diameter. For projectile diameters larger than the acceptor charge diameter, a constant initiation velocity is reached. This velocity corresponds to the threshold velocity obtained by impacting a projectile against a block of explosive with the same diameter

An explanation for this behavior could be related to the impact surface criterion, defined by Held [007]. Indeed, the impact surface is limited by the diameter of the acceptor charge. Having a projectile diameter larger than the acceptor charge diameter does not increase the impact surface. The explosive should also not be easier to initiate.

D. EFFECT OF A BARRIER ON IMPACT INITIATION

Discussion concerning the effect of a barrier (nature of the barrier, thickness) which has been tested in this thesis is presented below.

1. Ability of AUTODYN® to simulate impact initiation problems involving covered explosives

The plot of the results in figure 34[79] concerning the 2 mm tantalum barrier match nearly perfectly with the experiment results of James, Haskins and Cook [029], and are very consistent with the same ones obtained from Moulard [027] under similar conditions. This confirms the fact, that the simulation results obtained with AUTODYN® for a covered explosive are consistent with the reality, making AUTODYN® best adapted for simulating this art of problems.

2. Effect of the thickness of a barrier on impact initiation

The results obtained in chapter VI, subchapter D, part 1, show that the presence of a barrier in front on the impact side of the acceptor charge increases the projectile velocity which is necessary to initiate it. According to the plots, the thicker the barrier, the more important the threshold velocity.

This observation seems to confirm the idea that the presence of a barrier on the impact side of an acceptor charge acts as an attenuator, absorbing the energy of the shock. Having a look at figure 35[80] confirms this assumption. Indeed, considering a 8 mm diameter projectile launching against a covered (5 mm barrier) block of PBX 9404 at 700m/s (the threshold velocity with no barrier), the pressure along the centerline is decreasing within the steel barrier, reaching a value around 0.035 Mbar[81] (3.5GPa) at the interface Steel/PBX 9404. Without the steel barrier, the pressure at this interface would

[79] Chapter VI, subchapter D, part 2.

[80] See chapter VI, subchapter D, part 1.

[81] This value has been obtained by taking the average value between the value of the last cell along the centerline on the steel side (0.046 Mbar) and the value of the first cell along the centerline on the PBX 9404 side (0.024 Mbar).

have been 0.045 Mbar, according to figure 50[82], which should have been enough to obtain, at term, a detonation.

3. Effect of the nature of a barrier on impact initiation

Figure 35[83] shows the differences due to the nature of the barrier on impact initiation. According to the plots, the nature of the barrier does have an influence on impact initiation. However, it can't be find what exactly is responsible for these differences. Indeed, the densities alone can't explain it, because steel, for example, has the largest density (7.896 g/cm^3, at least three times higher as the two other ones) and its plot is, despite it, more or less contained between the two others.

E. EFFECT OF A CONFINEMENT ON IMPACT INITIATION

Discussion concerning the effect of a confinement on impact initiation, based on the simulation results obtained in the precedent parts, is presented below.

To make a statement about the effect of a confinement on impact initiation, it is meaningful to regroup some of the plots together, which could help to show this effect. This has been done in figure 56.

[82] See chapter VI, subchapter J, part 1.

[83] See chapter VI, subchapter D, part 2.

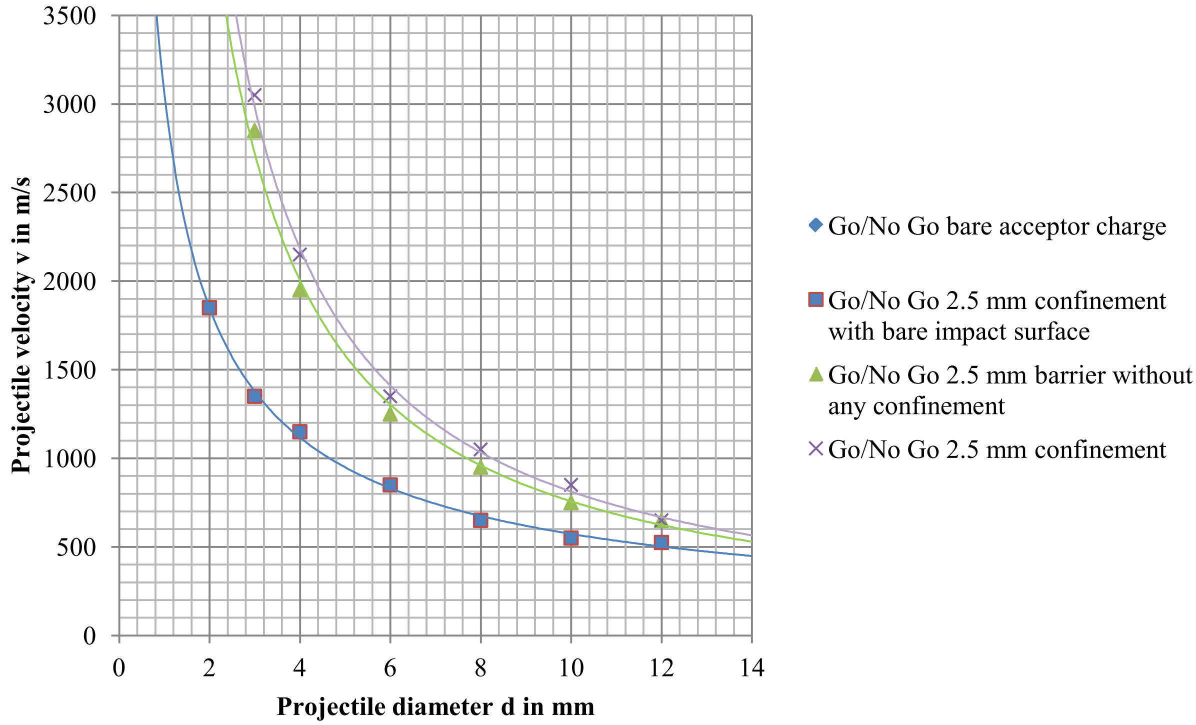

Figure 56: "Go/No Go" velocities as a function of the projectile diameter for a bare acceptor charge, a 2.5 mm confined bun uncovered acceptor charge, a 2.5 mm covered but unconfined acceptor charge and a 2.5 mm completely confined acceptor charge. Simulation results obtained for a steel projectile impacting a block of explosive PBX 9404 by a zoning of 2 cells/mm.

First of all, it seems that the presence of a confinement around an explosive with a bare impact surface[84], regardless to the run distance and to the run time, has no influence on impact initiation. Adding a 2.5 mm barrier on the impact side of the acceptor charge, making it completely confined in a 2.5 mm thick confinement, has a very strong influence. We could have expected, assuming our former results, that the threshold impact velocities would have increased to the values found for a block of PBX 9404 covered by a 2.5 mm thick steel barrier, but they haven't. The threshold velocities have increased to values that are higher than these ones.

In the case of a completely confined acceptor charge, the steel barrier is in contact with all other steel portions. The remain mass of steel is also more important. As steel seems

[84] In other words no confinement on the impact surface, but everywhere else.

to absorb the energy of the shock, it is very possible that a more important mass of steel absorbs more energy. This releases on the observation that increasing the thickness of the steel barrier make a detonation more difficult to obtain.

As a consequence, a confinement around an explosive with a bare impact side has no influence on impact initiation. However, a confinement all around an explosive make it more difficult to detonate than with the presence of a simple barrier, with the same thickness as the confinement, on the impact side of the acceptor charge.

F. EFFECT OF AN AIR GAP BETWEEN BARRIER AND ACCEPTOR CHARGE ON IMPACT INITIATION

The effect of the presence of an air gap between barrier and acceptor charge of an explosive is discussed in this subchapter. Interpretations and statements are based on the results obtained in the precedent chapters.

The plots of figure 38[85] are quite interesting. According to the description of the plots in the precedent chapter, large air gaps (larger than 0.5 mm) seem to make impact initiation more difficult, while small air gaps (less than 0.5 mm) seem to facilitate it for large diameters.

On the one hand, one important effect which could explain the trend that the presence of an air gap generally makes impact initiation more difficult is directly perceptible during the simulation. Indeed, the impact of the steel projectile in the steel barrier engenders a deformation of the barrier which extends within the air gap. This can be seen in figure 58. As a consequence, the effective surface which comes in contact with the block of explosive is smaller than it would be without an air gap. And, according to the surface criterion, it's more difficult to initiate an explosive with a smaller surface. Furthermore,

[85] See chapter VI, subchapter F.

the larger the air gap, the smaller the contact surface. This is exactly what has been observed for the 0.5 mm, 1 mm and 2 mm air gaps.

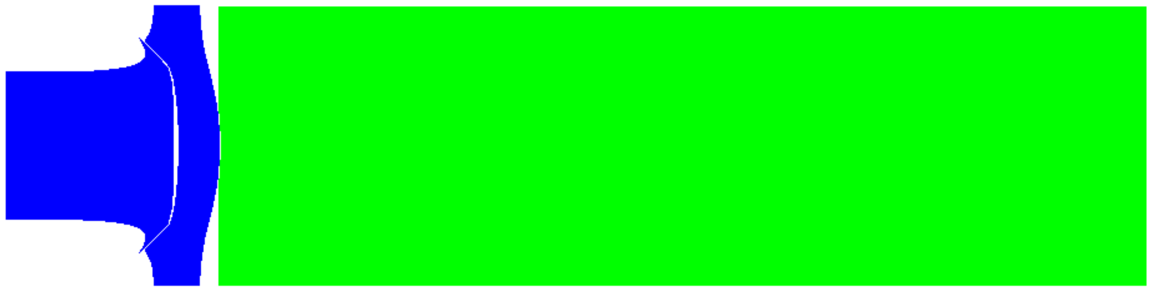

Figure 57: Visualization of the deformation effect due to the presence of an air gap between barrier and acceptor charge.

On the other hand, and as Held already observed[86], some other effects could engender a contrary effect, which has been observed above for small air gaps and large diameters. The main reason would be that the explosive could be pre-compressed by the bulging of the barrier plate while being impacted. The other reason mentioned, that a large-area spray of fragments emerging from the barrier increases the contact area with explosive is in that case not right, because the steel barrier is only deformed and not fragmented[87]. The resulting contact surface, as already explained above, is then smaller than it would be without an air gap. The difference with Held is that the simulation has been realized by impacting a projectile and not a jet. That's why his last assumption about this effect[88] could not be verified either.

The influence of an air gap on impact initiation is also a complex effect. On the one hand, large air gaps contribute to decrease the effective impact surface of the barrier on the acceptor charge making impact initiation more difficult, but on the other hand, the pre-compression of the acceptor charge due to the bulging of the barrier plate while being impacted contribute to facilitate the initiation of the acceptor charge, especially by small

[86] See Chapter II, subchapter A.

[87] See figure 57.

[88] See chapter II, subchapter A.

air gaps and large projectile diameters. The effect of air gaps on impact initiation seems also to be a mix of these two contrary effects.

G. STUDY OF OTHER EXPLOSIVES

A discussion concerning the study of other explosives is presented in this subchapter.

The charts which have been plotted under subchapter B of chapter VI have all been put together in the same figure:

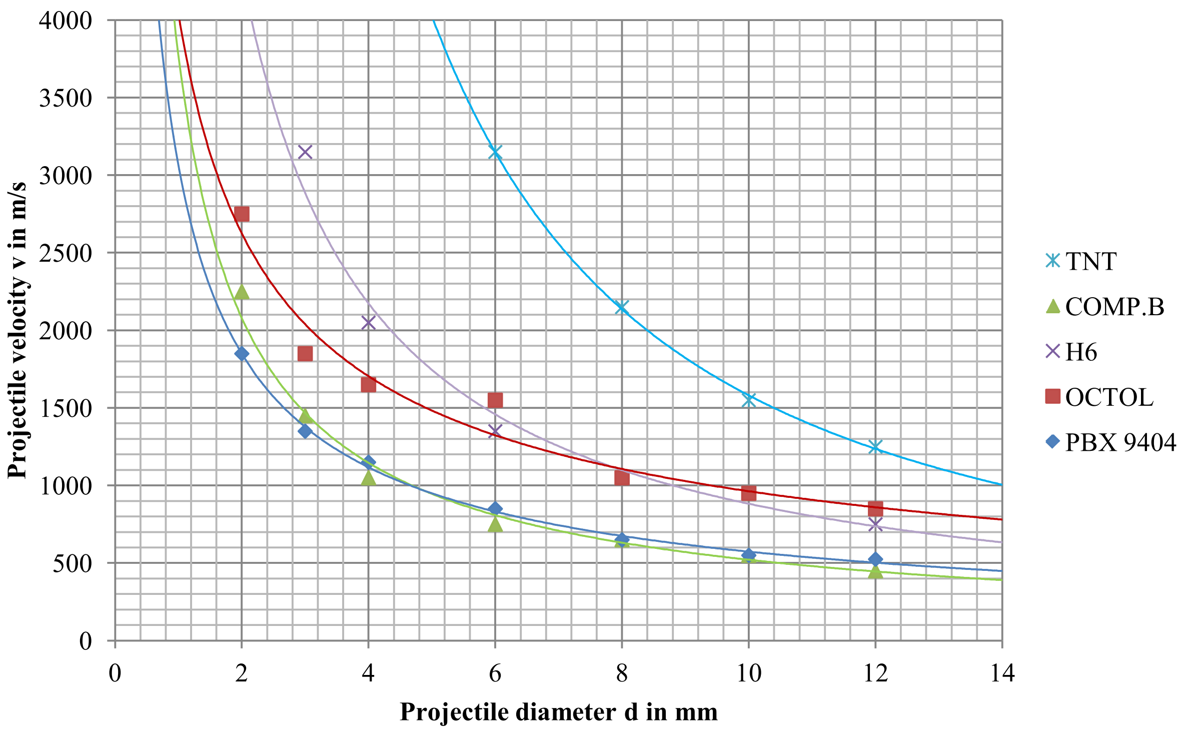

Figure 58: "Go/No Go" velocities as a function of the projectile diameter for different types of explosives. Simulation results obtained for a steel projectile impacting a bare block of explosive by a zoning of 2 cells/mm. The legend is ordered with regards to the explosive densities, going from the lowest (TNT) to the highest (PBX 9404).

All explosives seem to show very different trend with regards to impact initiation. As an example, a more than four times higher projectile velocity is needed to make TNT detonating with a 6 mm projectile diameter compared to make Comp. B detonating with this same projectile. The density alone is not responsible for this effect. Differences in the physical properties of the explosives make them reacting on a different way and with different sensitivities to initiation stimuli.

As a consequence, and as Held already observed in his studies [006], all explosives should have their own "projectile velocity" vs. "projectile diameter" chart. This chart has to be known in order to be successful in making an explosive detonating through impact initiation. Furthermore, the use of a "power" function to get a trend line of this behavior seems to be very appropriate. Testing a block of explosive with some diameters, preferably good distributed in the considered study area, is also enough to get a plot and an equation describing very well the "impact initiation condition".

The equations of the five explosives impacting in this thesis with a steel projectile are presented below in table 25. Each equation allows to define the critical diameter needed to obtain a detonation under knowledge of the projectile velocity used, or to evaluate the critical velocity under knowledge of the projectile diameter:

Explosive	Density (g/cm^3)	Equation
PBX 9404	1.84	$v = 3061*d^{-0.73}$
Octol (70/30)	1.80	$v = 4043*d^{-0.62}$
H6	1.75	$v = 8507*d^{-0.98}$
Comp. B (65/35)	4.72	$v = 3773*d^{-0.86}$
TNT (cast)	1.63	$v = 35246*d^{-1.35}$

Table 23: Equations connecting the projectile impact velocity with the projectile diameter for five different explosives and a steel projectile. Results obtained by simulations with a zoning of 2 cells/mm.

The information obtained in this part will be furthermore very helpful to estimate the values of the different initiation criterions checked in this thesis[89].

[89] See subchapter I of this chapter.

H. EFFECT OF THE PROJECTILE MATERIAL ON IMPACT INITIATION

The effect of the projectile material on impact initiation is discussed below.

The charts which have been plotted under subchapter C of chapter VI and the chart of part 2, subchapter B of chapter VI have all been put together in the same figure to facilitate comparisons and interpretations:

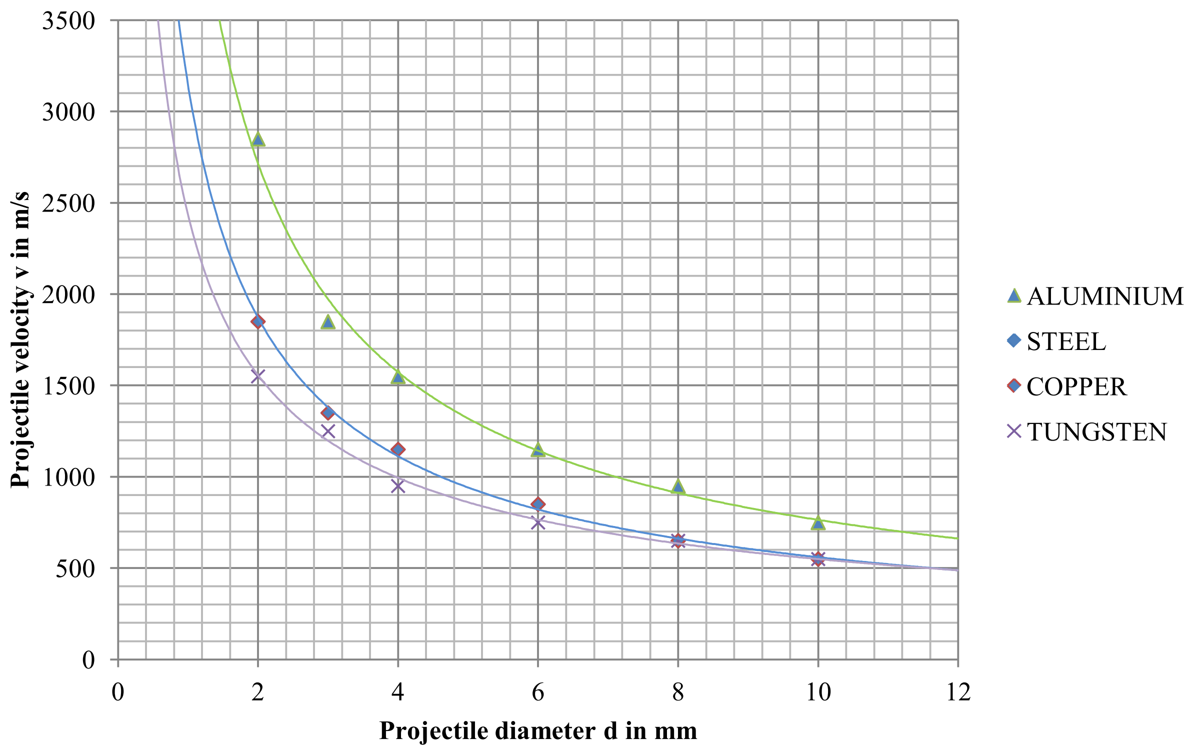

Figure 59: "Go/No Go" velocities as a function of the projectile diameter for different projectile materials. Simulation results obtained for a projectile impacting a bare block of explosive PBX 9404 by a zoning of 2 cells/mm. The legend is ordered with regards to the material densities, going from the lowest (aluminum) to the highest (tungsten).

These plots show clearly, that the impact initiation of a given explosive depends on the nature of the projectile.

The plots for steel and copper have exactly the same trend. One of the particularity of these two materials is that they have nearly the same density (7.90 g/cm^3 vs. 8.93 g/cm^3), while tungsten and aluminum have really different ones (19.22 g/cm^3 vs. 2.71 g/cm^3). If these four materials are ordered with density as a criterion, from the smallest densities to the largest, we get the succession aluminum, steel, copper and finally tungsten. This is exactly the succession obtained in figure 60. It seems to be the following rule: the more important the density, the easier the impact initiation.

Furthermore, it would be interesting to find a good mathematical correlation between the impact initiation and the density of the projectile. This correlation could be given by the Held u^2d, the Mader $\rho v^2 d$ or the Chick $\sqrt{\rho} v^2 d$. This will be checked in the next subchapter.

I. V^2D AND U^2D HELD CRITERIONS

The values of the two Held criterions, as well as the values of the Mader, Chick and the Pd energy criterions have been compared with each other to see what criterion seem to be the best to describe the critical conditions, combining the projectile impact velocity with the projectile diameter, needed to initiate an explosive with different projectile materials. Assuming the precedent results concerning the setup of the computational technique, the values of the presented criterions have been estimated using the simulations results for bare explosives by a standard arrangement[90], giving in that way an arrangement restriction to their use.

1. Explosive PBX9404 , different projectiles

According to the analyze of Dr. Held and some colleagues of him, the four initiation criterions should be constant for all diameters with regards to the same projectile. Having a simple look at the tables in chapter VI, subchapter I, part 1 can't convince us about it. The values are for each criterion all pretty different.

[90] This is the arrangement used in chapter V, subchapter A, in which the detonation process is not affected by any length, width, barrier, confinement or air gap effect.

To analyze in more details the disparities between the values for different diameters of the same projectile ("in the vertical") and the disparities between the values for a same diameter of different projectiles ("in the horizontal"), the ratio "largest value/smallest value" has been built in each of these two cases. After that, the average value has been calculated. This has been done for the v^2d, u^2d, ρv^2d, $\sqrt{\rho}v^2d$ and Pd criterions.

"In the vertical", the v^2d, u^2d, ρv^2d and $\sqrt{\rho}v^2d$ criterions give the same ratio variation average value of about 2.45. That means that the largest value is about 2.5 larger than the smallest one, attesting of large disparities. This value is the same for these four criterions, because they are directly linked with each other (the only difference is a density factor which has no influence by building a ratio). Concerning the Pd criterion, the ratio average value is about 1.17, more than two times smaller.

"In the horizontal", the ratio variation average values, all different because of the different density factors which can compress the individual values, have been plotted in figure 60.

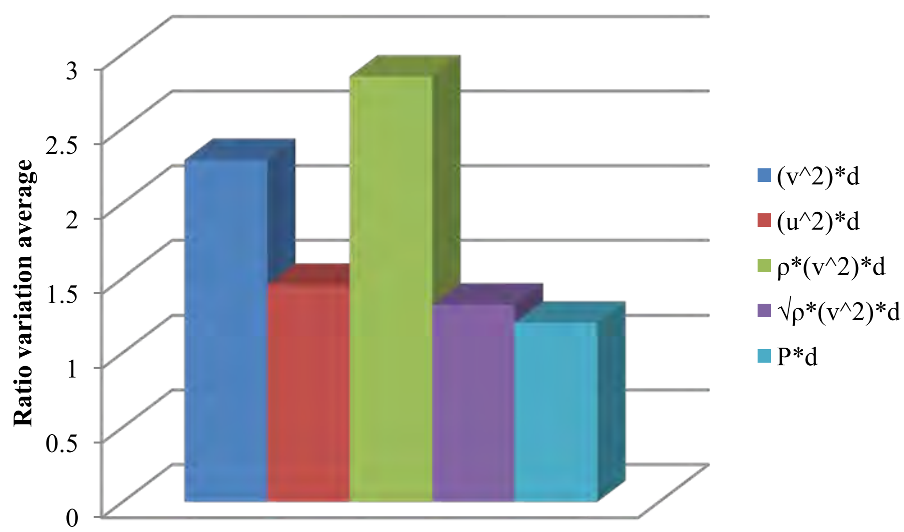

Figure 60: Horizontal criterion for the explosive PBX 9404 and different projectiles. Values obtained from the calculations presented in tables 6, 7, 9 and 10[91].

[91] See chapter VI, subchapter I, part 1.

According to this figure, the largest disparities appear for the v^2d (with 2.29) and ρv^2d (with 2.85) criterions. Concerning the v^2d criterion, as Held explained [016], this criterion is not adapted to compare values which have been obtained by impacting projectile of different materials on a same explosive. Indeed, this criterion does not take into account the differences between the projectile densities, which are really important for impact initiation, as shown before[92]. The ρv^2d takes it into account, but the correction factor seems to be too high. The u^2d (with 1.45) criterion, which takes into consideration the projectile density as well as the explosive density in the cratering velocity[93] u, seems better adapted. Held gave this criterion as a better one compared to the Chick $\sqrt{\rho}v^2d$ criterion [016], but it seems that the Chick $\sqrt{\rho}v^2d$ criterion (with 1.32), which is a sort of "compression" of the Mader ρv^2d criterion, shows less disparities between its values. Anyway, the smallest ratio variation average value is obtained by the P*d criterion (with 1.2).

Furthermore, the ratio "standard deviation σ/average" has been calculated for the five criterions with regards to the four projectiles and the explosive PBX 9404 to confirm the trend, that the Pd criterion is in that case better adapted:

	σ/average v^2d, u^2d, $\sqrt{\rho}v^2d$, ρv^2d	**σ/average Pd**
Steel	30.2 %	4.0 %
Copper	30.2 %	3.7 %
Aluminum	39.1 %	6.4 %
Tungsten	19.6 %	9.5 %

Table 24: σ/average for the tables 10 to 13[94]

These results are final.

[92] See subchapter H of this chapter.

[93] Definition in chapter II, subchapter A.

[94] See chapter VI, subchapter I, part 1.

2. Steel projectile, different explosives

The ratios "largest value/smallest value" of different explosives impacting by a steel projectile have only been calculated "in the vertical"[95]. The average has after that been estimated. Calculating them "in the horizontal" does not make sense, because all explosives are different, giving different values which can also not be compared with each other.

"In the vertical", the values obtained by the v^2d, u^2d, ρv^2d and $\sqrt{\rho}v^2d$ criterions are still the same between them, 3.1 in that case, because, as already explained, these four criterions are linked together. The Pd criterion, with a value of 1.57, about twice smaller, is quite better.

The ratio "standard deviation σ/average" has been calculated again for the five criterions with regards to the five explosives and the steel projectile to confirm the trend, that the Pd criterion is in that case, again, better adapted:

	σ/average v^2d, u^2d, $\sqrt{\rho}v^2d$, ρv^2d	**σ/average** **Pd**
PBX 9404	31.2 %	4.0 %
Comp. B	57.2 %	21.7 %
Octol	24.4 %	14.2 %
H6	62.8 %	21.4 %
TNT	52.2 %	27.8 %

Table 25: σ/average for the data of chapter VI, subchapter I concerning the explosives PBX 9404, Comp. B (65/35), Octol (70/30), H6 and TNT.

Here too, the results concerning the Pd criterion show much less disparities, making the Pd criterion doubtless better adapted.

[95] See precedent part.

3. Conclusions

According to the results obtained through the different experiments realized with different projectiles and different explosives, the initiation criterions given by Held, Chick or Mader are not constant values, but more a range of values, specific to an explosive, tending to get always smaller with the increase of the projectile diameter. Impacting different explosives with the same projectile make these four criterions equal. However, the Chick $\sqrt{\rho} v^2 d$ criterion seems to be the best adapted initiation of these four criterions for comparison purposes by impacting explosives with different projectiles. The Held u^2d remains good adapted too. However, a more accurate criterion, involving the projectile velocity as well as the projectile diameter, based on an energy basis seems to be better adapted; this is the Pd criterion. Standard deviations and ratio variation average values are indeed quite smaller.

Concerning the explosives which have been tested in this thesis, and assuming the fact that the values are issued from an impact initiation with a steel projectile, following results have been found with regards to the v^2d, u^2d, ρv^2d ,$\sqrt{\rho} v^2 d$ and Pd criterions for diameters going from 2 mm to 12 mm:

	v^2d ($mm^3/\mu s^2$)	**u^2d ($mm^3/\mu s^2$)**	**$\sqrt{\rho} v^2 d$ $\sqrt{(g/cm^3)}.mm^3/\mu s^2$**	**$\rho v^2 d$ ($g/cm^3.mm^3/\mu s^2$)**	**Pd (cal/cm²)**
PBX9404	4.5±1.4	2.05±0.6	12.7±4.0	35.7±11.1	793±32
Comp. B	4.7±2.7	2.2±1.3	13.3±7.6	37.3±21.3	691±150
Octol	11.0±2.7	5.1±1.2	31.0±7.6	87±21	1460±208
H6	13.7±8.6	6.3±4.0	38.5±24.2	108±68	1572±337
TNT	34.8±18.2	16.5±8.6	97.9±51.1	275±143	3049±849

Table 26: v^2d, u^2d ,$\sqrt{\rho} v^2 d$, ρv^2d and Pd criterions for diameters going from 2 mm to 12 mm. Results obtained by impacting a steel projectile on different bare explosives and issued from chapter VI, subchapter I.

J. PRESSURE AT THE IMPACT SURFACE, RUN DISTANCES AND RAREFACTION EFFECTS

Discussions concerning the results of the three analysis criterions, mainly used in this thesis to explain some of the effects which have been described above, are presented in this subchapter.

1. Pressure at the impact surface

With the results obtained in chapter VI, subchapter J, the theoretical results have been confronted to the simulation results to verify and validate the use of Hugoniot analysis.

Concerning the interface Steel/Steel, the simulations results, respectively given by the information caught from the fixed gauge on the explosive and from the moving gauge on the projectile, match perfectly with the calculations. AUTODYN® and theory are also very consistent. This also confirms and validates the use of Hugoniot analysis for inert-inert impacts.

Concerning the interface Steel/PBX 9404, some differences occur. The calculations and the simulation results given by the moving gauge are very close, but a constant difference of about 0.01 Mbar (1 GPa) remains for the complete study area. Because it is constant, it could be explained through the simulation code of AUTODYN® which could use other values or parameters than the ones which were used to calculate it. The simulation results obtained from the fixed gauge on the explosive show from a velocity between 500 m/s and 600 m/s a difference with the calculations which grows with the increase of the projectile velocity. This gauge is placed on the explosive which is in that case detonating for a projectile velocity of 550 m/s[96]. This detonation, even if it is just starting at the time when the gauge got the pressure value, makes the pressure increasing, probably being

[96] This is the Go/No Go threshold value for a 10 mm diameter steel projectile impacting a bare block of PBX 9404. See chapter VI, subchapter A, part 3.

responsible for the values differences with the calculations. The growth of the difference could be explained through the intensity of the detonation, which is increasing with the impact velocity.

Consistence between calculations and simulations concerning interface pressures confirm the fact, that the pressure analysis can be used if necessary to check and analyze results whom experiences have been simulated with AUTODYN®. This also confirms and validates the use of Hugoniot analysis for inert-reactive impacts.

2. Run distances

The different plots obtained in figure 54[97] give information about the length of run distances of different projectile diameters as a function of the projectile velocity. Results obtained for the 6 mm diameter and 8 mm diameter are close to the calculation results, but show small differences with it and even differences between them. The results from the 3 mm diameter projectile are very different from the other ones.

Interesting is, according to the theory, that the run distances should just depend on the initial impact pressure and some explosive constants. The initial impact pressure should itself just depend on Hugoniot constants and impact velocity. As a consequence, the run distances should not depend on the projectile diameter. However, the simulation results provide something else, showing that the projectile diameter has a strong influence on the run distances. This is true for the three different diameters which have been tested, and especially for the smaller one, whom strong differences could question the consistence of the results.

[97] See Chapter VI, subchapter J, part 2.

3. Rarefaction effects

According to the results obtained in the precedent chapter, it is possible to find the run distances x for which the distance x' over which the pressure is not affected by the rarefaction effects. With regards to the critical velocities needed to obtain a "prompt" detonation, the simulation results for the 6 mm projectile diameter show that the rarefaction effects can't affect the detonation process, because the distance x' is in each case larger than the run distance x. However, this is not the case concerning the calculation results for x for the velocities smaller than 750 m/s: in that case, rarefaction effects can affect the process (x' smaller than x) with a 1 mm projectile length and by velocities around 500 m/s or smaller for a 2 mm projectile length. The same effect appears for the 10 mm projectile diameter plot with velocities smaller than 600 m/s.

Having a look at the "projectile velocity" vs. "projectile diameter" plot for the 1 mm and 2 mm projectile lengths[98], give the information that the critical velocities noted down to initiate the block of explosive PBX 9404 with a steel projectile of these lengths and concerning a projectile diameter of 10 mm are a little higher as normally required[99]. This matches perfectly with the cases found above, confirming that the rarefaction effects can affect the detonation process by small projectile lengths. The reason for the effect of the projectile length on impact initiation studied before seems to have been found.

[98] See figure 30, chapter VI, subchapter B, part 1.

[99] Based on a 10 mm long projectile basis and a bare explosive, 750 m/s v05 s. 550 m/s (1 mm projectile length) and 650 m/s vs. 550 m/s (2 mm projectile length).

THIS PAGE INTENTIONALLY LEFT BLANK

VIII. CONCLUSIONS

Close examination of the experimental data proposed by Held and others to rate the relative threshold sensitivity of explosives to impact (incl., (v^2d), (u^2d), (ρv^2d) and ($\rho^{1/2}v^2d$)) have been found to deviate significantly from constancy. These deviations might result in part to shaped charge jet impact data, since accurate measure of impactor characteristics at impact are difficult. There is concluded that the product of interfacial impact pressure and well-defined projectile diameter is a much more reliable predictor of the impact sensitivity of a bare explosive based on the smaller deviation from mean values relative to the aforementioned terms. As important is that this energy term takes into account the density and Hugoniot properties of the impactor and explosive.

Therefore, experimental data from impacts against bare explosives, covered and confined with and without air gaps, and explosive and projectile dimensions have first been compared with simulation results obtained with the software ANSYS AUTODYN® under similar conditions. Results were conclusive, making AUTODYN® best adapted to simulate impact initiation problems with a great accuracy. Simulations with different zonings have shown that a zoning of 2 cells/mm gives a good accuracy, while keeping quite small simulation times.

This has then been used, on the one hand, to validate finite difference computations required to extend and properly evaluate the database and, on the other hand, to check by the same occasion some of the assumptions or statements formulated by Held in the last decades. In that way, it has been shown that the length of the projectile, materializing the pulse duration, has no influence on the impact initiation process as long as the projectile is long enough, by the critical Go/No Go velocities for a specific diameter, to avoid rarefaction effects. The limit found in this thesis is given by a ratio "projectile diameter/projectile length" of 4. Below this value, rarefaction affects occur, making initiation more difficult to obtain. In the same way, the length of the acceptor charge is unimportant too as long as it is longer than the run distance, which seems to depend on the projectile diameter and on the projectile velocity, that is needed to obtain a full detonation. Plotting the run distances as a function of the projectile velocity for different projectile diameters can help to scale the length of the explosive. Concerning the diameter of this same explosive, it has been shown that this diameter has no influence on impact initiation, as long as it is larger than the diameter of the projectile. For projectile diameters larger than acceptor charge diameters, a constant threshold velocity is reached and is given by the situation in which projectile diameter and acceptor charge diameter are equal. This confirms the utility of a critical impact area criterion. Furthermore, the presence of a barrier attenuates the shock intensity, making covered explosives less easy to initiate. The thicker the barrier, the more effective the attenuation. The nature of the barrier has a role in this process too. The presence of confinement on a non-covered explosive, surprisingly and contradicting the comments of Dr. Held, seems to have no influence on the impact initiation process. However, a covered and confined explosive is more difficult to initiate that a bare explosive, but even more difficult to initiate than a simple covered explosive with the same barrier thickness. Air gaps between barrier and explosive have a very complex effect on impact initiation. Small air gaps (at least less than 0.5 mm), concerning large diameters (at least more than 6 mm), seem to facilitate the initiation of explosives, while large air gaps have exactly the contrary effect.

These effects have been taken into consideration to setup correctly the simulations concerning the impact of a steel projectile on different projectiles (PBX 9404, cast TNT, H6, Comp. B 65/35 and Octol 70/30) and concerning the impact of projectiles made of different materials (steel, copper, aluminum, tungsten) on the explosive PBX 9404. The v^2d, u^2d, ρv^2d, $\sqrt{\rho}v^2d$ and Pd criterions have been calculated for this large choice of explosives and projectiles of much varied properties and sensitivities.

The average Pd-values for the explosives are reported below.

Explosive	**Pd (cal/cm^2)**	**% Deviation**
PBX9404	793±32	4.0
Comp. B	691±150	21.7
Octol	1460±208	14.3
H6	1572±337	21.4
TNT	3049±849	27.9

Pd values and % deviation established in this thesis.

Deviations from mean values of v^2d, u^2d, ρv^2d and $\rho^{1/2}v^2$ are from former treatments in most cases greater than 50 percent. Even with a well prepared explosive like PBX 9404, the v^2d varies over a range of more than 100 percent.

The differences in deviation between PBX9404 and the other explosives most likely results at least in part to preparation. That is, final content distribution and grain size are dependent on the rate of sedimentation of the denser components and the column length and rate of cool-down. Each of these factors can affect impact and shock sensitivity.

THIS PAGE INTENTIONALLY LEFT BLANK

IX. RECOMMENDATIONS

First of all, it is important to notify that the values obtained by the time independent Pd initiation criterion are between 20 and 50 times larger than the ones concerning the critical time dependent energy fluence presented by Cooper [022][100]. One research topic could also focus on comparing these two energy criterions, pointing out the main differences and giving reliable information concerning what one is in typical situations more adapted than the other one.

Some more values could be estimated for the Pd criterion, selecting a more important range of explosives and projectiles. This would contribute to give precise information about their sensitivities. Other initiation criterions could as well be developed and presented, increasing the accuracy of the critical initiation values of each explosive. The Pd energy criterion may not be the best one...

Furthermore, some of the effects which have been highlighted in this thesis seem to be very complex. This is for example the case of the presence of an air gap between barrier and acceptor charge and the effect of the nature of the barrier on impact initiation. Some basis explanations have been formulated to try to explain it, but a more deeper study could be needed to confirm it and to check other reasons that could influence it.

Last but not least, only a few number of assumptions and statements formulated by Dr. Held and concerning impact initiation could have been checked. A more complete study of this topic could also be performed. Other topics, which cover a large range in the immense field of ballistics, have also been treated by Held and could be critique in further studies.

These potential studies, which will take place in the future, may beneficiate from new more performing codes of the software AUTODYN® and more performing computer

[100] See chapter III, subchapter C, part 1, section c).

systems, which will allow to increase significantly the zoning, offering the possibility to obtain more accurate results on specific problems and define more specifically some of the limit values which have been found here.

APPENDIX A: MATERIAL PROPERTIES

The parameters of all the materials which have been used for the simulations in this Thesis are further contained. They have been taken from the AUTODYN® Library. They are very important because they describe the behavior of the considered material.

A. EXPLOSIVES

1. PBX 9404 (PBX9404JJ3)

Equation of State	**Lee-Tarver**
Reference density	1.84200E+00 (g/cm^3)
Parameter A	8.52400E+00 (Mbar)
Parameter B	1.80200E-01 (Mbar)
Parameter R1	4.60000E+00 (none)
Parameter R2	1.30000E+00 (none)
Parameter W	3.80000E-01 (none)
C-J Detonation velocity	8.80000E-01 (cm/us)
C-J Energy / unit volume	1.02000E-01 (Gerg/mm^3)
C-J Pressure	3.70000E-01 (Mbar)
Reaction zone width	2.50000E+00 (none)
Max change in reaction ratio	1.00000E-01 (none)
Ignition parameter I	4.40000E+01 (us)
Ignition reaction ratio exp.	2.22000E-01 (none)
Ignition critical compression	0.00000E+00 (none)
Ignition compression exp.	4.00000E+00 (none)
Growth parameter G1	0.00000E+00 (none)
Growth reaction ratio exp. c	0.00000E+00 (none)
Growth reaction ratio exp. d	0.00000E+00 (none)

Growth pressure exp. y	0.00000E+00 (none)
Growth parameter G2	8.50000E+02 (none)
Growth reaction ratio exp. e	2.22000E-01 (none)
Growth reaction ratio exp. g	6.66000E-01 (none)
Growth pressure exp. z	2.00000E+00 (none)
Max. reac. ratio: ignition	3.00000E-01 (none)
Max. reac. ratio: growth G1	0.00000E+00 (none)
Min. reac. ratio: growth G2	0.00000E+00 (none)
Maximum rel. vol. in tension	1.10000E+00 (none)
Unreacted EOS	JWL
Parameter A	9.52200E+03 (Mbar)
Parameter B	-5.94400E-02 (Mbar)
Parameter R1	1.41000E+01 (none)
Parameter R2	1.41000E+00 (none)
Parameter W	8.86700E-01 (none)
Von Neumann spike rel vol.	7.21000E-01 (none)
C-J Energy / unit volume	-1.50000E-03 (Gerg/mm^3)
Strength	**von Mises**
Shear Modulus	4.54000E-02 (Mbar)
Yield Stress	2.00000E-03 (Mbar)
Failure	**None**
Erosion	**None**
Material Cutoffs	-
Maximum Expansion	1.00000E-01 (none)
Minimum Density Factor	1.00000E-04 (none)
Minimum Density Factor (SPH)	2.00000E-01 (none)
Maximum Density Factor (SPH)	3.00000E+00 (none)
Minimum Soundspeed	1.00000E-10 (cm/us)
Maximum Soundspeed (SPH)	1.01000E+20 (cm/us)

Maximum Temperature	1.01000E+20 (K)
Reference:	Tarver & Hallquist 1981 - 7th Det. Symp. - p. 488

2. TNT (TNTCASTJJ1)

Equation of State	**Lee-Tarver**
Reference density	1.63000E+00 (g/cm^3)
Parameter A	3.71200E+00 (Mbar)
Parameter B	3.23060E-02 (Mbar)
Parameter R1	4.15000E+00 (none)
Parameter R2	9.50000E-01 (none)
Parameter W	3.00000E-01 (none)
C-J Detonation velocity	6.93000E-01 (cm/us)
C-J Energy / unit volume	7.00000E-02 ($Gerg/mm^3$)
C-J Pressure	2.10000E-01 (Mbar)
Reaction zone width	2.50000E+00 (none)
Max change in reaction ratio	1.00000E-01 (none)
Ignition parameter I	5.00000E+01 (/us)
Ignition reaction ratio exp.	2.22000E-01 (none)
Ignition critical compression	0.00000E+00 (none)
Ignition compression exp.	4.00000E+00 (none)
Growth parameter G1	0.00000E+00 (none)
Growth reaction ratio exp. c	0.00000E+00 (none)
Growth reaction ratio exp. d	0.00000E+00 (none)
Growth pressure exp. y	0.00000E+00 (none)
Growth parameter G2	4.00000E+01 (none)
Growth reaction ratio exp. e	2.22000E-01 (none)
Growth reaction ratio exp. g	6.66000E-01 (none)
Growth pressure exp. z	1.20000E+00 (none)

Max. reac. ratio: ignition	3.00000E-01 (none)
Max. reac. ratio: growth G1	0.00000E+00 (none)
Min. reac. ratio: growth G2	0.00000E+00 (none)
Maximum rel. vol. in tension	1.10000E+00 (none)
Unreacted EOS	JWL
Parameter A	1.79800E+01 (Mbar)
Parameter B	-9.31000E-01 (Mbar)
Parameter R1	6.20000E+00 (none)
Parameter R2	3.10000E+00 (none)
Parameter W	8.92600E-01 (none)
Von Neumann spike rel vol.	6.28500E-01 (none)
C-J Energy / unit volume	-1.54000E-03 (Gerg/mm^3)
Strength	**von Mises**
Shear Modulus	2.90000E-02 (Mbar)
Yield Stress	1.00000E-03 (Mbar)
Failure	**None**
Erosion	**None**
Material Cutoffs	-
Maximum Expansion	1.00000E-01 (none)
Minimum Density Factor	1.00000E-04 (none)
Minimum Density Factor (SPH)	2.00000E-01 (none)
Maximum Density Factor (SPH)	3.00000E+00 (none)
Minimum Soundspeed	1.00000E-10 (cm/us)
Maximum Soundspeed (SPH)	1.01000E+20 (cm/us)
Maximum Temperature	1.01000E+20 (K)
Reference:	Lee & Tarver 1980 - Phys. Fluids - p. 2362

3. H6 (H6SJ1)

Equation of State	Lee-Tarver
Reference density	1.75000E+00 (g/cm^3)
Parameter A	7.58020E+00 (Mbar)
Parameter B	8.51300E-02 (Mbar)
Parameter R1	4.90000E+00 (none)
Parameter R2	1.20000E+00 (none)
Parameter W	2.00000E-01 (none)
C-J Detonation velocity	7.36700E-01 (cm/us)
C-J Energy / unit volume	1.03000E-01 (Gerg/mm^3)
C-J Pressure	2.45000E-01 (Mbar)
Reaction zone width	2.50000E+00 (none)
Max change in reaction ratio	1.00000E-01 (none)
Ignition parameter I	4.00000E+02 (us)
Ignition reaction ratio exp.	2.22000E-01 (none)
Ignition critical compression	2.00000E-02 (none)
Ignition compression exp.	4.00000E+00 (none)
Growth parameter G1	3.77000E+02 (none)
Growth reaction ratio exp. c	2.22000E-01 (none)
Growth reaction ratio exp. d	6.67000E-01 (none)
Growth pressure exp. y	2.20000E+00 (none)
Growth parameter G2	0.00000E+00 (none)
Growth reaction ratio exp. e	0.00000E+00 (none)
Growth reaction ratio exp. g	0.00000E+00 (none)
Growth pressure exp. z	0.00000E+00 (none)
Max. reac. ratio: ignition	3.00000E-01 (none)
Max. reac. ratio: growth G1	1.00000E+00 (none)
Min. reac. ratio: growth G2	1.00000E+00 (none)

Maximum rel. vol. in tension	1.10000E+00 (none)
Unreacted EOS	Shock
Gruneisen coefficient	1.00000E+00 (none)
Parameter C1	2.75000E-01 (cm/us)
Parameter S1	1.90000E+00 (none)
Parameter Quadratic S2	0.00000E+00 (us/cm)
Relative volume, VE/V0	0.00000E+00 (none)
Relative volume, VB/V0	0.00000E+00 (none)
Parameter C2	0.00000E+00 (cm/us)
Parameter S2	0.00000E+00 (none)
Reference Temperature	3.73000E+02 (K)
Specific Heat	0.00000E+00 (Terg/gK)
Thermal Conductivity	0.00000E+00 (Terg/cmKus)
Strength	**von Mises**
Shear Modulus	4.00000E-02 (Mbar)
Yield Stress	2.00000E-03 (Mbar)
Failure	**None**
Erosion	**None**
Material Cutoffs	-
Maximum Expansion	1.00000E-01 (none)
Minimum Density Factor	1.00000E-04 (none)
Minimum Density Factor (SPH)	2.00000E-01 (none)
Maximum Density Factor (SPH)	3.00000E+00 (none)
Minimum Soundspeed	1.00000E-10 (cm/us)
Maximum Soundspeed (SPH)	1.01000E+20 (cm/us)
Maximum Temperature	1.01000E+20 (K)
Reference:	von Rosen 1997 - Unpublished

4. Comp B. (COMPBJJ3)

Equation of State	**Lee-Tarver**
Reference density	1.71700E+00 (g/cm^3)
Parameter A	5.24200E+00 (Mbar)
Parameter B	7.67800E-02 (Mbar)
Parameter R1	4.20000E+00 (none)
Parameter R2	1.10000E+00 (none)
Parameter W	3.40000E-01 (none)
C-J Detonation velocity	7.98000E-01 (cm/us)
C-J Energy / unit volume	8.50000E-02 ($Gerg/mm^3$)
C-J Pressure	2.95000E-01 (Mbar)
Reaction zone width	2.50000E+00 (none)
Max change in reaction ratio	1.00000E-01 (none)
Ignition parameter I	4.00000E+06 (us)
Ignition reaction ratio exp.	6.67000E-01 (none)
Ignition critical compression	0.00000E+00 (none)
Ignition compression exp.	7.00000E+00 (none)
Growth parameter G1	8.50000E+02 (none)
Growth reaction ratio exp. c	2.22000E-01 (none)
Growth reaction ratio exp. d	6.67000E-01 (none)
Growth pressure exp. y	2.00000E+00 (none)
Growth parameter G2	6.60000E+02 (none)
Growth reaction ratio exp. e	3.33000E-01 (none)
Growth reaction ratio exp. g	1.00000E+00 (none)
Growth pressure exp. z	3.00000E+00 (none)
Max. reac. ratio: ignition	2.20000E-02 (none)
Max. reac. ratio: growth G1	6.00000E-01 (none)
Min. reac. ratio: growth G2	0.00000E+00 (none)

Maximum rel. vol. in tension	1.10000E+00 (none)
Unreacted EOS	JWL
Parameter A	7.78100E+02 (Mbar)
Parameter B	-5.03100E-02 (Mbar)
Parameter R1	1.13000E+01 (none)
Parameter R2	1.13000E+00 (none)
Parameter W	8.93800E-01 (none)
Von Neumann spike rel vol.	6.93300E-01 (none)
C-J Energy / unit volume	-6.12000E-03 (Gerg/mm^3)
Strength	**von Mises**
Shear Modulus	3.50000E-02 (Mbar)
Yield Stress	2.00000E-03 (Mbar)
Failure	**None**
Erosion	**None**
Material Cutoffs	-
Maximum Expansion	1.00000E-01 (none)
Minimum Density Factor	1.00000E-04 (none)
Minimum Density Factor (SPH)	2.00000E-01 (none)
Maximum Density Factor (SPH)	3.00000E+00 (none)
Minimum Soundspeed	1.00000E-10 (cm/us)
Maximum Soundspeed (SPH)	1.01000E+20 (cm/us)
Maximum Temperature	1.01000E+20 (K)
Reference:	Tarver 1997 - Unpublished

5. Octol 7030 (OCT7030JJ3)

Equation of State	**Lee-Tarver**
Reference density	1.80400E+00 (g/cm3)
Parameter A	7.13950E+00 (Mbar)

Parameter B	1.28900E-01 (Mbar)
Parameter R1	4.50000E+00 (none)
Parameter R2	1.20000E+00 (none)
Parameter W	3.80000E-01 (none)
C-J Detonation velocity	8.33000E-01 (cm/us)
C-J Energy / unit volume	9.18000E-02 (Gerg/mm3)
C-J Pressure	3.20000E-01 (Mbar)
Reaction zone width	2.50000E+00 (none)
Max change in reaction ratio	1.00000E-01 (none)
Ignition parameter I	4.40000E+01 (/us)
Ignition reaction ratio exp.	2.22000E-01 (none)
Ignition critical compression	0.00000E+00 (none)
Ignition compression exp.	4.00000E+00 (none)
Growth parameter G1	0.00000E+00 (none)
Growth reaction ratio exp. c	0.00000E+00 (none)
Growth reaction ratio exp. d	0.00000E+00 (none)
Growth pressure exp. y	0.00000E+00 (none)
Growth parameter G2	1.30000E+03 (none)
Growth reaction ratio exp. e	2.22000E-01 (none)
Growth reaction ratio exp. g	6.67000E-01 (none)
Growth pressure exp. z	2.50000E+00 (none)
Max. reac. ratio: ignition	3.00000E-01 (none)
Max. reac. ratio: growth G1	0.00000E+00 (none)
Min. reac. ratio: growth G2	0.00000E+00 (none)
Maximum rel. vol. in tension	1.10000E+00 (none)
Unreacted EOS	Shock
Gruneisen coefficient	1.00000E+00 (none)
Parameter C1	2.21000E-01 (cm/us)
Parameter S1	2.51000E+00 (none)

Parameter Quadratic S2	0.00000E+00 (us/cm)
Relative volume, VE/V0	0.00000E+00 (none)
Relative volume, VB/V0	0.00000E+00 (none)
Parameter C2	0.00000E+00 (cm/us)
Parameter S2	0.00000E+00 (none)
Reference Temperature	3.73000E+02 (K)
Specific Heat	0.00000E+00 (Terg/gK)
Thermal Conductivity	0.00000E+00 (Terg/cmKus)
Strength	**von Mises**
Shear Modulus	4.96000E-02 (Mbar)
Yield Stress	2.00000E-03 (Mbar)
Failure	**None**
Erosion	**None**
Material Cutoffs	-
Maximum Expansion	1.00000E-01 (none)
Minimum Density Factor	1.00000E-04 (none)
Minimum Density Factor (SPH)	2.00000E-01 (none)
Maximum Density Factor (SPH)	3.00000E+00 (none)
Minimum Soundspeed	1.00000E-10 (cm/u)
Maximum Soundspeed (SPH)	1.01000E+20 (cm/us)
Maximum Temperature	1.01000E+20 (K)
Reference:	Davison 1992 - ADPA IM Tech. Symp. - p. 423

B. NON EXPLOSIVES

1. Steel (STEEL1006)

Equation of State	**Shock**
Reference density	7.89600E+00 (g/cm^3)
Gruneisen coefficient	2.17000E+00 (none)
Parameter C1	4.56900E-01 (cm/us)
Parameter S1	1.49000E+00 (none)
Parameter Quadratic S2	0.00000E+00 (us/cm)
Relative volume, VE/V0	0.00000E+00 (none)
Relative volume, VB/V0	0.00000E+00 (none)
Parameter C2	0.00000E+00 (cm/us)
Parameter S2	0.00000E+00 (none)
Reference Temperature	3.00000E+02 (K)
Specific Heat	4.52000E-06 (Terg/gK)
Thermal Conductivity	0.00000E+00 (Terg/cmKus)
Strength	**Johnson Cook**
Shear Modulus	8.18000E-01 (Mbar)
Yield Stress	3.50000E-03 (Mbar)
Hardening Constant	2.75000E-03 (Mbar)
Hardening Exponent	3.60000E-01 (none)
Strain Rate Constant	2.20000E-02 (none)
Thermal Softening Exponent	1.00000E+00 (none)
Melting Temperature	1.81100E+03 (K)
Ref. Strain Rate (/s)	1.00000E+00 (none)
Strain Rate Correction	1st Order

Failure	**None**
Erosion	**None**
Material Cutoffs	-
Maximum Expansion	1.00000E-01 (none)
Minimum Density Factor	1.00000E-04 (none)
Minimum Density Factor (SPH)	2.00000E-01 (none)
Maximum Density Factor (SPH)	3.00000E+00 (none)
Minimum Soundspeed	1.00000E-10 (cm/us)
Maximum Soundspeed (SPH)	1.01000E+20 (cm/us)
Maximum Temperature	1.01000E+20 (K)
Reference:	LA-4167-MS. May 1 1969. Selected Hugoniots: EOS 7th Int. Symp. Ballistics. Johnson & Cook

2. Copper

Equation of State	**Shock**
Reference density	8.93000E+00 (g/cm^3)
Gruneisen coefficient	1.99000E+00 (none)
Parameter C1	3.94000E-01 (cm/us)
Parameter S1	1.48900E+00 (none)
Parameter Quadratic S2	0.00000E+00 (us/cm)
Relative volume, VE/V0	0.00000E+00 (none)
Relative volume, VB/V0	0.00000E+00 (none)
Parameter C2	0.00000E+00 (cm/us)
Parameter S2	0.00000E+00 (none)
Reference Temperature	0.00000E+00 (K)
Specific Heat	0.00000E+00 (Terg/gK)

Thermal Conductivity	0.00000E+00 (Terg/cmKus)
Strength	**None**
Failure	**None**
Erosion	**None**
Material Cutoffs	-
Maximum Expansion	1.00000E-01 (none)
Minimum Density Factor	1.00000E-04 (none)
Minimum Density Factor (SPH)	2.00000E-01 (none)
Maximum Density Factor (SPH)	3.00000E+00 (none)
Minimum Soundspeed	1.00000E-10 (cm/us)
Maximum Soundspeed (SPH)	1.01000E+20 (cm/us)
Maximum Temperature	1.01000E+20 (K)
Reference:	LA-4167-MS. May 1 1969. Selected Hugoniots

3. Aluminum

Equation of State	**Shock**
Reference density	2.71000E+00 (g/cm^3)
Gruneisen coefficient	2.10000E+00 (none)
Parameter C1	5.38000E-01 (cm/us)
Parameter S1	1.33700E+00 (none)
Parameter Quadratic S2	0.00000E+00 (us/cm)
Relative volume, VE/V0	0.00000E+00 (none)
Relative volume, VB/V0	0.00000E+00 (none)
Parameter C2	0.00000E+00 (cm/us)
Parameter S2	0.00000E+00 (none)
Reference Temperature	0.00000E+00 (K)
Specific Heat	0.00000E+00 (Terg/gK)
Thermal Conductivity	0.00000E+00 (Terg/cmKus)

Strength	**von Mises**
Shear Modulus	2.69000E-01 (Mbar)
Yield Stress	2.90000E-03 (Mbar)
Failure	**None**
Erosion	**None**
Material Cutoffs	-
Maximum Expansion	1.00000E-01 (none)
Minimum Density Factor	1.00000E-04 (none)
Minimum Density Factor (SPH)	2.00000E-01 (none)
Maximum Density Factor (SPH)	3.00000E+00 (none)
Minimum Soundspeed	1.00000E-10 (cm/us)
Maximum Soundspeed (SPH)	1.01000E+20 (cm/us)
Maximum Temperature	1.01000E+20 (K)
Reference:	AFATL-TR-84-59. June 1984. Matuska D.A. HULL Users Manual

4. Tungsten

Equation of State	**Shock**
Reference density	1.81000E+01 (g/cm^3)
Gruneisen coefficient	1.58000E+00 (none)
Parameter C1	4.00000E-01 (cm/us)
Parameter S1	1.26800E+00 (none)
Parameter Quadratic S2	0.00000E+00 (us/cm)
Relative volume, VE/V0	0.00000E+00 (none)
Relative volume, VB/V0	0.00000E+00 (none)
Parameter C2	0.00000E+00 (cm/us)

Parameter S2	0.00000E+00 (none)
Reference Temperature	0.00000E+00 (K)
Specific Heat	0.00000E+00 (Terg/gK)
Thermal Conductivity	0.00000E+00 (Terg/cmKus)
Strength	**von Mises**
Shear Modulus	1.60000E+00 (Mbar)
Yield Stress	2.00000E-02 (Mbar)
Failure	**None**
Erosion	**None**
Material Cutoffs	-
Maximum Expansion	1.00000E-01 (none)
Minimum Density Factor	1.00000E-04 (none)
Minimum Density Factor (SPH)	2.00000E-01 (none)
Maximum Density Factor (SPH)	3.00000E+00 (none)
Minimum Soundspeed	1.00000E-10 (cm/us)
Maximum Soundspeed (SPH)	1.01000E+20 (cm/us)
Maximum Temperature	1.01000E+20 (K)
Reference:	AFATL-TR-84-59. June 1984. Matuska D.A. HULL Users Manual

5. Tantalum

Equation of State	**Shock**
Reference density	1.66000E+01 (g/cm^3)
Gruneisen coefficient	1.69000E+00 (none)
Parameter C1	3.42300E-01 (cm/us)
Parameter S1	1.21400E+00 (none)

Parameter Quadratic S2	0.00000E+00 (us/cm)
Relative volume, VE/V0	0.00000E+00 (none)
Relative volume, VB/V0	0.00000E+00 (none)
Parameter C2	0.00000E+00 (cm/us)
Parameter S2	0.00000E+00 (none)
Reference Temperature	0.00000E+00 (K)
Specific Heat	0.00000E+00 (Terg/gK)
Thermal Conductivity	0.00000E+00 (Terg/cmKus)
Strength	**von Mises**
Shear Modulus	6.56000E-01 (Mbar)
Yield Stress	5.00000E-03 (Mbar)
Failure	**None**
Erosion	**None**
Material Cutoffs	-
Maximum Expansion	1.00000E-01 (none)
Minimum Density Factor	1.00000E-04 (none)
Minimum Density Factor (SPH)	2.00000E-01 (none)
Maximum Density Factor (SPH)	3.00000E+00 (none)
Minimum Soundspeed	1.00000E-10 (cm/us)
Maximum Soundspeed (SPH)	1.01000E+20 (cm/us)
Maximum Temperature	1.01000E+20 (K)
Reference:	AFATL-TR-84-59. June 1984. Matuska D.A. HULL Users Manual

APPENDIX B: SIMULATION SETUP WITH AUTODYN

A. INTRODUCTION

ANSYS AUTODYN® is an engineering simulation software for modeling nonlinear dynamics of solids, fluids, gas and their interaction. This product, which has been developed by the company ANSYS, Inc. based in Canonsburg, Pennsylvania (United States of America), provides advanced capabilities within a robust, easy-to-use software tool to solve many nonlinear dynamics problems offering following solver technologies [023]:

- Finite element solvers for computational structural dynamics (FE)
- Finite volume solvers for fast transient computational fluid dynamics (CFD)
- Mesh-free particle solvers for high velocities, large deformation and fragmentation (SPH)
- Multisolver coupling for multiphysics solutions including between FE, CFD and SPH
- A wide suite of material models incorporating constitutive response and coupled thermodynamics
- Serial and parallel computation on shared and distributed memory systems

This panoply of different solvers makes ANSYS AUTODYN® a very appropriate tool to solve the problems considered in this thesis, with regards to Held's works, in the immense field of ballistics.

In the following subchapters, information are given to exactly set up the problems simulated in this thesis. This were obtained from some Workshops [031] or experiences from some research personals and research students or from experiences of my own. More specifically information concerning some of the most important tools, options or properties either used or mentioned in this Thesis are further contained [023].

B. PROBLEM SETUP FOR 2D FRAGMENT IMPACT (IMPACT INITIATION)

The problems considered in this thesis concern a 2D fragment impact which deals with impact initiation. To set up these problems, a new project has first to be started. A 2D axial geometry is chosen and allows to set up only "half of the problem". This means that all the dimensions along the y-axis, especially the width and diameters, have to be halved. The units chosen are cm, g and μs. It seems not to be very useful, but it is recommended from the interface to be used with the Lagrange solver. A contravene to this recommendation could bring some complications with it during the simulations.

After the new project has been created, the materials used in the simulation have either to be loaded or to be created. This can be done by clicking on "Materials" under the title "Setup" on the right side of the interface[101]. The next setup which has to be set concerns the initial conditions (under "Init. Cond." on the left panel). The different initial velocities, which will be assigned to our projectile, can be entered here. These velocities are only along the x-axis ("X-velocity")[102]. Therefore the Y-velocity are set to 0. After that, the Parts (under "Parts" on the left panel) have to be designed. The solver chosen is here the Lagrange-one, which allows to simulate impact initiation problems with regards to the Lee-Tarver model[103]. The "Part wizard" definition is kept. The dimensions of the parts, needed to realize the considered simulations, are now entered in a Cartesian coordinate system. The geometrical part picked out can be a box, a circle and so forth. It just depends on the form we have. In this Thesis, they are boxes. A zone size, also known as zoning, has thereafter to be defined. Therefore a number of cells in each direction (x- and y-direction in a 2D problem with a Cartesian coordinate system) has to be entered. The material, in which this part should be mainly composed of, can finally be selected. This complete operation has to be done for each part of the observed disposal (projectile

[101] More information are available in the ANSYS 13.0 Help [023].

[102] These velocities have to be entered with regards to the units used in this project.

[103] More information in part 4 of subchapter C.

and acceptor charge). The different parts which have been created can then be filled with other sorts of material. A delimitation of the filling, given through the numbering of cells or through the Cartesian coordinate system, has therefore to be indicated.

After that, the disposal has to be adjusted: gauges have for example to be placed and "Interactions", "Controls" as well as "Output" (present as well on the left panel) options have to be set up.

C. OTHER IMPORTANT TOOLS, OPTIONS OR PROPERTIES

1. Materials

The library contained in the software offers many different materials (different plastics, different metals, different explosives,...) which can be directly used. They are listed with regards to their equation of state (EOS), to their strength model and to their failure model. More information, like for example density, energy per unit volume and EOS parameters, are available by clicking on "Modify". Knowledge of all these material properties gives the possibility to create our own materials by clicking on "Create" and consequently completing the information fields .

2. Solvers

AUTODYN® uses four different solvers to provide solutions for the defined problems [023]:

- The Lagrange solver, mainly used for structural response and complex materials. This solver uses mesh-based Lagrangian methods. A grid, which size depends on the number of cells per mm (zoning), is defined inside the materials. No grid is required for exterior spaces. By interactions, the cells can become bigger or smaller. Their size is also not really fixed.

- The Euler solver, mainly used for solid, gas or fluid flow and blast waves. This solver uses mesh-based Eulerian methods. The grid is fixed in space and material flows through it. The external spaces have to be modeled with void cells. The cells have a fix size.

- The Arbitrary Lagrange Euler solver, called ALE solver, mainly used for fluid-structure interaction with strong structures. It is a sort of combination between the Lagrange and the Euler solver. It also uses a mesh-based hybrid Lagrangian/Eulerian method with predominantly Eulerian flow and predominantly Lagrangian deformation.

- The Mesh Free solver, mainly used for hypervelocity impact and brittle material fracture/fragmentation. It uses the particle-based Smooth Particle Hydrodynamics method (SPH). The geometry is represented as particles and none of these particles are required for exterior spaces.

A visual comparison of these four solver systems is given in figure 62:

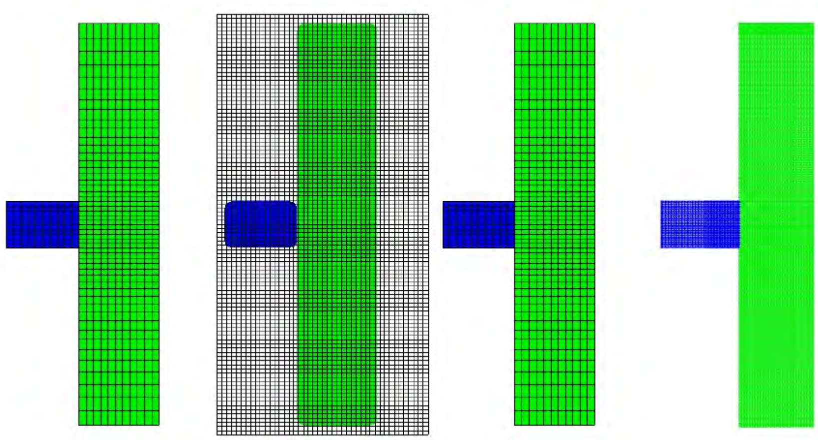

Figure 61 [031]: Visual comparison of the four solver models. From the left to the right: Lagrange, Euler Arbitrary Lagrange Euler, Smooth Particle Hydrodynamics.

It is possible and even recommended to select the "best" solver in the considerate simulation for each part of the disposal. The different parts can then interact with each other through bonding (joins), contact (Lagrange-Lagrange interactions) or coupling (Euler-Lagrange interactions). A visual comparison of contact and coupling interaction is given in figure 63:

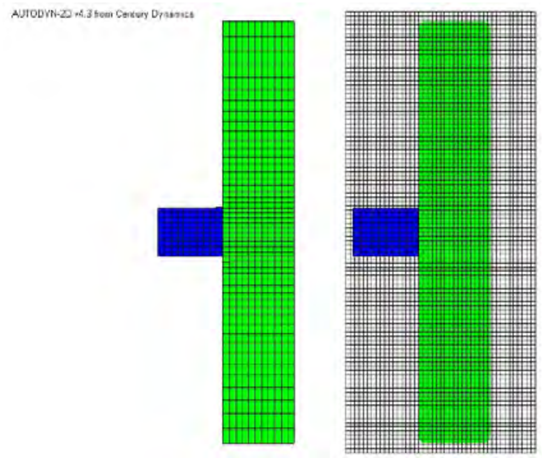

Figure 62 [031]: Visual comparison of the contact and coupling interaction. On the left: Lagrange/Lagrange contact and on the right: Euler/Lagrange contact.

Using the Lee-Tarver model in AUTODYN® implicates to select the Lagrange solver.

3. Zoning

Using the Lagrange, the Euler or the Arbitrary Lagrange Euler solver implicates to divide the space (the entire space or just the parts) in a grid with a specific number of cells. A cell is the smallest element in the disposal. That means that all physical information in the same cell are the same.

This action of dividing the space, which is called zoning, has to be done by creating the new parts. Therefore, a number of cells for both directions (x- and y-directions in 2D problems) has to be entered. The higher the number of cells per mm, the more accurate the simulation results, but the longer the simulation time. Simulations done by myself or by former NPS students have shown that a zone size of 2 cells/mm provides accurate enough simulation results while keeping the simulation time on an acceptable level. For some specific results, the zone size can be expend to 4 cells/mm.

Figure 63: Visual comparison of a disposal with a zoning of 1 cell/mm (left) and a zoning of 4 cells/mm (right).

A "graded zoning" can also be chosen. It allows the user to define the interacting fraction of a part with a better accuracy (more cells/mm) than the non-interacting one (less cells/mm). This should be especially done for big parts with small interacting portions in order to preserve a good accuracy while keeping "small" simulation times.

4. Equation of State (EOS)

See Chapter III, subchapter C.

5. Strength and Failure model

For a more physical post-burn behavior for medium and large expansions, the problems cannot be solved by only using the EOS. The Strength model has to be taken into consideration. It describes the transition between elastic and plastic strain, both in compression and release, and it gives a relation to define the onset of fracture. The methodology used in AUTODYN® is based on the formulations of Wilkins, who extended conventional numerical hydrodynamic codes to include the effects of material strength and resistance to shear distortion. More information about this model are available in the ANSYS 13.0 Help [023].

In the reality, materials cannot either withstand stresses which go over the material's local tensile strength. In order to prevent simulations from providing unphysical results, some models have been constructed to recognize when limits are reached, to deal with this, and to describe the properties of the material after this formulation has been applied. These different failure models depend on the different types of materials. This topic is discussed and described more specifically in the ANSYS 13.0 Help [023].

In this Thesis, both models are set up with the default application which is given to the considered materials. Consequently, no really attention has to be paid to them.

6. Interactions

Before starting the simulation, a gap, which is required for interaction logic, has to be defined [023]. Its size must be in the range 1/10 to 1/2 the dimension of the smallest element face of parts involved in interactions. However, it doesn't really matter how these dimensions are, because clicking on "Calculate", under the "Interaction" properties, provides an automatic calculation of the gap size (it will be set to 1/10 the dimension of the smallest element). After that, clicking on "Check" allows to check the validity of the gap size and that all parts involved in interactions are effectively separated by the specified gap size. A message will inform if the interaction is valid or not.

During the first problems set up in this thesis, the simulations used to stop after only a few seconds, delivering an error message as following: "Error, degenerate cells in...". This could be solved by selecting the option "Prevent erosion of degenerate elements" in the "Interaction" panel, which allows the interaction calculation to be used to stop elements from becoming degenerate. However, it is to notice that this option only works for Lagrange volume elements and can lead to unphysical results, especially if a large gap size is used. On the same way, the "Retain inertia of eroded notes" option, just above, is selected to prevent the eroded nodes from being removed from the model.

7. Gauges

The simulations done in AUTODYN® would not be very useful if the user was not able to get plenty of physical information during the simulation process. Therefore are gauges here. They give notably information, among others, about velocities, pressures, internal energies and densities.

Gauges have to be placed on the different parts of the disposal. There are two sorts of gauges: fixed gauges and moving gauges. Fixed gauges are, as their name implies, fixed on the considered position and only get information on this particular point. Moved gauges, on the contrary, move with the point they are assigned to. These gauges can be placed as simple points, arrays or blocks using the Cartesian coordinate system or the cells numerate system. Their total number is limited to 200.

At the end of the simulation, the option "History" gives the possibility to deal with all the information stored by the gauges. This point is treated in part 11 of this subchapter.

8. Controls

After the problem has been set up and before starting the simulation, controls have to be defined to assure the output of results that meet user's expectations. This can be done by clicking on "Controls" on the left panel.

The first visible controls are the "Wrapup criteria", in which parameters have to be specified. In "Cycle limit", the maximum number of cycles to be run has to be entered. It is not very useful to stop the simulation because of a cycle limit but much more interesting to let the simulation run until the problem is solved. That's why a very large number, like 100,000, is entered at that place. The "Time limit" is the time during which the simulation runs. Similar to the "Cycle limit", a very large number, like $1.0*10^{20}$ µs has to be entered in order to prevent the simulation from stopping before the problem has been solved. The "Energy fraction" gives the value of the energy error (in percent) that the simulation shouldn't exceed. The default value is set to 0.05 (5%). It can be that the default value is too small for the desired simulation. In that case, it could be increased to allow the simulation to go on. This energy error will first be checked at the cycle number specified in "Energy reference cycle". If the value entered in this field is large, the energy error may not be checked.

Other controls to be set up are the "Timestep options". The "Start time" is set to 0 µs. The "Minimum timestep" is, as its name implies, the minimum time value authorized for the considered simulation. If the timestep drops below this value, the problem will be terminated. However, it is still possible to enter another value in that field and to start the simulation again. Similar to the "Minimum timestep", the "Maximum timestep" is the maximum time value authorized for the considered simulation. If this value is exceeded, the simulation stops, but as for the "Maximum timestep", it is still possible to change the value and to start the simulation again. Entering a very small value for the "Minimum timestep" and a very large value for the "Maximal timestep" should however avoid a lot of inconvenient. All other parameters in the "Timestep options", as well as all other options in the "Controls" panel, can be left unchanged (default values). Further information about these options are provided from the ANSYS 13.0 Help [023].

9. Output

The output options are very important to provide significant results that can be used from the user. In the panel "Save", the backup parameters are defined. The data can be written at a set cycle frequency or at a time frequency. The start cycle or start time is first set to 0 to start saving data from the beginning of the simulation, the end cycle or end time is set to a large number (actually to the same value as under the "Controls" panel). In "Increment", the frequency to which the files are written can be chosen. In this Thesis, it is generally set to 10 cycles. What sort of data are saved in these files can be decided in

"Select variables" (pressures, velocities,...) and reviewed in "Review variables". In this thesis, this is left unchanged (default values) and also encompass pressures, velocities and all other parameters which are needed for the analysis. No attention is paid to the other output options because they merge into the "Save" ones.

10. Plots

The plots options, on the left panel, give the possibility to visualize information relative to the zoning, the material location, the material status (Hydro, Elastic) and the additional components like velocity vectors or gauges. Live information about variables like intern energy, temperatures, pressures or detonation progress are also available under the "Contour" option. Very interesting is the detonation progress visualization, known under "ALPHA", which allows the users of AUTODYN® to know when and where the explosive is detonating and when and where it is not, without performing any calculations. Indeed, this variable corresponds to the burn fraction, automatically and continually calculated with the AUTODYN® codes, and takes a value between 0 (no detonation - blue in the legend) and 1 (detonation complete - red in the legend). An example is given in figure 65:

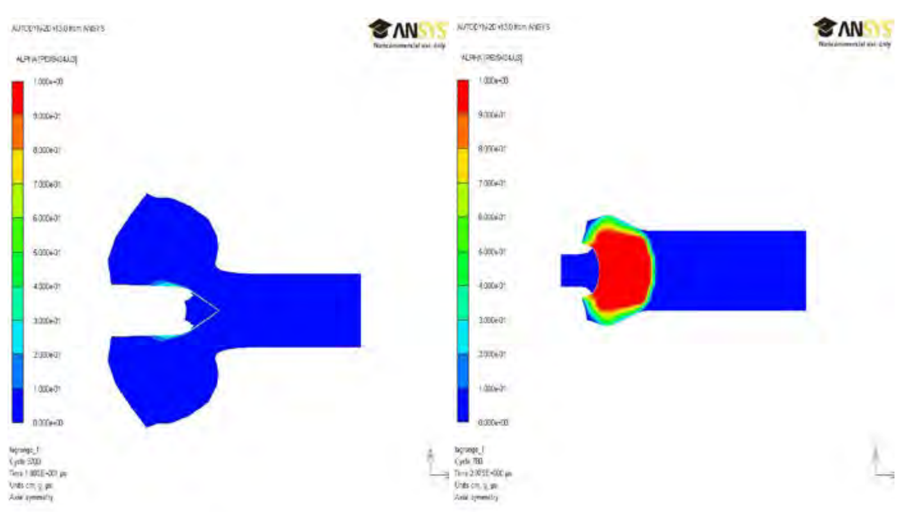

Figure 64: Use of the ALPHA variable and visualization of the detonation process. No detonation occurs on the left simulation (completely blue) while a detonation occurs on the right one (red in progress to the right).

11. History

After the simulation ends, and as indicated under part 7 of this subchapter, the information obtained through the gauges can be composed and displayed in the "History" panel. By selecting "Gauge points" and "Single variable plots" (plots of a single variable) or "Multi variable plots" (plots including multiple variables), the gauges can be chosen with regards to their attribution number and the desired variable (pressure, velocity, internal energy) can be drown as a function of the time or as a function of other parameters (pressure, velocity,...). The scale of the chart can be adjusted under "Set scales" as well as the plot styles under "Plot styles". Clicking on interesting points in the chart delivers information about the x- and y- Cartesian coordinates allowing a faithful analysis of the results. A picture of the chart can be taken by clicking on the camera button on the tools panel at the top of the window.

THIS PAGE INTENTIONALLY LEFT BLANK

APPENDIX C: DATA TABLES

A. EXPERIMENTAL RESULTS

The following results have been obtained in the literature and have been used in this thesis to confirm the ability of AUTODYN® to simulate impact initiation problems.

1. Experimental results concerning a bare block of explosive PBX 9404 and a steel projectile

a) Moulard experimental results

The arrangement and the conditions concerning this experiment have been described in detail in chapter V, subchapter A.

Projectile diameter in mm	No Go/Go velocities in m/s
2	1550-1650
3	1200-1300
4	1000-1100
6	800-900
8	650-750
10	500-600

Table 27: "Go/No Go" for different projectile diameters. Experimental results obtained for a steel projectile impacting a bare block of explosive PBX 9404 [027].

b) Weingart, Bahl and Vantine experimental results

In this experiment, a bare block of PBX 9404 has been impacted by flat-nosed steel projectiles of different diameters. Length of both explosive and projectile have not been reported.

Projectile diameter in mm	No Go/Go velocities in m/s
2	1350-1450
3	1150-1250
4	1000-1100
6	800-900
8	700-800
10	600-700
12	550-650

Table 28: "Go/No Go" for different projectile diameters. Experimental results obtained for a steel projectile impacting a bare block of explosive PBX 9404 [026].

c) LeRoy Green experimental results

In this experiment, a bare block of PBX 9404 has been impacted by a "long" cylindrical tool steel projectile of different diameters. Length of both explosive and projectile have not been reported.

Projectile diameter in mm	No Go/Go velocities in m/s
2	2000-2100
3	1300-1400
4	1100-1200
6	850-950
8	750-850
10	650-750
12	600-650

Table 29: "Go/No Go" for different projectile diameters. Experimental results obtained for a steel projectile impacting a bare block of explosive PBX 9404 [028].

d) James, Haskins and Cook experimental results

In this experiment, a bare block of PBX 9404 has been impacted by a "long" cylindrical tool steel projectile of different diameters. Length of both explosive and projectile have not been reported.

Projectile diameter in mm	No Go/Go velocities in m/s
2	1200-1300
3	1000-1100
4	900-1000
6	750-850
8	650-750
10	600-700
12	550-650

Table 30: "Go/No Go" for different projectile diameters. Experimental results obtained for a steel projectile impacting a bare block of explosive PBX 9404 [029].

2. Experimental results concerning a covered block of explosive PBX 9404 (2.0 mm barrier) and a steel projectile

a) James, Haskins and Cook experimental results

In this experiment, a covered (2.0 mm tantalum barrier) block of PBX 9404 has been impacted by a "long" cylindrical tool steel projectile of different diameters. Length of both explosive and projectile have not been reported.

Projectile diameter in mm	No Go/Go velocities in m/s
2	/
3	2100-2200
4	1600-1700
6	1150-1250
8	1050-1150
10	900-1000
12	750-850

Table 31: "Go/No Go" velocities for different projectile diameters. Results obtained by James, Haskins and Cook for a steel projectile impacting a covered (2.0 mm tantalum barrier) block of explosive PBX 9404.

b) Moulard experimental results

In this experiment, a covered (2.0 mm tantalum barrier) block of PBX 9404 has been impacted by a 10 mm long cylindrical steel projectile of different diameters. The explosive has a width of 15 mm and a length of 50 mm.

Projectile diameter in mm	**No Go/Go velocities in m/s**
2	/
3	2100-2200
4	1750-1850
6	1250-1350
8	1100-1200
10	900-1000
12	850-950

Table 32: "Go/No Go" velocities for different projectile diameters. Results obtained by Moulard for a steel projectile impacting a covered (2.0 mm tantalum barrier) block of explosive PBX 9404.

B. SIMULATION RESULTS

The following results have been obtained with AUTODYN® by performing the simulations described in this thesis. They are organized with regards to the parts in which they have been mentioned for the first time.

1. Chapter VI, subchapter A, part 1

Projectile diameter in mm	No Go/Go velocities in m/s
2	2600-2700
3	1600-1700
4	1100-1200
6	800-900
8	600-700
10	500-600

Table 33: "Go/No Go" velocities for different projectile diameters. Simulation results obtained for a steel projectile impacting a bare block of explosive PBX 9404 by a zoning of 1 cell/mm.

2. Chapter VI, subchapter A, part 2

Projectile diameter in mm	No Go/Go velocities in m/s
2	1800-1900
3	1300-1400
4	1100-1200
6	800-900
8	600-700
10	500-600
12	500-550

Table 34: "Go/No Go" velocities for different projectile diameters. Simulation results obtained for a steel projectile impacting a bare block of explosive PBX 9404 by a zoning of 2 cells/mm.

3. Chapter VI, subchapter A, part 3

Projectile diameter in mm	No Go/Go velocities in m/s
2	1800-1900
3	1200-1300
4	1000-1100
6	800-900
8	600-700
10	500-600

Table 35: "Go/No Go" velocities for different projectile diameters. Simulation results obtained for a steel projectile impacting a bare block of explosive PBX 9404 by a zoning of 4 cells/mm.

4. Results of chapter VI, subchapter D, part 1

Projectile diameter in mm	No Go/Go velocities in m/s
2	/
3	2100-2200
4	1500-1600
6	1300-1400
8	1000-1100
10	900-1000
12	700-800

Table 36: "Go/No Go" velocities for different projectile diameters. Simulation results obtained for a steel projectile impacting a covered (2.0 mm tantalum barrier) block of explosive PBX 9404 by a zoning of 2 cells/mm.

5. Results of chapter VI, subchapter D, part 2

Projectile diameter in mm	No Go/Go velocities in m/s
2	/
3	2500-2600
4	1700-1800
6	1200-1300
8	900-1000
10	800-900
12	700-800

Table 37: "Go/No Go" velocities for different projectile diameters. Simulation results obtained for a steel projectile impacting a covered (2.0 mm steel barrier) block of explosive PBX 9404 by a zoning of 2 cells/mm.

Projectile diameter in mm	No Go/Go velocities in m/s
2	/
3	2800-2900
4	1900-2000
6	1200-1300
8	900-1000
10	800-900
12	700-800

Table 38: "Go/No Go" velocities for different projectile diameters. Simulation results obtained for a steel projectile impacting a covered (2.5 mm steel barrier) block of explosive PBX 9404 by a zoning of 2 cells/mm.

Projectile diameter in mm	No Go/Go velocities in m/s
2	/
3	/
4	3400-3500
6	2000-2100
8	1400-1500
10	1100-1200
12	800-900

Table 39: "Go/No Go" velocities for different projectile diameters. Simulation results obtained for a steel projectile impacting a covered (5.0 mm steel barrier) block of explosive PBX 9404 by a zoning of 2 cells/mm.

Distance from the impact surface in mm	Pressure in Mbar
0.5	0.144
1.0	0.146
1.5	0.146
2.0	0.142
2.5	0.137
3.0	0.130
3.5	0.120
4.0	0.108
4.5	0.086
5.0	0.046
5.5	0.024
6.0	0.022
6.5	0.020

Table 40: Pressure for in the steel barrier (red) and in the explosive (blue) for different distances from the impact surface. Simulation results obtained for a steel projectile impacting a covered (5.0 mm steel barrier) block of explosive PBX 9404 by a zoning of 2 cells/mm.

6. Chapter VI, subchapter D, part 3

Projectile diameter in mm	No Go/Go velocities in m/s
2	/
3	2000-2100
4	1700-1800
6	1100-1200
8	800-900
10	700-800
12	600-700

Table 41: "Go/No Go" velocities for different projectile diameters. Simulation results obtained for a steel projectile impacting a covered (2.0 mm aluminum barrier) block of explosive PBX 9404.

7. Chapter VI, subchapter E, part 1

Projectile diameter in mm	No Go/Go velocities in m/s
2	/
3	3000-3100
4	2100-2200
6	1300-1400
8	1000-1100
10	800-900
12	600-700

Table 42: "Go/No Go" velocities for different projectile diameters. Simulations results obtained for a steel projectile impacting a completely confined (2.5 mm steel confinement) block of explosive PBX 9404.

8. Chapter VI, subchapter E, part 2

Projectile diameter in mm	No Go/Go velocities in m/s
2	1800-1900
3	1300-1400
4	1100-1200
6	800-900
8	600-700
10	500-600
12	500-550

Table 43: "Go/No Go" velocities for different projectile diameters. Simulation results obtained for a steel projectile impacting a confined but not covered (2.5 mm steel confinement) block of explosive PBX 9404.

9. Chapter VI, subchapter G, part 1

Projectile diameter in mm	No Go/Go velocities in m/s
2	/
3	/
4	/
6	3100-3200
8	2100-2200
10	1500-1600
12	1200-1300

Table 44: "Go/No Go" velocities for different projectile diameters. Simulation results obtained for a steel projectile impacting a bare block of explosive TNT by a zoning of 2 cells/mm.

10. Chapter VI, subchapter G, part 2

Projectile diameter in mm	No Go/Go velocities in m/s
2	/
3	3100-3200
4	2000-2100
6	1300-1400
8	1000-1100
10	900-1000
12	700-800

Table 45: "Go/No Go" velocities for different projectile diameters. Simulation results obtained for a steel projectile impacting a bare block of explosive H6 by a zoning of 2 cells/mm.

11. Chapter VI, subchapter G, part 3

Projectile diameter in mm	No Go/Go velocities in m/s
2	2200-2300
3	1400-1500
4	1000-1100
6	700-800
8	600-700
10	500-600
12	400-500

Table 46: "Go/No Go" velocities for different projectile diameters. Simulation results obtained for a steel projectile impacting a bare block of explosive Comp. B by a zoning of 2 cells/mm.

12. Chapter VI, subchapter G, part 4

Projectile diameter in mm	No Go/Go velocities in m/s
2	2700-2800
3	1800-1900
4	1600-1700
6	1500-1600
8	1000-1100
10	900-1000
12	800-900

Table 47: "Go/No Go" velocities for different projectile diameters. Simulation results obtained for a steel projectile impacting a bare block of explosive Octol by a zoning of 2 cells/mm.

13. Chapter VI, subchapter H, part 1

Projectile diameter in mm	No Go/Go velocities in m/s
2	1800-1900
3	1300-1400
4	1100-1200
6	800-900
8	600-700
10	500-600

Table 48: "Go/No Go" velocities for different projectile diameters. Simulation results obtained for a copper projectile impacting a bare block of explosive PBX 9404 by a zoning of 2 cells/mm.

14. Chapter VI, subchapter H, part 2

Projectile diameter in mm	No Go/Go velocities in m/s
2	2800-2900
3	1800-1900
4	1500-1600
6	1100-1200
8	900-1000
10	700-800

Table 49: "Go/No Go" velocities for different projectile diameters. Simulation results obtained for an aluminum projectile impacting a bare block of explosive PBX 9404 by a zoning of 2 cells/mm.

15. Chapter VI, subchapter H, part 3

Projectile diameter in mm	No Go/Go velocities in m/s
2	1500-1600
3	1200-1300
4	900-1000
6	700-800
8	600-700
10	500-600

Table 50: "Go/No Go" velocities for different projectile diameters. Simulation results obtained for a tungsten projectile impacting a bare block of explosive PBX 9404 by a zoning of 2 cells/mm.

C. OTHER DATA

The Hugoniot parameters, which have been used in this thesis to calculate the impact pressures needed for the values estimations of the Pd criterion, are tabulated in table 52. Hereby are:

ρ_0... Density of the unreacted explosive in $kg.m^{-3}$

c_0 ... Bulk sound speed in $m.s^{-1}$

s ... Constant dimensionless

	ρ_0 ($kg.m^{-3}$)	c_0 ($m.s^{-1}$)	s
Explosives	7890	1569	1.490
PBX 9404	1842	2310	2.767
TNT cast	1630	2570	1.880
H6	1760	2654	1.984
Comp. B (65/35)	1720	2710	1.860
Octol (70/30)	1800	3010	1.720
Non Explosives			
Steel	7896	4569	1.490
Copper	8930	3940	1.489
Aluminum	2785	5328	1.338
Tungsten	19224	4029	1.237
Tantalum	16654	3414	1.201

Table 51: Hugoniot values [022] for the explosives and projectiles used in this thesis.

THIS PAGE INTENTIONALLY LEFT BLANK

LIST OF REFERENCES

[001] Muthig, H., Leiber, C.O., Wanninger, P. (2011). Obituary Manfred Held 1933-2011. *Propellants, Explosives, Pyrotechnics, 36,* 103-104.

[002] (July 2008). Landwards science group Held captivated. Website of the *Council for Scientific and Industrial Research*. Retrieved from *www.csir.co.za*

[003] Kx. (February, the 9th 2011). Manfred Held. Website of the German journal *Donaukurier*. Retrieved from *www.Donaukurier.de*

[004] (February, the 14th 2011). A sad news. Website of the *Australian Institute of High Energetic Materials*. Retrieved from *www.ausihem.org*

[005] Held, M. (2000). Test setup for instrumented initiation tests. *Propellants, Explosives, Pyrotechnics, 25*(2), 49-53.

[006] Held, M. (1989, August). Initiation phenomena with shaped charge jets. Paper presented at the *9th International Symposium on Detonation,* Portland, OR, USA.

[007] Held, M. (1983). Critical area for the initiation of high explosive charges. Paper presented at the *Shock Waves in Condensed Matter. Ed.by JP Asay, RA Graham, and GK Straub, Elsevier Science Publishers, BV,* Santa Fe, NM.

[008] Walker, F.E. and Wasley, F.I. (1969). Critical energy for shock initiation of lieterogeneous explosives. *Explosivstoffe, 17,* 4-13.

[009] Held, M. (1968). Initiation of explosives, a multiple problem of the physics of detonation [Initiierung von Sprengstoffen, ein vielschichtiges Problem der Detonationsphysik]. *Explosivstoffe , 5*, 2-17.

[010] Weingart, R.C. (1976). Acceleration of thin flyers by exploding metal foils: application to initiation studies. Paper presented at the *6th International Symposium on Detonation*, Arlington, Virginia, USA.

[011] Vantine, H.C. (1980). The shock initiation of bare and covered PBX-9404 charges by projectile impact. *Lawrence Livermore National Laboratory, Report UCID-18547*.

[012] Moulard, H. (1981). Une condition de surface critique pour l'amorcage par onde de choc des explosifs solides. *Propellants and Explosives, 6*, 63-66.

[013] Held, M. (1987). Experiments of initiation of covered, but unconfined high explosive charges by means of shaped charge jets. *Propellants, Explosives, Pyrotechnics, 12*(2), 35-40.

[014] Held, M. (1987). Experiments of initiation of covered, but unconfined HE charges under different test conditions by shaped charge jets. *Propellants, Explosives, Pyrotechnics, 12(3)*, 97-100.

[015] Held, M. (1987). Discussion of the experimental findings from the initiation of covered, but unconfined high explosive charges with shaped charge jets. *Propellants, Explosives, Pyrotechnics, 12*(5), 167-174.

[016] Held, M. (1996). Initiation criteria of high explosives at different projectile or jet densities. *Propellants, Explosives, Pyrotechnics, 21*(5), 235-237.

[017] Chick, M., Bussel, T.,Frey, R., Boyce, G. (1986). Initiation of munitions by shaped charge jets. Proceedings of the 9th *International Symposium on Ballistics*, 421-430.

[018] Mader, C., Pimbley, G. (1983). Jet initiation and penetration of explosives. *Energetic Materials, 1*, 3-44.

[019] Mader, C. (1986). Recent advances in numerical modelling of detonation. *Propellants, Explosives, Pyrotechnics, 11*, 163-166.

[020] Zukas, J., Walters, W. (1998). Explosive effects and applications. Springer-Verlag, New York, USA.

[021] Brown, R. (2011). Physics of explosives. *Lesson PH4171*, Naval Postgraduate School, CA, USA.

[022] Cooper, P. (1996). Explosives engineering. Wiley-VCH, Inc, USA.

[023] (2010). ANSYS 13.0 Help, Canonsburg, Pennsylvania, USA.

[024] Hasenberg, D. (2010). Consequences of coaxial jet penetration performance and shaped charge design criteria. *Diplomarbeit*, Naval Postgraduate School, CA, USA.

[025] (1995). Technical demining - Task 85, Development, Mine neutralization, Munitions. *Office of special technology*, Fort Washington, Maryland, USA.

[026] Bahl, K., Vantine, H., Weingart, R. (1981). Proceedings of the 7^{th} *International Symposium on Detonation*, Annapolis, Maryland, USA.

[027] Moulard, H. (1981). Critical conditions for shock initiation of detonation by small projectile impact. Proceedings of the 7^{th} *International Symposium on Detonation*, Annapolis, Maryland, USA.

[028] LeRoy Green (1981). Shock initiation of explosives by the impact of small diameter cylindrical projectiles. Proceedings of the 7th *International Symposium on Detonation*, Annapolis, Maryland, USA.

[029] James, H., Haskins, P., Cook, M. (1996). Prompt shock initiation of cased explosives by projectile impact. *Propellants, Explosives, Pyrotechnics, 21*, 251-257.

[030] Kleinhanss, H., Lungenstrass, F., Zoellner, H. (...). Initiation threshold of high explosives in small flyer plate experiments. Proceedings of the ...th *International Symposium on Detonation*, ...

[031] (February 2010). Introduction to ANSYS AUTODYN®, *ANSYS training manual*, Release 12.1, 1st edition, Canonsburg, Pennsylvania, USA.

INITIAL DISTRIBUTION LIST

1. Defense Technical Information Center
   Ft. Belvoir, Virginia

2. Dudley Knox Library
   Naval Postgraduate School
   Monterey, California

3. Professor Ronald E. Brown
   Naval Postgraduate School
   Monterey, California

4. Professor Hendrik Rothe
   Helmut Schmidt University
   Hamburg, Germany

5. Professor Stefan Dickmann
   Helmut Schmidt University
   Hamburg, Germany

6. Prüfungsamt
   Helmut Schmidt University
   Hamburg, Germany

7. Prüfungsamt
   Helmut Schmidt University
   Hamburg, Germany

8. Prüfungsamt
   Helmut Schmidt University
   Hamburg, Germany